

**Comment Response Matrix
for
Nuclear Regulatory Commission (NRC)
Requests for Additional Information (RAIs) on the
Saltstone Disposal Facility Performance Assessment
(SRR-CWDA-2009-00017, Revision 0, dated October 29, 2009)**

Approved By:



T. C. Robinson
Manager, Closure & Disposal Assessments

July 23, 2010

APPROVED FOR PUBLIC RELEASE

Prepared by: Savannah River Remediation (SRR)
Closure & Waste Disposal Authority
Aiken, SC 29808



ACRONYM LIST FOR RESPONSES

ACI	American Concrete Institute
ALARA	As Low As Reasonably Achievable
ARP/MCU	Actinide Removal Process / Modular Caustic Side Solvent Extraction Unit
CBP	Cementitious Barriers Partnership
CSH	Calcium Silicate Hydrate
DCF	Dose Conversion Factor
DDA	Deliquification Dissolution Adjustment
DOE	U.S. Department of Energy
DSSF	Double-Shell Slurry Feed
FDC	Future Disposal Cell
FTF	F-Area Tank Farm
GCL	Geosynthetic Clay Liner
GSA	General Separations Area
HDPE	High Density Polyethylene
HELP	Hydrologic Evaluation of Landfill Performance
HTF	H-Area Tank Farm
INL	Idaho National Laboratory
LLW	Low-level Waste
NRC	U.S. Nuclear Regulatory Commission
MOP	Member of the Public
PA	Performance Assessment
PMP	Probable Maximum Precipitation
QAP	Quality Assurance Plan
RAI	Request for Additional Information
SA	Sensitivity Analysis
SDF	Saltstone Disposal Facility
SI	Sensitivity Index
SRS	Savannah River Site
SWPF	Salt Waste Processing Facility
SZ	Saturated Zone
TEDE	Total Effective Dose Equivalent
UA	Uncertainty Analysis
UTR-LZ	Upper Three Runs - Lower Zone
UTR-UZ	Upper Three Runs - Upper Zone
UZ	Unsaturated Zone
WCS	Waste Characterization System
PNNL	Pacific Northwest National Laboratory
SRNL	Savannah River National Laboratory
SPF	Saltstone Production Facility
NCSU	North Carolina State University

Performance Assessment Methods (PA):

<u>PA-1</u>	<p>The contribution of individual radionuclides to the dose was not provided for several deterministic sensitivity cases.</p> <p><u>Basis</u></p> <p>It is important to know which radionuclides are contributing to the dose in order to understand which radionuclides are most risk significant and to understand which factors the dose is likely to be sensitive to. A thorough understanding of these factors is critical to performance monitoring.</p> <p><u>Path Forward</u></p> <p>Provide the doses from individual radionuclides for Case B, Case C, Case D, Case E, the synergistic case, and the case presented in Section 5.6.6.7 of the PA, and for any new analyses that are performed in response to other comments in this document.</p>
--------------------	---

RESPONSE PA-1:

The following tables present the dose to the MOP in Sectors B and I for Cases B through E, the synergistic case, and the other cases presented in SDF PA Section 5.6.6. The dose results presented in the following tables are based on the radionuclide concentrations computed by the PORFLOW model. Only those radionuclides that contribute approximately 1%, or greater, to the total dose in either Sectors B or I are presented.

Table PA-1.1: Peak Dose to MOP at 100 Meters in Sector B for Cases A through E

MOP Dose in Sector B Within 10,000 Years			MOP Dose in Sector B Within 20,000 Years		
Radionuclide	Dose (mrem/yr)	Contribution	Radionuclide	Dose (mrem/yr)	Contribution
Case A (10,000 years)			Case A (15,080 years)		
I-129	5.2E-02	3.8%	I-129	1.4E+00	48.3%
Ra-226	1.3E+00	94.0%	Ra-226	1.4E+00	47.6%
Tc-99	1.3E-02	0.9%	Tc-99	8.7E-02	3.0%
Total	1.4E+00	--	Total	2.9E+00	--
Case B (4,180 years)			Case B (15,740 years)		
I-129	1.1E-01	2.8%	I-129	8.3E-02	1.4%
Pb-210	4.8E-02	1.2%	Pb-210	6.3E-02	1.0%
Ra-226	3.5E+00	90.1%	Ra-226	4.6E+00	75.7%
Rn-222	4.0E-02	1.0%	Rn-222	5.2E-02	0.9%
Tc-99	1.8E-01	4.7%	Tc-99	1.1E+00	18.9%
Total	3.9E+00	--	Total	6.0E+00	--
Case C (7,360 years)			Case C (15,420 years)		
I-129	1.0E-01	2.0%	I-129	1.0E-01	1.8%
Pb-210	6.4E-02	1.3%	Pb-210	7.0E-02	1.3%
Ra-226	4.8E+00	93.2%	Ra-226	5.1E+00	92.9%
Rn-222	5.5E-02	1.1%	Rn-222	5.9E-02	1.1%
Tc-99	8.7E-02	1.7%	Tc-99	7.5E-02	1.4%
Total	5.1E+00	--	Total	5.5E+00	--
Case D (9,800 years)			Case D (16,180 years)		
I129	1.6E-02	1.2%	I129	4.4E-02	2.1%
Np237	5.6E-04	0.0%	Np237	4.0E-02	1.9%
Pa231	4.9E-04	0.0%	Pa231	6.0E-02	2.9%
Pb210	1.6E-02	1.3%	Pb210	1.5E-02	0.7%
Ra226	1.2E+00	94.7%	Ra226	1.1E+00	51.4%
Rn222	1.4E-02	1.1%	Rn222	1.2E-02	0.6%
Tc99	2.1E-02	1.6%	Tc99	8.4E-01	40.3%
Total	1.3E+00	--	Total	2.1E+00	--
Case E (9,400 years)			Case E (9,400 years)		
Pb210	7.4E-01	1.3%	Pb210	7.4E-01	1.3%
Ra226	5.4E+01	96.5%	Ra226	5.4E+01	96.5%
Rn222	6.2E-01	1.1%	Rn222	6.2E-01	1.1%
Total	5.6E+01	--	Total	5.6E+01	--

Table PA-1.2: Peak Dose to MOP at 100 Meters in Sector I for Cases A through E

MOP Dose in Sector I Within 10,000 Years			MOP Dose in Sector I Within 20,000 Years		
Radionuclide	Dose (mrem/yr)	Contribution	Radionuclide	Dose (mrem/yr)	Contribution
Case A (10,000 years)			Case A (15,080 years)		
I-129	8.6E-02	20.8%	I-129	2.7E+00	86.6%
Pb-210	4.1E-03	1.0%	Pb-210	4.7E-03	0.2%
Ra-226	3.2E-01	76.6%	Ra-226	3.9E-01	12.6%
Rn-222	4.9E-03	1.2%	Rn-222	5.3E-03	0.2%
Total	4.2E-01	--	Total	3.1E+00	--
Case B (4,180 years)			Case B (15,740 years)		
Ra-226	1.1E+00	67.9%	Ra-226	1.4E+00	77.5%
Tc-99	2.4E-01	15.0%	Tc-99	1.7E-01	9.0%
I-129	2.0E-01	12.4%	I-129	1.5E-01	7.9%
Rn-222	4.0E-02	2.5%	Rn-222	5.2E-02	2.8%
Total	1.6E+00	--	Total	1.9E+00	--
Case C (7,360 years)			Case C (15,500 years)		
I-129	1.8E-01	9.2%	I-129	1.8E-01	8.3%
Pb-210	4.5E-02	2.3%	Pb-210	5.0E-02	2.3%
Ra-226	1.5E+00	78.6%	Ra-226	1.8E+00	79.8%
Rn-222	5.5E-02	2.8%	Rn-222	5.8E-02	2.6%
Tc-99	1.3E-01	6.9%	Tc-99	1.5E-01	6.8%
Total	1.9E+00	--	Total	2.2E+00	--
Case D (9,840 years)			Case D (15,580 years)		
I-129	1.9E-02	5.8%	I-129	7.0E-02	12.7%
Pb-210	1.1E-02	3.3%	Pb-210	1.6E-02	2.9%
Ra-226	2.9E-01	86.2%	Ra-226	4.3E-01	77.2%
Rn-222	1.4E-02	4.2%	Rn-222	2.0E-02	3.7%
Tc-99	1.7E-03	0.5%	Tc-99	1.8E-02	3.3%
Total	3.3E-01	--	Total	5.5E-01	--
Case E (9,400 years)			Case E (15,060 years)		
I-129	1.6E-01	1.1%	I-129	8.0E+00	41.6%
Pb-210	4.9E-01	3.4%	Pb-210	3.9E-01	2.0%
Ra-226	1.3E+01	90.7%	Ra-226	1.0E+01	53.5%
Rn-222	6.2E-01	4.4%	Rn-222	5.0E-01	2.6%
Total	1.4E+01	--	Total	1.9E+01	--

Table PA-1.3: Peak Dose to MOP at 100 Meters in Sector B for Other Cases Presented in Section 5.6.6

MOP Dose in Sector B Within 10,000 Years			MOP Dose in Sector B Within 20,000 Years		
Radionuclide	Dose (mrem/yr)	Contribution	Radionuclide	Dose (mrem/yr)	Contribution
No Closure Cap (9,800 years)			No Closure Cap (15,060 years)		
I-129	5.3E-02	2.6%	I-129	1.6E+00	44.5%
Pb-210	2.2E-02	1.1%	Pb-210	2.6E-02	0.7%
Ra-226	1.6E+00	79.2%	Ra-226	1.9E+00	53.0%
Tc-99	3.3E-01	16.0%	Tc-99	1.4E-02	0.4%
Total	2.1E+00	--	Total	3.5E+00	--
Ten Times Sulfate (10,000 years)			Ten Times Sulfate (12,140 years)		
I-129	1.7E-01	9.7%	I-129	2.0E-01	4.0%
Pb-210	2.0E-02	1.2%	Pb-210	1.7E-02	0.3%
Ra-226	1.5E+00	84.8%	Ra-226	1.2E+00	24.1%
Rn-222	1.7E-02	1.0%	Rn-222	1.4E-02	0.3%
Tc-99	5.6E-02	3.2%	Tc-99	3.5E+00	69.9%
Total	1.7E+00	--	Total	5.1E+00 (a)	--
No Sulfate Case (10,000 years)			No Sulfate Case (15,600 years)		
I-129	1.9E-02	2.2%	I-129	3.1E-02	1.3%
Pb-210	1.1E-02	1.3%	Pb-210	2.9E-02	1.2%
Ra-226	7.9E-01	95.1%	Ra-226	2.1E+00	89.6%
Rn-222	9.0E-03	1.1%	Rn-222	2.4E-02	1.0%
Tc-99	1.6E-03	0.2%	Tc-99	1.5E-01	6.3%
Total	8.3E-01	--	Total	2.3E+00	--
Synergistic Case (6,380 years)			Synergistic Case (15,760 years)		
I-129	4.9E-01	2.8%	I-129	1.7E+00	6.2%
Ra-226	1.7E+01	94.9%	Ra-226	2.6E+01	91.8%
Tc-99	2.4E-01	1.3%	Tc-99	2.8E-01	1.0%
Total	1.8E+01	--	Total	2.8E+01	--
Oxidized Walls (860 years)			Oxidized Walls (15,820 years)		
I-129	2.5E-03	0.6%	I-129	1.2E-01	4.6%
Pa-231	3.2E-08	0.0%	Pa-231	2.6E-02	1.1%
Ra-226	2.9E-11	0.0%	Ra-226	2.3E+00	92.8%
Tc-99	4.3E-01	99.4%	Tc-99	9.6E-03	0.4%
Total	4.3E-01	--	Total	2.5E+00	--
Increased Saltstone Conductivity (9,860 years)			Increased Saltstone Conductivity (15,680 years)		
I-129	2.0E-01	3.7%	I-129	4.4E-01	4.1%
Pa-231	1.2E-03	0.0%	Pa-231	1.2E-01	1.1%
Ra-226	5.1E+00	95.5%	Ra-226	9.9E+00	92.0%
Tc-99	1.3E-02	0.2%	Tc-99	1.6E-01	1.5%
Total	5.4E+00	--	Total	1.1E+01	--

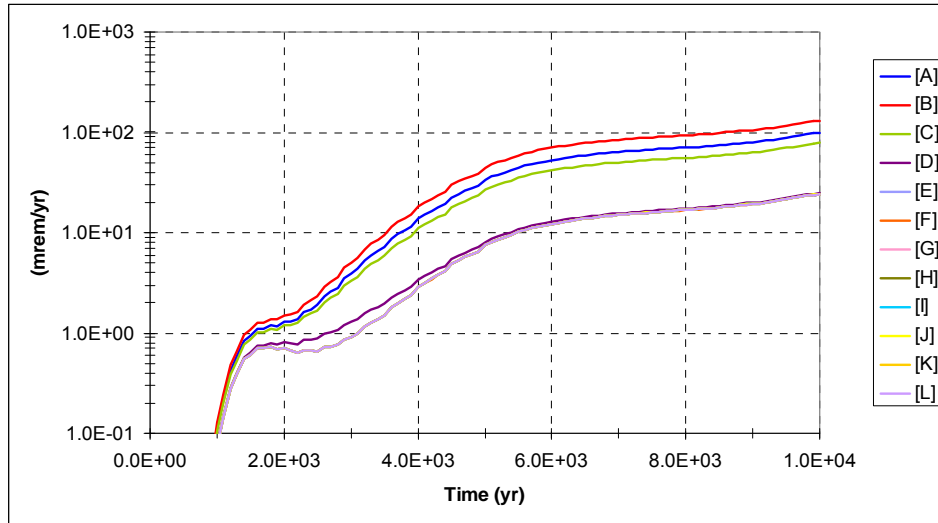
(a) Figure 5.6-81 indicates the peak dose as 5.1 mrem/yr; not 4.8 mrem/yr as stated in PA Table 5.6-19.

Table PA-1.4: Peak Dose to MOP at 100 Meters in Sector I for Other Cases Presented in Section 5.6.6

MOP Dose in Sector I Within 10,000 Years			MOP Dose in Sector I Within 20,000 Years		
Radionuclide	Dose (mrem/yr)	Contribution	Radionuclide	Dose (mrem/yr)	Contribution
No Closure Cap (10,000 years)			No Closure Cap (15,060 years)		
I-129	9.0E-02	15.3%	I-129	3.0E+00	83.7%
Pb-210	1.6E-02	2.7%	Pb-210	1.8E-02	0.5%
Ra-226	4.5E-01	76.9%	Ra-226	5.5E-01	15.1%
Rn-222	2.0E-02	3.4%	Rn-222	2.1E-02	0.6%
Tc-99	9.7E-03	1.6%	Tc-99	1.6E-03	0.0%
Total	5.9E-01	--	Total	3.6E+00	--
Ten Times Sulfate (2,420 years)			Ten Times Sulfate (12,600 years)		
I-129	8.7E-01	98.6%	I-129	3.5E-01	24.5%
Pb-210	4.1E-04	0.0%	Pb-210	2.8E-02	2.0%
Ra-226	1.1E-02	1.3%	Ra-226	9.0E-01	63.9%
Rn-222	5.4E-04	0.1%	Rn-222	3.5E-02	2.5%
Tc-99	7.3E-05	0.0%	Tc-99	8.0E-02	5.6%
Total	8.9E-01	--	Total	1.4E+00	--
No Sulfate Case (10,000 years)			No Sulfate Case (15,600 years)		
I-129	2.3E-02	9.9%	I-129	4.6E-02	7.6%
Pb-210	7.2E-03	3.1%	Pb-210	1.9E-02	3.1%
Ra-226	1.9E-01	83.0%	Ra-226	5.0E-01	82.5%
Rn-222	9.0E-03	3.9%	Rn-222	2.4E-02	3.9%
Tc-99	1.8E-04	0.1%	Tc-99	1.6E-02	2.7%
Total	2.3E-01	--	Total	6.1E-01	--
Synergistic Case (10,000 years)			Synergistic Case (Peak Dose at 17,320 years)		
I-129	1.7E+00	83.2%	I-129	3.0E+00	55.6%
Ra-226	2.2E-01	10.6%	Ra-226	9.2E-01	17.0%
Tc-99	1.3E-01	6.1%	Tc-99	1.5E+00	27.3%
Total	2.1E+00	--	Total	5.4E+00	--
Oxidized Walls (10,000 years)			Oxidized Walls (15,080 years)		
I-129	7.2E-02	72.2%	I-129	2.3E+00	96.7%
Ra-226	2.8E-02	27.6%	Ra-226	7.7E-02	3.3%
Total	1.0E-01	--	Total	2.3E+00	--
Increased Saltstone Conductivity (10,000 years)			Increased Saltstone Conductivity (15,040 years)		
I-129	2.4E-01	80.3%	I-129	3.8E+00	95.7%
Ra-226	5.8E-02	19.6%	Ra-226	1.7E-01	4.3%
Total	3.0E-01	--	Total	3.9E+00	--

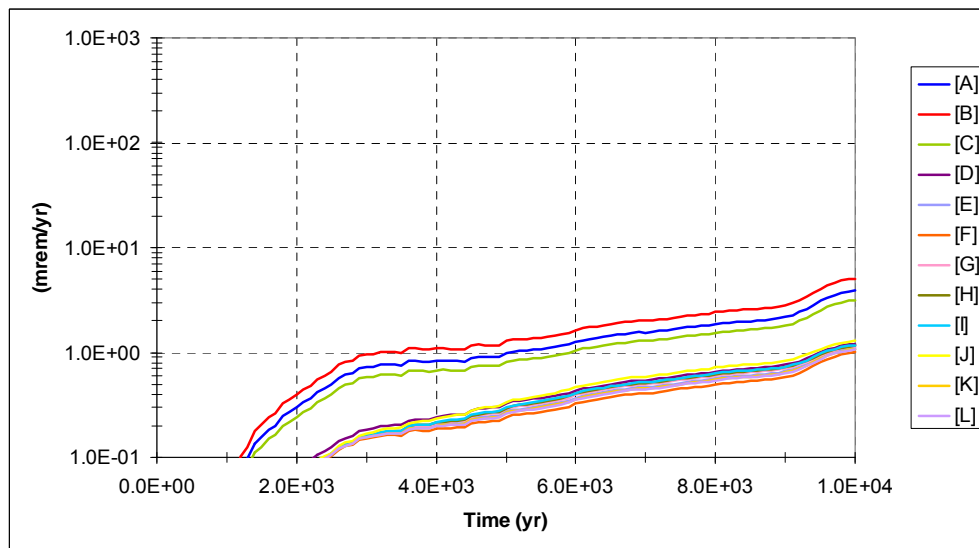
<p><u>PA-2</u></p>	<p>Probabilistic sensitivity analyses were not provided for cases representing bulk saltstone degradation.</p> <p><u>Basis</u></p> <p>Probabilistic sensitivity analyses were performed only for Cases A and C. Although Case C represents a fast flow pathway through saltstone, neither Case A nor Case C represents degradation of the bulk saltstone matrix. Case E, which represents saltstone degradation, was not included in the sensitivity analysis. Dose sensitivities in a case with degraded saltstone are expected to be different from the sensitivities in a case without degraded saltstone. For example, because chemical transitions would be achieved earlier in a case in which bulk saltstone has a greater hydraulic conductivity, parameters affecting the transport of radionuclides sensitive to pH transitions in saltstone may have a greater effect on dose. Similarly, parameters related to slower-moving radionuclides (e.g., plutonium) may have a more significant effect on dose in a case in which more water moves through the bulk saltstone. The sensitivity of these parameters is important to identifying issues that should be tracked during monitoring.</p> <p><u>Path Forward</u></p> <p>Provide a probabilistic sensitivity analysis for a case that reflects saltstone degradation, or explain why the sensitivity analyses performed in the PA are expected to reflect the sensitivities of dose in a case that reflects saltstone degradation. If a new sensitivity analysis is performed, it should be consistent with any modifications made in response to the comments in this document.</p>
<p><u>RESPONSE PA-2:</u></p> <p>This response provides results for the probabilistic uncertainty and sensitivity analysis for the severely degraded saltstone Case E over 10,000 years. Degraded saltstone is assumed to take the form of cracked grout and has been modeled by increasing its hydraulic conductivity to a value of 1.7E-3 cm/sec.</p> <p>As emphasized in SDF PA Section 5.6.4, the results of the uncertainty and sensitivity model are not intended to predict future potential dose for comparison to performance objectives (the SDF PORFLOW model has been used for assessment of peak doses versus performance objectives). Rather, the goal of this SDF modeling is to characterize the context of uncertainty and sensitivity surrounding the PA calculations involving doses to MOP exposed via groundwater. Case E is an extreme case based on the very high hydraulic conductivity value used, which is approximately two orders of magnitude higher than backfill soil. The relative influence of Case E on the composite "AllCases" result is evident by comparing Figure PA-2.1 and Figure PA-2.2 below.</p>	

**Figure PA-2.1: Peak Mean Dose to a MOP, Any Sector- Case E
(modified from Figure 5.6-38 in SDF PA)**



Note: Dose from Sector L directly overlies Sector J dose.

**Figure PA-2.2: Peak Mean Dose to a MOP, Any Sector- All Cases
(modified from Figure 5.6-39 in SDF PA)**



Following the uncertainty modeling methodology described in the SDF PA Section 5.6.4, the uncertainty associated with an extremely degraded bulk saltstone matrix (Case E) was determined by simulating 5,000 separate realizations, each sampling a unique stochastic input parameter. In this way, uncertainty from the input parameters is propagated through to the dose calculation.

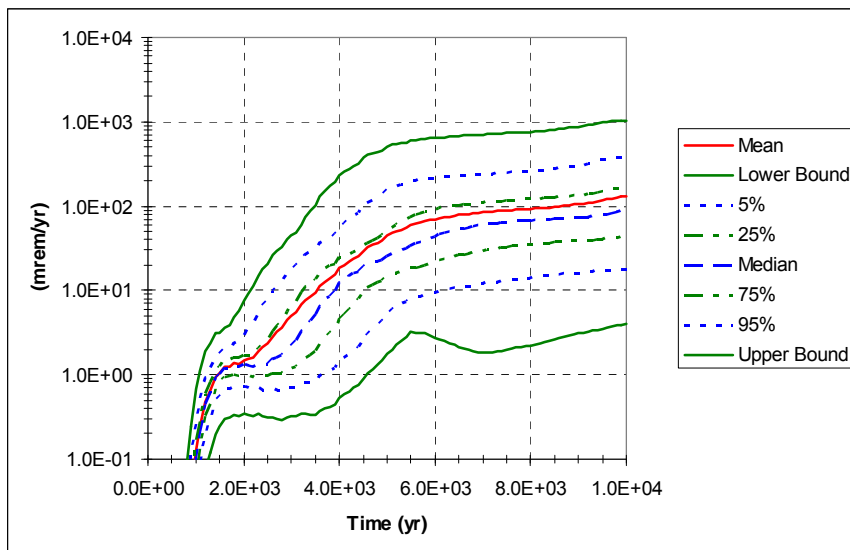
An alternative way to describe the uncertainty associated with a degraded bulk saltstone is by looking at key model endpoints which drive the dose and the uncertainty associated with dose. Table PA-2.1 provides a summary of selected endpoints for Case E.

Table PA-2.1: Summary for Selected SDF Endpoint – Case E Only

Endpoint	Mean	Median (50th percentile)	95th Percentile
Maximum MOP dose at any Sector within 10,000 years (mrem/yr)	131.8	89.6	387.0
Maximum MOP dose at Sector B within 10,000 years (mrem/yr)	131.8	89.6	387.0
Maximum MOP dose at Sector J within 10,000 years (mrem/yr)	24.4	16.1	73.4
Maximum aqueous concentration of Tc-99 at Sector B within 10,000 years (pCi/L)	2.7	1.7	8.9
Maximum aqueous concentration of Tc-99 at Sector J within 10,000 years (pCi/L)	0.1	0.1	0.3
Maximum aqueous concentration of I-129 at Sector B within 10,000 years (pCi/L)	31.0	30.0	59.6
Maximum aqueous concentration of I-129 at Sector J within 10,000 years (pCi/L)	1.1	1.1	2.1
Maximum aqueous concentration of Ra-226 at Sector B within 10,000 years (pCi/L)	129.0	91.5	371.0
Maximum aqueous concentration of Ra-226 at Sector J within 10,000 years (pCi/L)	4.5	3.2	13.0

Table PA-2.1 indicates that the maximum MOP dose at any sector within 10,000 years occurs in Sector B. The maximum MOP dose at Sector J within 10,000 years is also provided. While the dose to Sector J is presented in the table, only Sector B results will be discussed since it is the location of the maximum MOP dose. The uncertainty associated with the dose to Sector B is provided in Figure PA-2.3. Based on the results of the figure, by the end of the performance period, there is an order of magnitude uncertainty in dose to the MOP for Sector B. Referring back to Table PA-2.1, most of Sector B's peak dose as well as the uncertainty in Sector B, is from the contribution from Ra-226.

Figure PA-2.3: Statistical Time History of a MOP Dose, Sector B within 10,000 Years – Case E



Deviating from the methodology presented in the SDF PA Section 5.6.5 slightly, the GoldSim built-in multi-variate analysis tool was used directly (instead of using the gradient boost methodology) to determine which variables have distributions that exert the greatest influence on the response. The response, in this case, is the dose to the MOP to Sector B within 10,000 years for the degraded saltstone case. The influence of the 700 stochastic parameters included in the model were evaluated. The GoldSim built-in multi-variate analysis tool returned an R^2 value of 0.75, indicating that 75% of the variability is explained from the stochastic parameters analyzed. The three parameters with the most influence on the dose to Sector B are included in Table PA-2.2 below. Sensitivity index values below 4 are not reported.

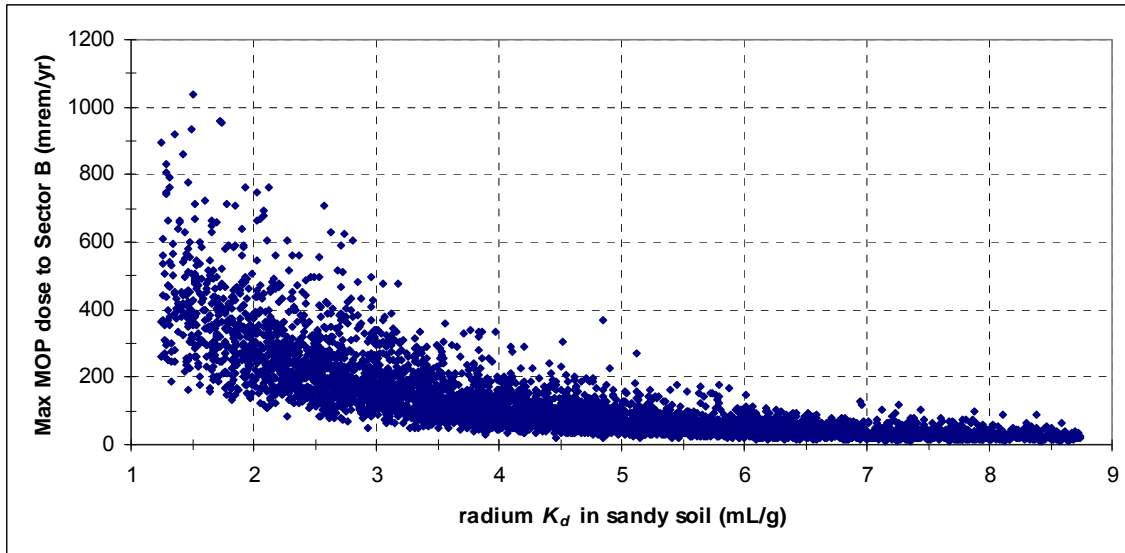
Table PA-2.2: Most Sensitive Parameters for the Max. MOP dose at Sector B within 10,000 years.

Input Parameter	SI Rank	Sensitivity Index
K_d for radium in sandy soil	1	69
Unsaturated zone thickness - FDCs	2	10
Vegetable consumption – local fraction	3	4

SI = Sensitivity Index

The primary driver of the uncertainty for the dose to Sector B within 10,000 years is the K_d for radium in sandy soil. This is expected because radium is the radionuclide contributing the most to the total dose to this sector. Figure PA-2.4 is provided to demonstrate the dependency of the dose for this sector on radium K_d in sandy soil. When a high radium K_d is sampled (e.g., > 4 mL/g), the dose to Sector B remains low. In contrast, as radium K_d in sandy soil decreases to values less than 4mL/g, the uncertainty in the maximum dose to Sector B increases.

Figure PA-2.4. Correlation of Max MOP dose to Sector B to radium K_d in sandy soil



The other two parameters that influence the dose to Sector B include the unsaturated zone thickness below the FDCs and the amount of locally grown vegetables consumed by the MOP. As the unsaturated zone thickness decreases, the uncertainty in dose increases, whereas as more locally grown vegetables are consumed by the MOP, the uncertainty in their dose increases.

Although the dose sensitivities in a case with degraded saltstone are expected to be different from the sensitivities in a case without degraded saltstone, this sensitivity analysis demonstrates that the radium K_d for sandy soil becomes the most important factor to dose for this case, indicating that parameters independent of the cracked waste form (and those parameters that occur downstream from the waste form, like unsaturated zone thickness and consumption rate of locally grown vegetables) have greater influence.

PA-3

The determination of key radionuclides described in Section 5.2.2 of the PA may not have captured all of the risk significant radionuclides. The determination of key radionuclides is significant to the results of the PA because many of the analyses used to support the PA only include the key radionuclides (e.g., the PORFLOW analyses for Cases B-E).

Basis

The determination of the key radionuclides was based on the all-pathways doses calculated for the Case A scenario. In this case, it is assumed that there is no degradation or fracturing of the saltstone, and, consequently, there is very little water passing through the saltstone. These assumptions may be optimistic and may not adequately represent the actual performance of the disposal system (see, e.g., Saltstone Performance comments). In the cases where degradation and fracturing of the saltstone occur, other radionuclides may also be important contributors to dose. For example, Table 5.6-15: "Most Sensitive Parameters for Endpoints of Interest – Case C" lists the K_d values for plutonium in clayey and sandy soils as being important parameters, which

	<p>indicates that plutonium is an important radionuclide for Case C. Because Pu-238 happens to be a parent of the key radionuclide Ra-226, its transport was considered; however the process used in determining the key radionuclides (Section 5.2.2) did not identify this radionuclide, which indicates that the process may not be sufficient to capture all radionuclides that are potentially important to dose in reasonably foreseeable scenarios.</p> <p>In addition, the response to other comments may affect the dose modeling results. It is important to consider if changes made to the model as part of the response to other comments results in a significant dose from additional radionuclides (e.g., a dose above the 0.05 mrem/yr criteria used in Section 5.2.2 of the PA).</p> <p><u>Path Forward</u></p> <p>Determine if any additional radionuclides are significant contributors to dose in cases other than Case A, and if so, add these radionuclides to the key radionuclide list and provide the dose results. Evaluate whether changes made to the model based on the responses to other comments in this document results in a significant dose from any additional radionuclides. If so, add these radionuclides to the list of key radionuclides and provide the dose results.</p>
--	--

RESPONSE PA-3:

As discussed in the response to clarifying comment C-8, the key radionuclide determination was not used to screen radionuclides from the GoldSim model inventory list. The GoldSim model includes nearly all of the radionuclides included in the Base Case PORFLOW modeling (some of the radionuclides included in the SDF PA Section 3.3 inventory were not modeled in GoldSim because transport modeling was not required (e.g., their half-lives are so short they are only significant as a result of in-growth at the evaluation location). The radionuclides included in the abridged GoldSim transport inventory (listed in SDF PA Appendix Table I6-1) were used for all GoldSim modeling results (e.g., the UA, SA and benchmarking). This approach ensured that GoldSim model results included the less-mobile radionuclides even if they were not determined to be key radionuclides.

The benchmarking in the SDF PA Section 5.6.2.3 included comparison of the peak doses between the two models. The dose comparisons for Cases A through E in the SDF PA Section 5.6.2.3 show good agreement between the PORFLOW and GoldSim models' dose results. This agreement provides assurance that less-mobile radionuclides that were determined not to be key radionuclides (and therefore not included in the PORFLOW alternate case runs) do not present a significant dose risk in 10,000 years and not including them in the PORFLOW alternate case runs is acceptable. If these radionuclides posed a potentially significant dose contribution in 10,000 years, it would have been apparent in the GoldSim dose results. Further discussion regarding the benchmarking analysis is provided in the response to RAI PA-4.

Since the GoldSim model results include the less-mobile radionuclides and did not identify any radionuclides of concern different from the key radionuclides (identified through the PORFLOW Base Case), it is reasonable to conclude that there are not any additional radionuclides that are significant contributors to dose in cases other than Case A that are not already addressed through the key radionuclide list.

<p><u>PA-4</u></p>	<p>Benchmarking based only on key radionuclides identified in the base-case analysis does not provide adequate support for the interpretation of alternate-case GoldSim model results.</p> <p><u>Basis</u></p> <p>As discussed in Section 5.6.2 of the PA, benchmarking was performed only for radionuclides that were significant to dose in the base case. Because the base case assumed very little water flow through the disposal units and waste form, the key radionuclides identified in the base case are all relatively mobile in cementitious materials and soils.</p> <p>The GoldSim model, which is not benchmarked for radionuclides important in other cases, may not represent transport of those radionuclides well. For example, divergence between the PORFLOW and GoldSim model results at 20,000 years is attributed to differences in plutonium transport (SRNL-TR-2009-00052).</p> <p>An understanding of the applicability of the GoldSim model to less-mobile radionuclides is needed to support an interpretation of the results of the GoldSim model in alternate cases. For example, the peak of the mean dose for Case C in GoldSim within 20,000 years is 492 mrem/yr while in PORFLOW it is only 5.54 mrem/yr (SRR-CWDA-2009-00017). A better understanding of the applicability of the GoldSim model to less-mobile radionuclides would provide a better basis for determining how to interpret the GoldSim results.</p> <p><u>Path Forward</u></p> <p>Explain the applicability of the GoldSim model to radionuclides that are important in alternate cases but were not used in the benchmarking analysis, or provide benchmarking of the less mobile radionuclides.</p>
<p><u>RESPONSE PA-4:</u></p> <p>As discussed in the response to clarifying comment C-8, the key radionuclide determination was not used to screen radionuclides from the GoldSim model inventory list. The GoldSim model includes nearly all of the radionuclides included in the Base Case PORFLOW modeling. Some of the radionuclides included in the SDF PA Section 3.3 inventory were not modeled in GoldSim because transport modeling was not required (e.g., their half-lives are so short they only are significant as a result of in growth at the evaluation location). The radionuclides included in the abridged GoldSim transport inventory (listed in Appendix Table I6-1 of the SDF PA) were used for all GoldSim modeling results (e.g., the benchmarking analysis, the uncertainty analyses, and the sensitivity analyses). This approach ensured that GoldSim model results included the less-mobile radionuclides even if they were not determined to be key radionuclides.</p> <p>As stated in the SDF PA Section 5.6.2.2, “the purpose of the benchmarking is to ensure reasonable transport modeling agreement between the SDF PORFLOW and GoldSim models, not to calibrate the radionuclide concentration results between them. Although every attempt was made to ensure transport modeling was as similar as possible for the two models, the different solution formulations of the two codes ensured that there would be some differences</p>	

between the two models. Before benchmarking began, the PORFLOW results were used to determine which radionuclides were most important to dose. It was found that the radionuclides of most importance to dose were Ra-226 and I-129 for Case A (see the SDF PA Section 5.2.2). However, Tc-99 was also analyzed in the benchmarking as it is highly mobile during transport when released from the waste form.” The benchmarking in the SDF PA Section 5.6.2.3 was performed not just on concentrations for significant radionuclides, but also for peak doses between the two models. The dose comparison benchmarking for Cases A through E in the SDF PA Section 5.6.2.3 shows good agreement between the PORFLOW and GoldSim models’ dose results. This agreement provides assurance that less mobile radionuclides that were determined not to be key radionuclides (and therefore not included in the PORFLOW alternate case runs) do not present a significant dose risk in 10,000 years and not including them in the PORFLOW alternate case runs is acceptable. If these radionuclides posed a potentially significant dose contribution in 10,000 years, it would have been apparent in the GoldSim dose results.

The fact that the peak of the mean dose for Case C in GoldSim within 20,000 years is 492 mrem/yr while the PORFLOW deterministic dose is only 5.54 mrem/yr (per SDF PA) can be explained as follows. The GoldSim probabilistic peak of the mean dose is much higher than the PORFLOW deterministic dose due to modeling differences and the stochastic distributions associated with some of the less mobile radionuclides, not due to the less mobile radionuclides not being included in the PORFLOW alternate case runs. The GoldSim model, as stated at the end of the SDF PA Section 5.6.4, includes a direct transfer path from the waste zone to the saturated zone for Case C to simulate the fast flow path. Thus, the less mobile radionuclides through the disposal unit concrete, such as Pu-239, enter the saturated zone with no retardation from the concrete. In the PORFLOW model not all of the flow traverses directly into the saturated zone in Case C, but is computed based on the size of the model elements and their hydraulic properties. As can be seen in the Case C partial dependence plots (the SDF PA Section 5.6.5.5), the wide distributions used for some plutonium associated stochastics (e.g., soil K_d values) can have a significant impact on the Case C GoldSim results, such that the results are not driven as much by the presence of plutonium but rather by the amount of retardation that is assumed to be provided by the soil. Realizations at the extreme low end of the plutonium soil K_d distribution can significantly impact the peak of the mean dose for Case C, as illustrated below.

To demonstrate how significantly the plutonium associated stochastic on K_d in soil impacts the Case C GoldSim results, additional GoldSim runs were made with two different plutonium K_d distributions in sandy and clayey soils (used only for the purposes of this sensitivity analysis). The GoldSim model using the sandy and clayey soil K_d distributions for plutonium as described in the SDF PA Section 5.6.3.3 was run with 1,000 realizations (the PA analysis used 5,000 realizations). Another GoldSim run was made with 1,000 realizations but with tighter distributions of the sandy and clayey soil K_d for plutonium. The distribution of the sandy soil K_d for plutonium was tightened by increasing the minimum value from 67.5 mL/g to 200 mL/g and reducing the maximum from value from 473.5 mL/g to 360 mL/g. This tightened distribution resulted in a median value of 268 mL/g which is essentially the deterministic value of 270 mL/g. The distribution of the clayey soil K_d for plutonium was tightened by increasing the minimum value from 2,950 mL/g to 4,500 mL/g and reducing the maximum value from 8,850 mL/g to 7,700 mL/g. This tightened distribution resulted in a median value of 5,886 mL/g which is essentially the deterministic value of 5,900 mL/g. The results from these two GoldSim runs are presented in Table PA-4.1 and show the significance that the plutonium K_d distribution has on the Case C results.

Table PA-4.1: Case C Results for Different Plutonium Soil K_d Distributions

GoldSim Runs	Peak MOP Dose in Sector B				Peak MOP Dose Sector J			
	10,000 years		20,000 years		10,000 years		20,000 years	
	Mean	Median	Mean	Median	Mean	Median	Mean	Median
PA Table 5.6-13 (5,000 realizations)	12.4	8.6	262	160	9.4	2.3	431	212
PA K_d Distribution (1,000 realizations)	11.8	8.7	263	159	8.0	2.3	440	221
Tightened K_d Distribution (1,000 realizations)	8.8	8.3	40.0	20.0	2.5	2.0	58.2	18.3

PA-5

Additional information is needed about the benchmarking factors and other GoldSim parameter adjustments based on benchmarking to the PORFLOW model.

Basis

The benchmarking parameters described in the benchmarking summary (Section 5.6.2) of the PA include (1) the factors in Table 5.6-1, (2) adjustments to the K_d values for Tc, (3) the saturated zone flow rate, (4) a factor applied to saturated zone cells to account for “dilution” shown in PORFLOW (Section 5.6.2.3.2) (5) the plume correction factor, and (6) the contribution of Vaults 1 and 4 to unexpected regions (Section 5.6.2.3.2).

It is unclear whether this list is exhaustive or whether other benchmarking factors or other adjustments were applied to the GoldSim model. For example, Section 5.6.3.8.1 of the PA indicates that the thickness of the saturated zone and the development of its distribution were based, in part, on the results of the benchmarking process; however, it is unclear whether this adjustment corresponds to the factor applied to saturated zone cells listed in (4), above. Based on the summary in the PA, and the description in the “Saltstone Disposition Facility Stochastic Transport and Fate Model Benchmarking” (SRNL-TR-2009-00052), the meaning of benchmarking factor (4), and the reference to PORFLOW “dilution” in the description of benchmarking factor (4) is unclear. It also is not clear how benchmarking factor (4) was derived, what its value is, and to which parameter in the GoldSim model it is applied.

In addition, the physical basis for some of the benchmarking factors is not clear. For example, while a reasonable explanation is provided for the plume correction factor and contribution of Vaults 1 and 4 to unexpected regions in Section 5.6.2.3.2, no explanation is provided of the physical basis for the benchmarking factors provided in Table 5.6-1. In some cases, the factors in Table 5.6-1 adjust the flow by an order of magnitude. An

adequate understanding of the benchmarking adjustments is important to understanding the basis for the GoldSim model and the resulting uncertainty analyses.

Path Forward

Provide a list of all benchmarking factors and any other parameter adjustments that were made based on benchmarking results for each case, including the final value of the factor or magnitude of the adjustment. Describe how each factor applies to the conceptual model (e.g., indicate whether the factor adjusts a flow rate, accounts for dispersion, or adjusts an aspect of the structural model such as the saturated zone thickness). Note the type of analysis used to calculate each benchmarking factor or parameter adjustment (e.g., benchmarking based on flux between the unsaturated and saturated zone or concentrations at 100 m). Provide a description of the meaning of benchmarking factor (4) in the basis of this comment. Provide an explanation of the physical basis of benchmarking factors that adjust the PORFLOW output by an order of magnitude or more.

RESPONSE PA-5:

The benchmarking between the PORFLOW and GoldSim models was conducted in two distinct phases to capture specific model parameters associated with each phase. The two phases were: 1) contaminant flux entering the water table from each disposal unit type and 2) concentration at 100m within each of the sectors. The success of the benchmarking effort was shown by the comparison of the dose to the MOP at 100m in the various sectors between doses calculated based on PORFLOW concentrations and doses calculated based on the concentrations computed by the GoldSim transport model.

The first phase focused on the contaminant flux entering the water table below each of the three different disposal unit types (Vault 1, Vault 4, and FDCs). Each disposal unit type has differing disposal cell geometries and characteristics that result in different flow values that are computed by PORFLOW for each case. As stated in the SDF PA Section 5.6.2.3.1, and repeated below, the flow values abstracted from the PORFLOW runs are identified within the GoldSim model as:

- PF_Flowgrout – the flow of liquid through saltstone
- PF_FlowWall – the flow of liquid through the wall of the disposal unit
- PF_Flowdirt – the flow of liquid in the soil region adjacent to the wall
- PF_FlowUZ – the flow of liquid in the unsaturated zone below the disposal unit

For each case, Cases A through E, and each disposal unit type, the flow values were adjusted by use of multiplicative factors in an attempt to reproduce the flux behavior shown by PORFLOW. The results of this portion of the benchmarking are shown in PA Figures 5.6-1 through 5.6-9.

The flow values used in the GoldSim model were abstracted from the PORFLOW results as described in the SDF PA Section 4.4.4.2. This flow abstraction converts the 2-D flow fields calculated using PORFLOW to the 1-D flow fields used in the GoldSim calculations. This abstraction process averages the flow velocity (cm/yr) obtained from PORFLOW in the various horizontal and vertical nodes or cells for each of the model regions at each time period used by PORFLOW. The PF_Flowgrout and PF_Flowdirt data elements are each comprised of a matrix of 20 by 44 entries representing 20 flow values in vertical slices through the saltstone

and the soil adjacent to the wall respectively for each of the 44 PORFLOW time periods. Data element PF_FlowWall is a 1 by 44 vector which has a single flow velocity through the disposal unit wall for each time step. Data element PF_FlowUZ is comprised of a 4 x 44 matrix representing four flow velocities in the vertical direction for each time period. Table PA.5-1 illustrates the “compression” of PORFLOW data for input into GoldSim.

Table PA.5-1: Flow Velocity Nodes per Time Period in PORFLOW and GoldSim

Disposal Unit (model used)	Grout (cm/yr)	Wall (cm/yr)	Dirt (cm/yr)	UZ¹ (cm/yr)
Vault 1 (PORFLOW)	1,113	150	444	852
Vault 4 (PORFLOW)	1,533	224	456	1,236
FDC (PORFLOW)	1,872	264	1,080	1,275
All types (GoldSim)	20	1.0	20	4.0

¹UZ = Unsaturated Zone

The benchmarking modified the flow velocities by applying multiplicative factors to the respective data elements as shown in PA Table 5.6-1. Recognizing that the flow abstraction is reducing the number of velocity nodes used in PORFLOW by averaging the PORFLOW velocities, it is not unreasonable to require a relatively large benchmarking factor adjustment.

The only other benchmarking adjustment utilized for the flux comparison is the treatment of the K_d value for technetium, which is addressed in the SDF PA Section 5.6.2.3.

The second phase of the benchmarking effort focused on the concentrations at 100m in the various sectors. While PORFLOW uses data from the GSA database to simulate the transport of contaminants via the aquifers to the 100m point, a representative saturated zone velocity value was determined based on the timing of the movement of a trace element computed by PORFLOW. Thus, the saturated zone flow rate is not a benchmarking factor; but rather a modeling parameter to transport contaminants to the 100m location as discussed in the SDF PA Section 5.6.3.8.2. PORFLOW computes the concentrations of the radionuclides in the three aquifers associated with Z-Area, the UTR-UZ, the UTR-LZ, and the Gordon Aquifer at the 100m distance in each sector. The highest concentration of any of the three aquifers at each time step and 100m sector location is used to determine the dose to the MOP at each of the 100m sector locations. To simulate the attenuation provided by the aquifers, GoldSim uses the disposal units width normal to the flow, defined as the width of the saturated zone, “SatWidth”, and the thickness of the saturated zone, defined as 12m, “SatThickness”. The use of SatWidth and SatThickness is to compute concentration in the GoldSim model and are not benchmarking factors. These model parameters are discussed in the SDF PA Section 5.6.3.8.1. The statement in the SDF PA Section 5.6.3.8 acknowledges that the parameters of saturated zone velocity, saturated zone width, and saturated zone thickness were developed during GoldSim benchmarking but are not considered benchmarking factors.

The contribution from the various disposal units to the 100m concentrations in each of the 12 sectors were developed using the GoldSim plume function which is described in the SDF PA Section 4.4.4.2.2 and in the SDF PA reference SRNL-TR-2009-00051. This initial contribution assessment was based on the streamline paths developed from PORFLOW which are shown in PA Figure 4.4-70. Tables PA-5.2 and PA-5.3 identify the disposal units that contribute to each of the 12 sectors based on the development of the plume function using the PORFLOW streamline paths.

Table PA-5.2: Disposal Unit Contributions to the Southern Sectors (Based on PORFLOW Streamlines)

Disposal Unit	Sector A	Sector B	Sector C	Sector D	Sector E	Sector F
V1	x	x	x	x		
V4	x	x	x			
V14A	x	x				
V14B	x	x				
V14C	x	x	x			
V14D	x	x	x			
V15A	x	x				
V15B	x	x				
V16A	x	x	x			
V16B	x	x	x			
V16C	x	x	x			
V16D	x	x	x			
V17A			x	x		
V17B			x	x		
V17C					x	
V17D				x	x	
V18A		x	x	x		
V18B		x	x	x		
V18C		x	x	x		
V18D		x	x	x		
V19A					x	x
V19B					x	x
V19C					x	x
V19D					x	x
V20A				x	x	
V20B				x	x	
V21A				x	x	
V21B				x	x	
V21C				x	x	
V21D				x	x	

Table PA-5.3: Disposal Unit Contributions to the Northern Sectors (Based on PORFLOW Streamlines)

Disposal Unit	Sector G	Sector H	Sector I	Sector J	Sector K	Sector L
V2A					X	X
V2B					X	X
V5A	X	X				
V5B	X	X				
V5C	X	X				
V5D	X	X				
V6A	X	X	X			
V6B	X	X	X			
V6C	X	X	X			
V6D	X	X	X			
V7A			X	X		
V7B			X	X		
V7C			X	X		
V7D			X	X		
V8A	X					
V8B	X	X				
V8C	X	X				
V8D	X	X				
V9A	X	X	X			
V9B		X	X			
V9C		X	X			
V9D		X	X			
V10A				X	X	
V10B				X	X	
V10C				X	X	
V10D					X	X
V11A	X	X				
V11B	X	X	X			
V11C	X	X	X			
V11D		X	X			
V12A				X	X	X
V12B					X	X
V12C				X	X	X
V12D						X
V13A					X	X
V13B						X

Following the development of the plume function a benchmarking factor of 0.5 was applied to all of the GoldSim computed 100m concentrations based on initial comparison of the PORFLOW generated concentrations. Further benchmarking identified additional adjustments that are described below.

1. Adjustment for the Flow Divide

Benchmarking identified that a factor of 5 was required for the contribution from Vaults 7A through 7D in Sector J because of the flow divide shown in PA Figure 4.4-70. This benchmarking factor effectively multiplies the plume function value and the radionuclide concentration contribution by a factor of 5 for those disposal units in Sector J.

2. Vault 4 Contributions in Sectors A, B, and C

The Vault 4 contribution to the concentrations in Sectors A, B, and C were multiplied by 70, 140, and 70, respectively. These specific adjustments to the Vault 4 contribution are attributed to the width of the saturated zone applied to Vault 4 which was set equal to 600 feet, the length of Vault 4; as well as to align to the highest PORFLOW concentration values.

3. Additional Disposal Unit Contributions

The final benchmarking conducted on the 100m concentrations was to include contributions from specific disposal units to sectors that are not apparent based on the PORFLOW streamline paths shown in PA Figure 4.4-70. The radionuclide concentrations in the Southern Sectors E and F were increased by adding a contribution from Vault 1. This additional contribution is 2% from Vault 1 to Sector E and 1% from Vault 1 to Sector F. The radionuclide concentrations in the Northern Sectors G through L were increased by adding a contribution from the disposal units in the Southern Sectors. The radionuclide concentrations in Sectors G and H were increased by adding a contribution from Vault 1. The concentrations in Sectors G and H include 4% and 5% of the radionuclide concentrations from Vault 1, respectively. For Sectors I through L the radionuclide concentrations include 5% of the radionuclide concentrations computed in Sector A.

The resulting comparisons of PORFLOW concentrations to the GoldSim concentrations, modified as described above, are shown in the SDF PA Section 5.6.2.3.2.

PA-6

Results of analyses run to times beyond or far beyond the performance period appear to underestimate dose by excluding radionuclides and pathways based on their contribution to the base case analysis at 10,000 or 20,000 years. Although an estimate of the dose at extremely long times is not likely to be necessary for a compliance determination, it is important to understand the basis for any reported results and, when reporting the information, to note important limitations.

Basis

As discussed in Section 5.2.2, the selection of key radionuclides was based on the peak dose to a member of the public within 20,000 years in the base case. Because of the limited amount of water flowing through saltstone in the base case, the radionuclides causing an appreciable off-site dose within 20,000 years in the base case are all relatively mobile (i.e., Tc-99, I-129, Ra-226, Np-237, and Pa-231).

Section 5.5.1.5 indicates a peak dose associated with the key radionuclides is calculated through 40,000 years. However, it is not clear that it is appropriate to neglect the dose from less-mobile radionuclides that do not reach a member of the public within 20,000 years but may reach a member of the public within 40,000 years from the analysis. In addition, it is not clear if parents of the key

	<p>radionuclides were included in the 40,000-year analysis.</p> <p>Similarly, Section 5.6.4 reports doses from Case A run in GoldSim out to 450,000 years. Although an analysis of the dose at this very long time is not likely to be necessary for the demonstration of compliance in this case, it could cause confusion to report a dose that is a significant underestimate of the expected dose at very long times. Additional information would be necessary to evaluate whether the reported dose at 450,000 years is a reasonable estimate. For example, the parameters used in the flow and chemical models out to 450,000 years are not discussed. It appears the results reported for 450,000 years could be misinterpreted if the Case A flow parameters, which are based on the assumption that saltstone does not physically degrade, are not modified during the 450,000 year period. Furthermore, it is not clear if pathways and phenomena that were not considered in the base case or were determined to be insignificant contributors to dose in the base case at 10,000 years, but that may be more important at very long times (e.g., radon emanation, climate change, landform evolution) were included in the estimate of the dose at 450,000 years.</p> <p><u>Path Forward</u></p> <p>Revise the calculated dose at 40,000 years to reflect contributions from radionuclides that may have been transport-limited in the base case analysis but may reach a member of the public within 40,000 years. Provide the assumptions about the physical and chemical state of saltstone and the disposal units that were used in the 40,000 and 450,000 year analyses. Either explain how the reported dose in the 450,000 year analysis reported in Section 5.6.4 is expected to compare to the expected dose, considering potential doses from relevant radionuclides and pathways excluded from the analysis, or indicate that the 450,000 year dose should not be considered in the interpretation of results. The discussion of the 450,000 year analysis should clearly state limitations and assumptions.</p>
--	---

RESPONSE PA-6:

No screening was performed to remove radionuclides from the GoldSim model inventory list (as discussed in the response to clarifying comment C-8), therefore the calculated dose at 40,000 years does reflect contributions from radionuclides that may be transport-limited in the Base Case. The GoldSim model used for the uncertainty/sensitivity analyses in the SDF PA Section 5.6.4 includes nearly all of the radionuclides included in the Base Case PORFLOW modeling. Some of the radionuclides included in the SDF PA Section 3.3 inventory were not modeled in GoldSim because transport modeling was not required (e.g., their half-lives are so short they only are significant as a result of in growth at the evaluation location). The radionuclides included in the abridged GoldSim transport inventory (listed in PA Appendix Table I6-1) were used for all GoldSim modeling results (e.g., benchmarking, uncertainty analyses, and sensitivity analyses). This approach ensured that GoldSim model results included the less mobile radionuclides even if they were not determined to be key radionuclides.

The 40,000 year PORFLOW model documented in the SDF PA Section 5.5.1.5 and the 450,000 year GoldSim probabilistic model documented in the SDF PA Section 5.6.4 both assume the same rates for physical degradation of the saltstone and disposal units as was assumed for the 20,000 year model run. The timing of the physical property transitions for the longer timescale model analyses are consistent with the 20,000 year model run. The timing of key model changes are indicated by disposal unit type in PA Table 4.4.6, Table 4.4.7, and Table 4.4.9 for Vault 1, Vault 4, and FDCs, respectively. The chemical transition times indicated in Table 4.2-17 for saltstone and disposal unit concrete are also utilized in the 40,000 year and 450,000 year models.

It should be noted that the long term results presented in the SDF PA Section 5.6.4 are meant only to help identify the model's sensitivity to certain parameters and their uncertainty, and are provided for trend spotting only. The dose results presented in this section should not be compared to performance objectives, and the limitations of modeling out hundreds of thousands of years must be considered when reviewing these results.

Inventory (IN)

IN-1

The reported inventory of some of the radionuclides disposed of in Vaults 1 and 4 as of March 31, 2009 (X-CLC-Z-00027) exceeds the total inventory of these radionuclides assumed in the PA for these vaults (Tables 3.3-1 and 3.3-3 in the PA), even when accounting for the decay of these radionuclides to the year 2030.

Basis

As seen in the IN1-1 below, the inventory provided in Table 3.3-1 of the PA for Am-241 in Vault 1 and the inventories provided in Table 3.3-3 for Ni-59 and Ra-226 is less than the reported inventory disposed of to date (as reported in X-CLC-Z-00027).

Table IN1-1: Inventory Data for Selected Radionuclides

Radionuclide	Inventory in PA (decayed to 10/1/2030) (Ci)	Current SDF Inventory (as of 3/31/09) (Ci)	Current SDF Inventory (decayed 20 years) (Ci)
Vault 1			
Am-241	4.70E-04	5.83E-04	5.65E-04
Vault 4			
Ni-59	0.4	0.447	0.446
Ra-226	4.1	5.35	5.3

The calculation of the inventory in 2030 only accounted for decay and did not include ingrowth. Saltstone contains parent radionuclides for both Ra-226 and Am-241, so additional amounts of these radionuclides would ingrow over time.

Additionally, the PA states that the inventory was decayed to October 1, 2030, but the starting date of this calculation was not provided, so it is not clear exactly how many years of decay were assumed.

Path Forward

Provide the expected inventory for these radionuclides in Vaults 1 and 4. If the expected inventory is more than the inventory assumed in the PA, provide an updated estimate of the inventory of these radionuclides in Vaults 1 and 4 and the SDF decayed to October 1, 2030. Provide an assessment of the effect of the increased inventory on the dose. Provide the number of years of decay assumed in the inventory calculation.

RESPONSE IN-1:

The PA inventories for Ni-59 and Ra-226 disposal in the SDF were developed using waste tank inventories which were adjusted based on treatment processes. In some cases these waste tank sample analyses resulted in analytical detection limits. As material is added to the SDF disposal units, inventories will be developed using the current sample results from the SDF feed tank. This feed tank sample analysis, for certain radionuclides, will result in analytical detection limits. Since analytical detection limits are not constant, new inventory estimates could result in greater values than the projected PA inventory. To more accurately estimate/bound the inventories of Ni-59 and Ra-226 and to assess whether the PA inventories are bounding, alternative methods of estimating Ni-59 and

Ra-226 inventories were developed following PA inventory development and will be applied to future additions. [SRNL-L3100-2009-00189]

The alternative method of estimating the Ra-226 inventory is based on the in-growth from the decay of Th-230. Using this method, the Ra-226 maximum total SDF inventory is shown to be 2E-03 Ci, significantly less than the total PA projected inventory of 4.1 Ci. [SRNL-L3100-2009-00189] Since essentially the entire Ra-226 PA inventory is in Vault 4, the PA modeled inventory is reasonably bounding.

For the alternative method of estimating the Ni-59 inventory, ratios of Ni-59 to Ni-63 have been analyzed in the waste and can be used for estimating. Taking into account the decay from present to the time of closure, a ratio of 0.020 is shown to be conservative in estimating the inventory. [SRNL-L3100-2009-00189] Using the alternative method of estimating and the current Ni-63 inventory in Vault 4 of 1.21 Ci, the current Ni-59 Vault 4 inventory is estimated at 0.024 Ci. [X-CLC-Z-00027] When this is compared to the PA modeled inventory of 0.4 Ci, the PA modeled inventory is shown to be reasonably bounding. The alternative approaches described above will be utilized, as appropriate to determine updated concentrations that are to be reported when final characterization information is available, per permit requirements.

The method to project the inventories of Am-241 did not account for the in-growth from Pu-241 decay. If this in-growth from the decay were included, the current Vault 1 inventory of Am-241 would approximately double. However, as detailed in the note with PA Table 3.3.2, the inventory values shown for Vault 1 were doubled in the PA model (i.e., double the values reported in the table) to account for potential future use of Vault 1 for low level contaminated materials. Therefore the potential dose impacts from the current Vault 1 inventory of Am-241 and in-growth of Am-241 from Pu-241 are bounded by the PA. In addition, the Vault 4 PA Am-241 and Pu-241 inventories (Table IN-1.1) are much larger, and the much larger inventories of these isotopes in Vault 4 did not result in any impact on dose.

Table IN-1.1: Inventory Comparison

Radionuclide	Inventory in PA (decayed to 10/1/2030) (Ci)	Current SDF Inventory (as of 3/31/09) (Ci)
Vault 1		
Am-241	4.70E-04	5.83E-04
Vault 4		
Am-241	1.3E+02	8.69E+00
Pu-241	2.4E+03	1.20E+02

The decay duration used to estimate the PA projected inventories was the time difference from the inventory basis date of 8/14/2007 to the estimated closure date of 10/1/2030.

IN-2

More information is needed about the basis for the uncertainty distributions for the radionuclide inventories used in the GoldSim calculations.

Basis

The derivation of the source inventory uncertainty distributions used in the GoldSim probabilistic analysis is described in the SDF PA Section 5.6.3.2. These distributions represent the uncertainty associated with the ability of the WCS system to predict the inventories in the tank waste that will be disposed of at the SDF. Figure 5.6-32 of the PA

	<p>presents the ratios of sample analysis results to predicted values for samples from 8 tanks for C-14, Cs-137, Pu-239, Sr-90, and U-238. Minimum and maximum values for the uncertainty distributions were selected based on the range of ratios observed in this figure. The distribution for radionuclides other than the five considered individually was assumed to have a minimum value of 0.1 and a maximum value of 10. However, the basis for this assumed distribution is not clear. It is also not clear why the assessment of the ratios of sample results to predicted values was only performed for the five radionuclides listed above and why the key radionuclides Ra-226 and Pa-231 and their parents were not considered in this assessment.</p> <p>The uncertainty distributions were implemented in GoldSim using the truncated log-normal distribution. The geometric mean was assumed to be 1 and the distributions were truncated as described above. In addition, a value of 1.1 was used for the geometric standard deviation. The basis for the use of this standard deviation is not clear, and the use of such a small standard deviation does not seem to capture the variability shown in Figure 5.6-32 of the PA.</p> <p><u>Path Forward</u></p> <p>Provide more information regarding the basis for the uncertainty distributions assumed for the radionuclide inventories in the GoldSim calculations, particularly the geometric standard deviation used in the GoldSim model. Provide the basis for the assumed uncertainty distribution for the radionuclides not evaluated in Figure 5.6-32 of the PA.</p>
--	--

RESPONSE IN-2:

The exclusive use of ratios from C-14, Cs-137, Pu-239, Sr-90, and U-238 was due to the limited sample analysis and/or availability of estimated values in WCS. These radionuclides were the only ones available for comparison. WCS tracks both saltcake and supernate concentrations. For supernate concentrations, samples are taken frequently and analyzed and WCS is updated with the results, however, no history is kept which hampers comparisons with previous sample results. For saltcake concentrations, there have been limited samples and analyses performed to allow for comparisons.

The distribution range for radionuclides other than the five considered was based on the evaluation of Figure 5.6-4. The ratios for Cs-137 shown in Figure 5.6-4 were considered biased high for the reason described in the SDF PA Section 5.6.3.2. Therefore, the Cs-137 ratios were not considered in setting the maximum range of 10 times for the other radionuclides. Using the other four radionuclides, the maximum ratio was 10 times the predicted value as reflected in SDF PA Figure 5.6-32. Therefore this was used for setting the other radionuclides' maximum value. In evaluating the minimums, two of the radionuclides (C-14 and Pu-239) ranged down to approximately 0.1 times the predicted value. While the other two (Sr-90 and U-238) ranged down significantly less than that, it was felt using a minimum less than 0.1 could be non-conservative. Therefore, the other radionuclides' minimum value was set at 0.1.

The value for the geometric standard deviation, 1.1, was chosen to ensure that the geometric mean of each distribution would be equivalent to the estimated deterministic value for the respective radionuclide inventory.

<p><u>IN-3</u></p>	<p>Information is needed on the process that will be used to ensure that the inventory will be distributed among the Future Disposal Cells (FDCs) in a configuration that provides reasonable assurance that the performance objectives will be met.</p>
---------------------------	--

	<p><u>Basis</u></p> <p>The total inventory for the SDF is estimated in Table 3.3-7 of the PA and the projected average inventory in the FDCs was provided in PA Table 3.3-5. The sequence in which the waste will be disposed, and consequently the amount of inventory that will be located in particular disposal cells, has not yet been determined. Based on the variability in the concentrations of the radionuclides in the various waste tanks in the tank farms, it is expected that the variability in the inventory from FDC to FDC could be significant.</p> <p>The PORFLOW model used to demonstrate compliance with the performance objectives assumed that the inventory in each of the FDCs will be equal to the average inventory for all of the FDCs. In the probabilistic uncertainty analysis in GoldSim, the location uncertainty of the inventory was evaluated by randomly selecting the order in which the waste tanks would be emptied and the order in which the FDCs would be filled. Although the model simulates various disposal configurations, it is unclear if all configurations provide reasonable assurance of an acceptable dose. It appears that unfavorable configurations (i.e., configurations in which higher activity waste is placed into neighboring vaults) might result in an unacceptable dose. Without an understanding of the dose implications for the unfavorable configurations and a commitment that unfavorable configurations will not be implemented, the NRC will need to monitor to the assumption used in the PORFLOW calculations used to demonstrate compliance (i.e., that the FDCs all contain an inventory that is equal to the average FDC inventory provided in Table 3.3-5).</p> <p><u>Path Forward</u></p> <p>Provide information on the process that will be used to ensure that the placement of the different tank waste into the different FDCs is done in a way that provides reasonable assurance that the performance objectives will be met.</p>
<p><u>RESPONSE IN-3:</u></p> <p>While the deterministic model considered the average inventory for the FDCs, the probabilistic model incorporated variability into the disposal sequence. One significant conservatism in this disposal sequence variation approach was that the maximum waste tank concentrations were used without consideration to the path each tanks' material would take before reaching SPF. Due to the transfers that need to take place to process the waste tank contents, the material in each tank will be added to other tanks, which, will in turn be added to even more tanks before reaching the SPF. These tank transfers were not taken into account in developing the stochastics for the disposal sequence variability. While this activity will not completely average the contents from all of the tanks, it will tend to move them to the average. Tanks that are low in concentration of a specific constituent will tend to increase and those high in concentration will tend to decrease. Therefore, the sensitivity analysis should be considered reasonably bounding and the expectation would be for the results to move to the mean.</p> <p>To illustrate the transfer paths material has to take prior to reaching SPF, the tank currently projected to have the maximum concentration for I-129 is Tank 1. To move the Tank 1 material to the SPF feed tank (Tank 50), this material would travel through a minimum of two other tanks prior to reaching Tank 50.</p> <p>In addition, the stochastics did not link the maximum concentrations for each constituent by tank. Each constituent's maximum concentration was picked independent of other constituents' related tank concentrations.</p>	

Also, the maximum inventory of the FDCs, assuming no mixing, is within several factors of the average inventory. The cumulative probability distributions for Tc-99 and I-129 used in the sensitivity analysis are presented in Figures IN-3.1 and IN-3.2. They show the maximum inventories are limited to a few factors greater than the average inventory. For example, Tc-99's maximum inventory was approximately 1,800 Ci as compared to an average inventory of 540 Ci. For I-129, the maximum inventory was approximately 0.85 Ci versus 0.38 Ci. It also shows a limited number of FDCs at the higher inventories. For example, there were two FDCs with a Tc-99 inventory greater than approximately 1,450 Ci and eight FDCs with inventories greater than approximately 1,050 Ci. This represents a minimal increase in dose risk from these few FDCs when balanced with those FDCs with less than average inventories.

Figure IN-3.1: Cumulative Probability Density for FDC Inventories of Tc-99

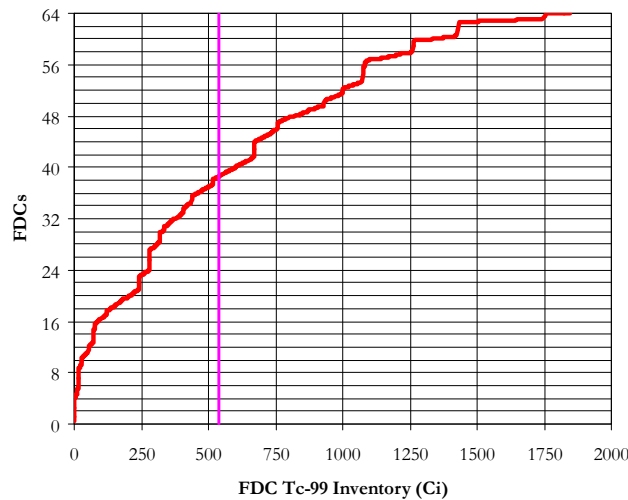
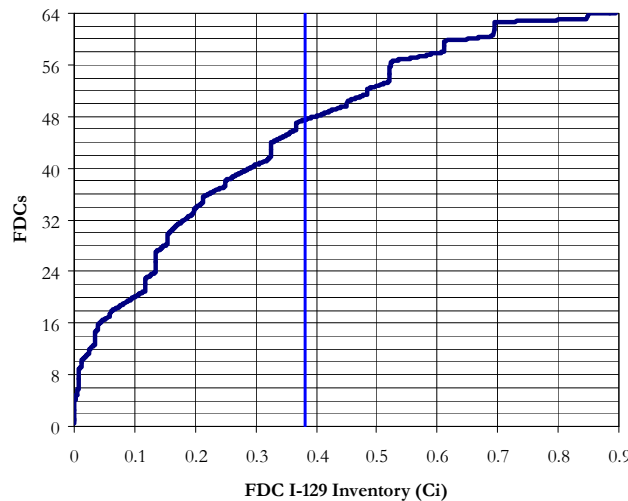


Figure IN-3.2: Cumulative Probability Density for FDC Inventories of I-129



IN-4

More information is needed about the inventory expected to remain in the sheet drain systems for Vault 4 and the FDCs and the inventory expected to remain in the transfer lines at the time of closure.

	<p><u>Basis</u></p> <p>Sections 3.2.1.2.5 and 3.2.1.3.5 of the PA state that after the operational period the drainwater collection system will be emptied and filled with grout. However, it is not clear if measures will be taken to clean the drainwater collection system and it is not clear how much inventory could remain in this system at the time of closure. If inventory remains in these systems at the time of closure, this inventory may be transported into the environment more rapidly than inventory in the saltstone wasteform because the sheet drain system is located at the edge of the vault and this system may provide a fast pathway into the environment. In addition, the inventory remaining in the sheet drains may be less encapsulated in the grout than the inventory in the saltstone. Information on the expected time of operation of the sheet drain system also was not provided. Thus, it is not clear how long the sheet drain systems will remain operational and when they will be grouted.</p> <p>It is also not clear how much inventory could remain in the transfer lines at the time of closure. If inventory remains in the transfer lines, an intruder could inadvertently drill through the transfer lines or be exposed through other scenarios and receive a dose from this inventory.</p> <p><u>Path Forward</u></p> <p>Provide a description of the measures that will be taken to empty and clean the drainwater system and transfer lines, and provide an estimate for when the operation of the sheet drain system will stop and when it will be grouted. Provide an estimate of the inventory expected to remain in the sheet drain systems and transfer lines at the time of closure. If this inventory is not negligible, provide an estimate of the potential dose from this inventory that could result to an offsite member of the public and to an intruder who drills through a line or is exposed to the inventory in a transfer line by another pathway.</p>
--	--

RESPONSE IN-4:

After grout placement operations have concluded, a cold cap consisting of “clean” water and dry feeds material will be placed over the saltstone monolith. After the clean cap is in place, the drainwater systems will be pumped free of drainwater to the extent practical. The drainwater system includes a filter feature that serves to preclude solids from entering the sheet drain system. Therefore, the predominant material entering the sheet drain is solubles contained in the drainwater, which are not expected to remain in the sheet drain system. In addition, the final cold cap will produce clean drain water that will serve as the final flush of the sheet drain system. Thus inventory of the sheet drain system at the time of closure is negligible. Drainwater components will be filled with “clean” grout.

After grout operations are completed, transfer lines to and drainwater return lines from the facility will be removed and disposed of as low level waste. Since the transfer lines will be removed prior to closure they will not contribute to the inventory of the SDF after closure.

This information will be included in the SDF Closure Plan when it is revised as part of the SDF PA implementation.

Infiltration and Erosion Control (IEC):

<p><u>IEC-1</u></p>	<p>The PA does not describe what portion of the water entering the perimeter drainage channel will infiltrate back into the native soil or backfill, or what, if any, effect such infiltration will have on vadose zone or saturated zone flow.</p> <p><u>Basis</u></p> <p>Until the HDPE/GCL layer in the closure cap is degraded, most of the precipitation infiltrating the cap will be diverted to the perimeter drainage channels as subflow through the drainage layer. Based on WSRC-STI-2008-00244, Section 4.4.17, the perimeter drainage channel appears to coincide with the “toe of side slope” in the PA, Figure 3.2-21. Focused infiltration along the perimeter drainage channels could alter the pattern of flow in the vadose zone, create local perched, saturated lenses, and/or flow back toward the disposal vaults. Divergence of natural percolation away from the closure cap footprint also could alter groundwater flow patterns in the saturated zone. Based on SRNL-STI-2009-00115, infiltration in the vadose zone models was specified based on simulated infiltration through the closure cap using the HELP model. The lower boundary condition in the vadose zone model was the water table based on the calibration of the GSA/PORFLOW model (SRNL-STI-2009-00115). Based on the model description in SRNL-STI-2009-00115, the vadose zone model simulations do not consider the effect of focused infiltration along the perimeter drainage channel outside the footprint of the closure cap. The saturated zone model does not represent the effect of the closure cap on infiltration to the water table or focused infiltration from the perimeter drainage channel that might affect groundwater flow patterns or velocities (SRR-CWDA-2009-00017).</p> <p><u>Path Forward</u></p> <p>Provide a technical basis for neglecting the effect of focused infiltration along the perimeter drainage channels on flow in the vadose zone and flow in the saturated zone.</p>
<p><u>RESPONSE IEC-1:</u></p> <p>Focused infiltration along the perimeter drainage channels is neglected when modeling flow in the vadose zone and flow in the saturated zone in the SDF PA. Prior to closure cap degradation, most precipitation falling on the cap will run-off to the perimeter drainage channels. The increased localized infiltration could affect flow patterns in the vadose zone and SZ. However, a 50 foot extension of the closure cap beyond the sides of the disposal units is assumed sufficient in preventing any adverse impacts on contaminant transport out of the disposal units. The SDF PA Section 3.2.2.9 explicitly identifies this as a conservative assumption, therefore it “is acceptable for use for PA modeling” (Section 3.2.2.9).</p> <p>This assumption is supported by the initial scoping model developed for HTF flow and transport (PORTAGE-08-022, Rev 0). This PORFLOW model looked at two cases: one with an intact closure cap and one with a degraded closure cap. Results indicate that the “<i>intact cap case shows a reduction in the velocities below the cap. The diversion of water down and around tanks can be seen in the figures [(i.e., Figure 3-18 through 3-22 of PORTAGE-08-022, Rev 0)]. Noteworthy in both simulations is that the movement of water in the immediate area of the tanks is primarily vertical. ... Since the flow is primarily vertical, there is little chance for any contaminant transport interaction between waste tanks until sufficient transport distance</i></p>	

occurs that regional horizontal flow dominates and the streamlines turn horizontal." [PORTAGE-08-022, page 63] The conclusions of the scoping HTF model can be applied to the expected results of a SDF model evaluating the impact of an intact closure cap on flow (in the UZ and SZ).

As a precaution, an open design issue (Issue #6 in Table 34 of WSRC-STI-2008-00244), will track whether or not the "50-foot extension of the closure cap beyond the sides of the disposal cells [is] sufficient to prevent infiltration ... from impacting contaminant transport." If it is found that the current design adversely impacts contaminant transport out of the disposal units, the closure cap design will be modified to appropriately remediate these impacts.

IEC-2

The cross-sections of disposal units in WSRC-STI-2008-00244 illustrate the lower backfill layer and other materials in the closure cap covering the cells, but do not indicate what materials will be used to backfill around the cells.

Basis

The cross-sections through the Saltstone Disposal Facility (Figures 6, 7 and 8 in WSRC-STI-2008-00244) indicate that some of the disposal cells (e.g., 6A/B, 12A/B) will be constructed below the preclosure grade. Photographs of the Saltstone Disposal Facility (e.g., SRNL-STI-2009-00115) show the disposal cells as free-standing structures suggesting that backfilling around the cells will be required prior to placing the lower backfill layer of the closure cap. The properties of backfill materials placed around the disposal cells will influence water movement and settlement in the vadose zone around the disposal cells. Illustrations showing the distribution of materials assigned to the computational grid in the vadose zone model (e.g., SRNL-STI-2009-00115, Figure 56) indicate that the backfill material will be same as that in the lower backfill layer.

Path Forward

Explain the nature and properties (e.g., hydraulic conductivity, porosity, bulk density) of the backfill material that will be placed around the disposal cells and the manner in which it will be placed and compacted.

RESPONSE IEC-2:

The cross-sections through the SDF (Figures 6, 7 and 8 in WSRC-STI-2008-00244) indicate some disposal cells (e.g., 6A/B, 12A/B) will be constructed below the pre-closure grade. Although the referenced cross-sections do not graphically depict the material immediately adjacent to the cells, controlled compacted backfill will be used, consistent with the inputs used in HELP (WSRC-STI-2008-00244, Section 5.4.2) and PORFLOW (WSRC-STI-2006-00198, Table 5-18) modeling. The properties of controlled compacted backfill are described in Section 5.3 and Table 5-18 of WSRC-STI-2006-00198. The physical properties are reproduced in Table IEC-2.1 below.

Table IEC-2.1: Physical Properties of Control Compacted Backfill

Material	Horizontal Conductivity (K _h) cm/s	Vertical Conductivity (K _v) cm/s	Effective Diffusion Coefficient (De) cm ² /s	Porosity (η) unitless	Bulk Density (ρ _b) g/cm ³	Particle Density (ρ _s) g/cm ³
Lower backfill ¹	7.6E-05	4.1E-05	5.3E-06	0.35	1.71	2.63

¹ Controlled Compacted

The manner in which backfill will be placed and compacted is in accordance to the specifications described in Part 3 of C-SPP-Z-00006, Section 02320.

IEC-3

Additional information is needed to support conclusions about the long-term performance of the side slopes of the closure cap.

Basis

The physical stability of the closure cap side slopes is important for the long-term stability and performance of the closure cap as a whole. WSRC-STI-2008-00244 discusses the following physical mechanisms that could degrade the closure cover:

- Static-loading induced settlement
- Seismic-induced liquefaction and subsequent settlement
- Seismic-induced slope instability
- Seismic-induced lateral spread
- Seismic-induced direct rupture due to faulting

The reference (WSRC-STI-2008-00244) concludes these phenomena will be unimportant to the stability of the SDF closure cover. In addition to the mechanisms discussed in WSRC-STI-2008-00244, the following mechanisms also could affect the closure cap side slopes:

- Slumping of the side slope
- Downslope creep of the riprap
- Vegetation growth on side slopes

	<p>Slumping and downslope creep of the riprap could expose the backfill underlying the side slope riprap leading to erosion of the side slope and ultimately the closure cap as a whole. Subflow from the closure cap drainage layer flowing through the side slope riprap could significantly increase the water content of the backfill beneath the side slope, leading to slumping. Frost heave could also lead to downslope creep of the side slope riprap that would ultimately expose the underlying backfill to erosion. Although WSRC-STI-2008-00244 presents engineering calculations to support the sizing of riprap on the side slopes to resist the effects of erosion due to surface water runoff, no calculations are presented related to the stability of the side slope to slumping or the stability of the riprap to frost heave creep.</p> <p>Modeling of the closure cap performance includes the effects of degradation due to pine tree propagation onto the vegetative cover, which is extensively discussed in WSRC-STI-2008-00244. Although the PA and supporting documents discuss the effects of vegetation on the performance of the closure cap, the possibility of vegetation developing on the side slopes of the closure cap is not addressed. Development of vegetation on the side slopes could have either a beneficial or deleterious effect on the slope performance and stability. For example, vegetation growth on the riprap on the side slopes and in the toe of the side slopes could reduce the ability of the side slope and perimeter drainage channel to conduct water away from the cover. Alternately, development of vegetation on the side slopes could be beneficial because development of vines or deep-rooted plants could stabilize the side slopes. On the other hand, windfall of trees on the side slopes could dislodge the riprap and expose the backfill to erosion. In particular, windfall due to extreme weather events can result in common-mode disruption that overtakes natural repair processes.</p> <p>Although a barrier analysis discussed in the PA concluded that complete failure of the cap did not have a significant effect on dose, this conclusion is based on uncertain assumptions that ensure very limited water flow through the waste form (see, e.g., comments on Saltstone Performance in this document). Because of the importance of the hydraulic isolation of saltstone to long-term performance and because of the uncertainty in other factors limiting flow through saltstone during the 10,000 year performance period (e.g., limited degradation of the wasteform and disposal units), long-term performance of the cap as an erosion and infiltration barrier is considered an important element of establishing reasonable assurance that the performance objectives will be met.</p> <p><u>Path Forward</u></p> <p>Either provide a technical basis for neglecting side slope slumping and riprap creep as degradation mechanisms, or provide engineering calculations to demonstrate the resistance of the side slopes to these degradation mechanisms. Provide a technical basis for neglecting the effects of vegetation on the side slopes and toe of the side slopes, or provide an engineering assessment of the effects of vegetation on the stability and performance of the side slopes, toe of the side slopes, and closure cap as a whole. An assessment of the effects of vegetation on the side slopes and toe of the side slopes should be consistent with the response to comment IEC-4.</p>
--	--

RESPONSE IEC-3

Introduction

This response provides a technical basis for neglecting the following degradation mechanisms; 1) slumping of the side slope and down-slope creep of the riprap and 2) vegetation growth on side slopes.

In general, these degradation mechanisms were neglected because; 1) the erosion barrier riprap sizing and thickness calculations (WSRC-STI-2008-00244, Appendix A) used conservative assumptions to develop an overly-robust riprap design and 2) the side slopes of the closure cap are not expected to experience significant vegetative growth.

Closure Cap Footprint

Closure cap degradation and infiltration was evaluated using a model that included the footprint of the closure cap (which extends 50 feet beyond the edge of the saltstone disposal units) however, the model did not include degradation of the side slope, toe of the side slope, or the riprap. [WSRC-STI-2008-00244] For PA purposes, the 50 foot extension of the closure cap beyond the sides of the disposal units is assumed sufficient. Regardless, the open design issue (Issue #6 in Table 34 of WSRC-STI-2008-00244) will track whether or not the “50-foot extension of the closure cap beyond the sides of the disposal cells [is] sufficient to prevent infiltration ... from impacting contaminant transport.” If it is found that the current design is not sufficient in preventing infiltration, the closure cap design will be modified to appropriately remediate this.

Slumping of the Side Slope and Down-Slope Creep of the Riprap

With respect to movement of the side slope riprap, the erosion barrier riprap sizing and thickness calculations in Appendix A of WSRC-STI-2008-00244 were performed to provide a riprap surface with an underlying gravel bedding layer to prevent gully formation on the side slopes and to provide long-term slope stability. The side slope riprap has been sized based upon the PMP and the methodology outlined by ISSN: 0733-9429/91/0008-0959 and NUREG-1623. A PMP is defined as the theoretically greatest depth of precipitation for a given duration that is physically possible over a given storm size area at a particular geographic location. The PMP utilized for the side slope riprap sizing was 52.6 in/hr, which represents a rainfall amount that is significantly greater than the SRS 100,000 year return period rainfall event of 7.4 in/hr. The methodology outlined by ISSN: 0733-9429/91/0008-0959 and NUREG-1623 results in a riprap size which will not move with the flow resulting from the PMP. This means that the side slope riprap is stable relative to potential movement.

In addition to the conservativeness of riprap sizing relative to the use of the PMP, the sizing has a number of additional conservative assumptions affecting the riprap slope degradation design parameters (WSRC-STI-2008-00244, Appendix A):

- *Flow Concentration Factor (F):*
A conservative flow concentration factor (F) of 5 (rather than 3, as used for the cap surface) has been utilized for the erosion barrier. [WSRC-STI-2008-00244 pp. 183]
- *Runoff Coefficient (C):*
In order to be conservative, the runoff coefficient (C) will be taken as the lower end of that for concrete (i.e. $C = 0.8$). [WSRC-STI-2008-00244 pp. 183]
- *Median Size of the Side Slope Riprap (D_{50}):*

The flow at failure (Q_{failure}) is the flow required to move the riprap such that the underlying filter fabric or bedding stone is exposed. Using the ISSN: 0733-9429/91/0008-0959 method, the required D_{50} (median size) of the side slope riprap was determined to be 10.1 inch. [WSRC-STI-2008-00244 pp. 187]

- *Riprap Layer Thickness:*

The more conservative NCSU 1991 criterion requiring a riprap layer thickness at least 1.5 times the maximum stone diameter (D_{100}) is used to determine the riprap layer thickness of 24 inch, as opposed to NUREG-1623 which suggests 1.5 times the mean stone diameter (D_{50}). [WSRC-STI-2008-00244 pp. 187]

Although slumping of the side slope and down-slope creep of the riprap were not evaluated when developing the conclusions about the long-term performance of the side slopes of the closure cap, these built-in conservatisms provide for a robust riprap pre-conceptual design that can be expected to negate any potentially adverse effects of additional degradation mechanisms.

Further, slope stability, including slumping of the side slope and down-slope creep of the riprap, will be appropriately considered and handled as part of the closure cap final design so that it is not a significant degradation mechanism requiring consideration within the PA as outlined in Section 6.1 of WSRC-STI-2008-00244. Additionally as stated in Section 2.0 of WSRC-STI-2008-00244, Rev. 0:

The closure cap design and infiltration information is preliminary ... it provides sufficient information for planning purposes ... to estimate infiltration over time through modeling. It is not intended to constitute final design. Final design and a re-evaluation of infiltration will be performed near the end of the operational period. Technological advances, increased knowledge, and improved modeling capabilities are all likely and will result in improvements in both the closure cap design and infiltration estimates.

Precipitation and Vegetation Growth on Side Slopes

Eight water balance and infiltration studies (Table 2 of WSRC-STI-2008-00244) found that precipitation is distributed into evapotranspiration (median of 31.2 in/yr), infiltration (median of 14.8 in/yr), and runoff (median of 1.6 in/yr). The vegetative soil cover on the closure cap has been designed to promote evapotranspiration, minimize erosion, and prevent the initiation of gullying due to a PMP event.

The side slopes of the closure cap shall be covered with a riprap (rock) overlaying a stone-bedding layer (SDF PA Figure 3.2-21). The slope of the side slopes, the thickness and size of side slope riprap (2 feet thick layer of 10 inch median sized riprap), the 6 inch thick gravel bedding layer, and lack of topsoil will make the side slopes inhospitable to most vegetation. [WSRC-STI-2008-00244] Due to the slope of the side slopes any runoff and lateral drainage from the top of the closure cap will quickly drain off the side slopes. The side slopes would generally present a relatively dry, rock environment. Under these conditions only short-lived annual herbaceous plants, which could not damage the side slopes, would be expected, and significant woody plants would not be expected.

Additionally, the side slopes account for roughly a third of the aerial surface of the total closure cap, none of which overlies the waste disposal vaults (based on WSRC-STI-2008-00244, Figure 5). Therefore, the effect of side slope vegetation is considered negligible. Further, if any vegetative growth on the side slopes did occur, which is unlikely, any growth would reduce flow velocities, thus reducing erosion effects.

<p><u>IEC-4</u></p>	<p>During the transition from Bahia grass to a pine tree forest the closure cap could be affected by external factors such as drought or fire, thus changing the assumptions required for the stability calculation.</p> <p><u>Basis</u></p> <p>The vegetative cover physical stability calculations based on the permissible velocity method presented in WSRC-STI-2008-00244 assume that the closure cap is vegetated with Bahia grass. Possible evolution of the vegetative cover after the period of institutional control is discussed in WSRC-STI-2008-00244 Section 6.2. The transition from a well-maintained Bahia grass cover to a mature pine forest covering the entire closure cap is estimated to take several hundred years. As the vegetation on the cap changes and is possibly impacted by fire or severe drought, the resistance of the cover to erosion may change (see, e.g., LA-UR-01-4658, 2001; PNNL-17859, 2008). The stability calculations presented in WSRC-STI-2008-00244 Appendix A assume that the closure cap has a Bahia grass vegetative cover yielding a maximum permissible runoff velocity of 3.22 feet per second. The calculated runoff velocity based on the probable maximum precipitation was 2.98 feet per second. The maximum permissible runoff velocity and calculated runoff velocity may be different if the cover is not well-maintained Bahia grass or the vegetation has been stressed by fire or drought.</p> <p>As described in comment IEC-4, although the PA concluded that complete failure of the cap did not have a significant effect on dose, that conclusion is based on uncertain assumptions about the hydraulic performance of other elements of the disposal system. Thus, long-term performance of the cap as an erosion and infiltration barrier is considered an important element of establishing reasonable assurance that the performance objectives will be met.</p> <p><u>Path Forward</u></p> <p>Provide estimates of the vegetative cover physical stability to erosion based on the permissible velocity method for the cover conditions that may exist between the end of active maintenance and establishment of a mature pine tree or bamboo cover.</p>
----------------------------	--

<p><u>RESPONSE IEC-4:</u></p> <p>Possible biological stressors and external factors such as droughts, disease, or fire are expected to occur based on typical events in the SRS region, and have the potential to impact the vegetative cover transition over the closure-cap. Section 6.2 of WSRC-STI-2008-00244 discusses the possible evolution of vegetative cover after institutional controls over the closure cap, and the possible impacts from environmental and biotic stressors:</p> <p><i>“During [the transition from bahia grass to pine forest]..., numerous biotic and abiotic factors will influence the exact nature and timing of succession. These could include drought, insects, diseases, fire, etc. The basic biology and ecology of bahia and many of the early invaders will typically be altered only slightly due to biotic factors. This can result in a minimum lengthening of the time sequence of advancement. The possible exception is the occurrence of fire during the early successional years. This would tend to delay the advancement of the shrub and pine community until an interval after the last fire occurrence. When the interval between fires is long enough for the encroaching pine saplings to become tall enough to withstand fire disturbance and</i></p>

survive, the successional pattern to a pine dominated stand will proceed. This is the normal successional pattern for the SRS region.”

As stated above, stressors will delay pine forest succession. The SDF PA Section 3.2.2.6.2 identifies pine tress as “the most deeply rooted naturally occurring climax plant species which will degrade the GCL through root penetration”. Degradation of the GCL leads to accelerated degradation of the closure cap, and the onset of increased infiltration. Therefore, ignoring periods of drought, disease, and fire is a conservative approach since this assumption results in an increased infiltration rate earlier than if any of these stressors were assumed to occur.

Additionally, although studies conducted in steeply sloping mountainous regions have identified the potential for wildfires to increase surface soil erosion (LA-UR-01-4658), increased erosion due to destabilization from drought and fire is not expected on the gently sloping (1.5% slope over 825 feet slope length) SDF conceptual closure cap.

As noted in the SDF PA Section 3.2.2, the design information provided is for planning purposes sufficient to support evaluation of the closure cap. Final design and a re-evaluation of infiltration will be performed near the end of the operational period. Technological advances, increased knowledge, and improved modeling capabilities are all likely to have occurred prior to closure and will result in improvement in both the final closure cap design and infiltration estimates.

IEC-5

Differential settlement could occur due to the presence of the relatively rigid disposal cells within the lower backfill and non-uniform thickness of the backfill. This could affect the drainage efficiency of the upper drainage layer and the integrity of the geomembrane layer.

Basis

Static-loading-induced settlement is identified as a potential mechanism degrading the closure cap (Table 3.2-6 of the PA and WSRC-STI-2008-00244 Section 6.1). Settlement due to static loading is stated to be only a few inches and to be uniformly distributed over the closure cap.

The closure cap will be constructed over disposal cells and a lower backfill of nonuniform thickness. The disposal cells are concrete structures filled with saltstone that will be relatively rigid with respect to the backfill on which the closure cap is constructed. Based on cross sections in WSRC-STI-2008-00244, the combined thickness of the backfill and closure cap will vary from as little as 20 feet to as much as 60 feet across the Saltstone Disposal Facility. Settlement of the soil within the backfill between the disposal cells could be greater than that over the disposal cells. Such differential settlement could affect the local slope of the drainage layer and create stresses on the HDPE geomembrane.

Path Forward

Provide engineering calculations to justify the assumption that static-loading-induced settlement will only be a few inches and will be uniformly distributed over the closure cap.

RESPONSE IEC-5:

With respect to the PA differential settling of the closure cap (controlled compacted backfill) is not expected to impact the geomembrane layer or drainage. This expectation for SDF is based upon the analogous calculations for FTF discussed below.

The 2 to 3 inches of static settlement cited in the PA is based upon F-Area tank calculations. Table 4 of K-CLC-F-00073 Rev. 1 shows that at 10,000 years post-closure, the maximum static settlement of the F-Tank closure cap is estimated to be 2.2 inches. This estimate is based upon F-Area tank closure cap pressure (greater than 10 ksf), which is more than twice the pressure of the Saltstone disposal unit closure cap (4.2 ksf). This indicates that the SDF closure cap will actually experience less differential settling. Therefore, applying a range of 2 to 3 inches is a conservative approach.

Additionally, calculations for static-loading induced settlement of closure caps over selected F-Area tanks estimated that the “*differential settlement for any given tank is less than 0.1 inches,*” thus supporting a uniform distribution. [K-CLC-F-00073, Section 3.1] The Saltstone Vault Degradation Prediction calculation, with respect to seismically induced differential settlement, states:

The location of the differential settlement region under the vault is assumed to be a uniformly distributed variable. Structural analyses indicate that multiple differential settlement regions, on the average, are not as severe as a single differential settlement region. A conservative bias is introduced by only postulating one single differential settlement region per seismic event”
 [T-CLC-Z-00006, Rev. 0, Appendix H, pp. 592]

Although this assumption was prepared for seismic-induced differential settlement under the disposal unit, it is expected that this assumption is still conservative when applied to static loading-induced differential settlement of the closure cap.

Static settlement will be appropriately considered and handled as part of the final design of the closure cap. Static settlement is not a significant degradation mechanism requiring consideration within the PA as outlined in Section 6.1 of WSRC-STI-2008-00244. Additionally as stated in Section 2.0 of WSRC-STI-2008-00244, Rev. 0:

The closure cap design and infiltration information is preliminary ... it provides sufficient information for planning purposes ... to estimate infiltration over time through modeling. It is not intended to constitute final design. Final design and a re-evaluation of infiltration will be performed near the end of the operational period. Technological advances, increased knowledge, and improved modeling capabilities are all likely and will result in improvements in both the closure cap design and infiltration estimates.
 [WSRC-STI-2008-00244, Rev 0, Section 2.0]

IEC-6

Additional justification is needed for the hydraulic conductivity assigned to the foundation layer of the infiltration and erosion cap.

Basis

As described in WSRC-STI-2008-00244 Appendix I, the HDPE/GCL is treated as a combined layer in the HELP model with fully penetrating holes after a 300 year service life. According to the HELP model documentation (Schroeder et al., 1994), simulated flow through the holes in the HDPE/GCL combined layer is controlled by

the size and number of holes, and the hydraulic conductivity and thickness of the underlying vertical percolation layer. The underlying layer is the foundation layer that is assigned a saturated, vertical hydraulic conductivity of 1×10^{-6} cm/s, but with other relevant hydraulic properties equal to those of SRS compacted backfill. The hydraulic properties of control compacted backfill are described in WSRC-STI-2008-00244, Section 5.4.2. A vertical, saturated hydraulic conductivity of 4.1×10^{-5} cm/s is assigned to this material. This value is 41 times greater than the vertical, saturated hydraulic conductivity assigned to the foundation layer in the HELP model. This lower value controls percolation through the closure cap as the HDPE/GCL layer degrades (develops more holes).

The technical basis for the hydraulic conductivity assigned to the foundation layer in the HELP model is not discussed, with the exception of the statement that bentonite will be incorporated into local soils used in the foundation layer (WSRC-STI-2008-00244). If a higher value of hydraulic conductivity was assigned to the foundation layer, the calculated percolation rate through the closure cap would be higher at earlier times, although it might not be significantly greater after the HDPE/GCL layer is fully degraded.

Path Forward

Clarify whether the hydraulic conductivity value of 1×10^{-6} cm/s is a specification for the saturated, vertical hydraulic conductivity of the foundation layer in the future cap design or whether there is a technical basis for selecting this value for use in the HELP model. Provide any existing technical basis for the value assigned to the hydraulic conductivity of the foundation layer in the HELP model.

RESPONSE IEC-6

As stated in WSRC-STI-2008-00244, Section 4.4.3, based on design specifications, it is a functional requirement for the closure cap foundation layer to have a hydraulic conductivity less than or equal to $1E-06$ cm/s. Bentonite, which reduces soil permeability (because of its hydraulic conductivity of $5E-09$ cm/sec), will be blended with the SRS backfill material to achieve this targeted, specified hydraulic conductivity.

The purpose of the foundation layer is to provide a relatively low permeability layer directly above the lower backfill. In addition, it will provide structural support and required contours for slope of 4% for overlying layers and a smooth surface free from deleterious materials suitable for installation of the GCL. Appropriately, this value is less than the value used for the SRS compacted backfill layers.

Use of the higher vertical saturated hydraulic conductivity value of $4.1E-05$ cm/s for typical backfill layers within the HELP model is considered appropriate, since the backfill has been designated as a vertical percolation layer which will promote drainage of infiltrating water away from and around the disposal cells.

Saltstone Performance (SP)

<p><u>SP-1</u></p>	<p>Additional justification is required for the assumption that saltstone is hydraulically undegraded for 20,000 years.</p> <p><u>Basis</u></p> <p>Section 4.2.3.2.4 of the PA indicates that, in the base case, degradation of the saltstone material is not assumed to occur during the performance period. The same section of the PA also acknowledges that the potential for physical degradation of the saltstone is uncertain. The assumption that saltstone will not degrade during the performance period appears to be based on the conclusion of “<i>Thermodynamic and Mass Balance Analysis of Expansive Phase Precipitation in Saltstone</i>” (WSRC-STI-2008-00236) that fracturing due to expansive phase precipitation is unlikely to occur in saltstone because the maximum amount of porosity filled is 34 percent. However, the PA does not provide a basis for neglecting other types of degradation, such as shrinkage cracking, corrosion cracking, or dissolution of salts and low solubility matrix phases. Furthermore, DOE deferred responses to several NRC comments on the expansive phase precipitation report (NRC, 2009a), and characterized the report as preliminary research (SRR-CWDA-2009-00011). NRC acknowledged that the report was an initial step in a research program but cautioned that the use of research as support for assumptions and parameters in performance assessments should be consistent with the maturity of the research (NRC, 2009a).</p> <p>Because of the preliminary nature of the expansive phase precipitation report and the potential for other types of degradation, additional support is needed for the assumption that saltstone remains undegraded in the base case during the performance period (and in calculations carried to 20,000 years). NRC comments on the expansive phase report to which DOE deferred a response include the following:</p> <ol style="list-style-type: none">1) The conclusions of the expansive phase precipitation report are based on geochemical modeling results. It is unclear whether there are data and observations available for comparison to constrain the modeling calculations.2) The expansive phase study does not consider the effects of organic additives or pozzolanic replacement on the dissolution and precipitation of cement-related compounds, which may have an effect on the generation of expansive phases. Future research could consider the effect that sulfide from the blast furnace slag might have on the phases and reactions present in this system.3) Experiments that are designed to collect data on initial mineralogical conditions, fundamental thermodynamic data and reaction kinetics would provide much needed model support for this study.4) Geochemist’s Workbench is based on an equilibrium reaction model. However, reaction kinetics could result in metastable products that are often associated with an increase in volume. Subsequent studies might consider expansive phases produced by intermediate or metastable
---------------------------	---

	<p>reaction products.</p> <p>5) The conclusions reached in this study area could be integrated with other ongoing or recently completed studies. Dixon (SRNL-STI-2008-00421) recently completed a study on the physical properties of grout, which included bulk porosity measurements. Updated measurements of the bulk porosity of saltstone grout may be useful in assessing whether expansive phase precipitation is likely to result in grout degradation.</p> <p>In addition to expansive phase precipitation, additional mechanisms could cause degradation of saltstone. Degradation mechanisms that may cause discrete fracturing along certain features of the wastefrom, such as corrosion cracking along reinforcement bars or shrinkage cracking around the wastefrom perimeter or support columns, are addressed non-mechanistically in the PA by sensitivity cases B-D and the synergistic case, which postulate fractures through the waste. Mechanisms that may cause a network of smaller-scale cracking, such as dissolution of salts or low-solubility matrix phases, are addressed non-mechanistically in sensitivity Case E and in an increased saltstone hydraulic conductivity case discussed in Section 5.6.6.7. However, as discussed in SP-3, SP-4, SP-5, and SP-6, the degree of conservatism of these cases is unclear. Furthermore, because the base case result is an important factor in the compliance determination, it is important to be able to support assumptions about saltstone degradation used in the base case. For these reasons, additional support is needed for the assumption that saltstone does not degrade hydraulically in the base case.</p> <p><u>Path Forward</u></p> <p>Provide additional basis for assuming no hydraulic degradation of saltstone occurs in the base case or provide an updated base case analysis that reflects estimated saltstone hydraulic degradation (e.g., changes in hydraulic conductivity and effective diffusivity). Specifically, address the specific comments on the expansive phase report included in the basis, additional degradation mechanisms noted in the basis, and any other relevant degradation mechanisms that could cause hydraulic degradation of saltstone. If a new analysis is provided, the assumptions should be consistent with the response to other comments in this document.</p>
--	---

RESPONSE SP-1:

Additional research into saltstone material degradation is planned and on-going, as noted in item 2 of Table 8.2-1 in the SDF PA. The first phase of the long-range testing has been completed and is documented in SRNS-STI-2009-00477. The research is meant to take the next step, after the initial expansive phase work documented in WSRC-STI-2008-00236, in understanding the potential degradation mechanisms and degradation rates for saltstone. SRNS-STI-2009-00477 describes initial laboratory testing performed on actual saltstone wastefrom simulates and a comparison to model predictions from the STADIUM® computer code. The testing indicated that “the durability (stability) of the saltstone matrix upon immersion in water was found to be better than that of Portland cement paste with a similar water to cement ratio and a lower total porosity.” The testing also indicated that the code predictions for cement leach rates were similar to actual tested materials for the short duration of exposure in the report. While the leached zone did not show any obvious signs of

degradation, additional work is planned and ongoing for longer exposure times and research into the physical signs of degradation and degradation properties for longer exposure times.

The physical testing is meant to provide assurance that any long-term code predictions of material conditions are reasonable. The testing also provides real physical data and observations to inform any future modeling and provides a means to study the impacts of multiple potential degradation mechanisms such as those noted in the basis section of this comment.

As noted in Basis Item 5, SRNL-STI-2008-00421 has been issued which evaluated the porosity of various saltstone samples. The 90 day cured porosities were 0.55, 0.59, and 0.59 for DDA, ARP/MCU, and SWPF stimulant mixes respectively. These values all exceed the value of 0.46 utilized in WSRC-STI-2008-00236 and further support the conclusion that expansive phase degradation is unlikely.

SP-2

A basis is required for the modeled extent of saltstone fracturing.

Basis

As described in SP-1, various mechanisms may cause degradation of cementitious waste forms. Fracturing is addressed non-mechanistically in the PA by Cases B, C, and D. However, the relationship between the total fracture area and fracture geometry assumed in Case C and the total fracture area and geometry that may occur in various plausible degradation cases is not clear. For example, it is not clear if the total fracture area represented in Case C adequately represents the fracturing that could occur due to the degradation mechanisms discussed in SP-1.

Once fracturing is initiated, increased water infiltration can increase the rate of subsequent degradation. For example, increased infiltration through the wasteform can speed dissolution of low-solubility phases or increase the rate of introduction of species that could form expansive precipitates, such as sulfates. As fracturing occurs, the volume-to-surface-area of saltstone blocks between fractures would increase, decreasing the diffusive length required for radionuclides to travel from the wasteform. In addition, as the volume-to-surface-area of blocks between fractures increases, the rate of leaching could increase, increasing the rate of subsequent fracturing.

Although fracturing is represented in the PA as a low-probability case, initial fracturing of saltstone has been observed (see, e.g., SRNL-ESB-2008-00017).

Path Forward

Provide a basis for the extent of fracturing assumed to occur in Case C. Address the potential acceleration of fracturing that could occur as the average volume-to-surface-area ratio of intact saltstone blocks decreases. Address the mechanisms noted in the basis as well as other mechanisms by which fractures could increase the rate of subsequent fracturing. Alternately, provide a new estimate of saltstone fracturing during the performance period, including a basis for the new estimate, and the effect of the new estimate on dose.

RESPONSE SP-2:

In Case C for Vaults 1 and 4, the model crack through saltstone is intended to capture the impact of transverse structural cracks predicted to form after differential settlement and seismic events (SRNL-STI-2009-00115, Rev. 1, Section 3.3). The single longitudinal crack in the Vaults 1 and 4 half-width models is equivalent to two 600 foot longitudinal cracks in the full width. The equivalent number of transverse cracks, in terms of cumulative crack length, is six for Vault 4 and 12 for Vault 1. Physical cracks are predicted to range from none up to a few (T-CLC-Z-00006), less than the number of equivalent transverse cracks represented in the models.

For the FDCs, a single (annular) crack was positioned such that the surface and cross-sectional areas of the fracture approximately match the cumulative areas of the support columns. The postulated crack between saltstone and concrete can account for a number of physical mechanisms, such as shrinkage or the presence of sheet drains. Differences in the size and number of saltstone cracks could potentially impact flow through the Vaults and FDCs. Impact of flow variability on the model results has been assessed not through a crack sensitivity study but through various sensitivity analyses of hydraulic conductivity. The SDF PA Section 5.6.6.7 evaluated the impact of increasing the saltstone hydraulic conductivity and Section 5.6.6.1, evaluated the impact of alternate disposal unit configurations, such as configuration E, which assumes a degraded, fully cracked saltstone condition that results in a hydraulic conductivity of 1.7E-3 cm/sec. These sensitivity studies provide information regarding the effect crack variability (as it impacts flow) would have on the PA results.

SP-3

The moisture characteristic curve for intact saltstone implemented in the PORFLOW model does not sufficiently account for experimental uncertainties and is inconsistent with literature results for material similar to saltstone and other cementitious materials.

Basis

The PA relies on moisture characteristic curves to determine the flow through unsaturated cementitious materials. Because direct measurements of unsaturated hydraulic conductivity were considered to be time and cost prohibitive, the SRS report, "*Hydraulic and Physical Properties of Saltstone Grouts and Vault Concretes*" (SRNL-STI-2008-00421) relied on theoretical and indirect methods to predict the unsaturated hydraulic conductivity based on measurements of saltstone samples for a suction range of 0 to 55 bars. A monitoring follow-up item related to characteristic curve uncertainty (ML091320439-012) was closed based on the DOE conclusion that the saltstone remained sufficiently close to saturation that the shape of the characteristic curves was not risk-significant (NRC, 2009b). However, even in the small range of saturations considered in the PA (i.e., a minimum of 98% saturation for saltstone), the characteristic curves used for saltstone predict significantly reduced unsaturated hydraulic conductivities as compared to saturated hydraulic conductivities (see Figure 1, below).

The PA implements curves substantially different from those found in literature. For example, the curves in the PA are significantly different from the curves discussed in "*Hydraulic Property Data Package for the E-Area and Z-Area Soils, Cementitious Materials, and Waste Zones*" (WSRC-STI-2006-00198) (Figure 1). The moisture

characteristic curves discussed in WSRC-STI-2006-00198, which were derived by Rockhold et al. (1993), Savage and Janssen (1997), and Baroghel-Bouny (1999) for different cementitious materials by different methods, all have very similar characteristics. The similarity of the curves is significant because the curve derived by Rockhold et al. (1993) was based on a Hanford double-shell slurry feed (DSSF) grout formulation that is very similar to saltstone (WSRC-STI-2006-00198). Both saltstone and the DSSF grout consist of approximately 47% blast furnace slag, 47% fly ash, and 6% Portland cement with similar salt concentrations (WSRC-STI-2006-00198).

Difficulties with experimental methods introduced additional uncertainty into the characteristic curve for saltstone implemented in the PA. The curve developed in “*Numerical Flow and Transport Simulations Supporting the Saltstone Disposal Facility Performance Assessment*” (SRNL-STI-2009-00115) is based on experiments conducted at the Idaho National Laboratory (INL) which experienced experimental challenges that are not typically encountered in traditional soil and rock testing, as discussed in “*Hydraulic and Physical Properties of MCU Saltstone*” (WSRC-STI-2007-00649). These challenges resulted in the following non-standard conditions which introduce uncertainty into the results: (i) modification of standard tests, (ii) inconsistent sample preparation, (iii) hydraulic analyses being obscured by the generation of gas within the saltstone samples, (iv) inability to meet the requirements of minimizing the effects of the matrix potential gradient for the samples, (v) limited drainage of the samples, and (vi) the assumption of a residual moisture retention value in the samples that is in contrast with the literature (WSRC-STI-2006-00198; Vanapalli, 1998).

Case E and the increased hydraulic conductivity case discussed in Section 5.6.6.7 address the uncertainty in flow through saltstone by assuming it the bulk saltstone to be degraded. Cases B-D and the synergistic case address uncertainty in the flow through saltstone by assuming saltstone to be fractured. However, due to the uncertainty in the characteristic curves for intact saltstone and fractured saltstone, as discussed in this comment and comment SP-4, it is not clear how conservative these sensitivity cases are. In addition, because the base case result is an important factor for compliance determination, it is important to be able to support assumptions about the characteristic curves used for the base case.

Path Forward

Provide additional justification for the moisture characteristic curve for intact saltstone implemented in the PA model by addressing the experimental sources of uncertainty described in the basis. Alternately, provide updated results of Cases A, B, C, D, the synergistic case, and the sensitivity case in Section 5.6.6.7 that use a characteristic curve for intact saltstone that is more consistent with results in the literature. Any updated analysis should be consistent with the response to SP-4.

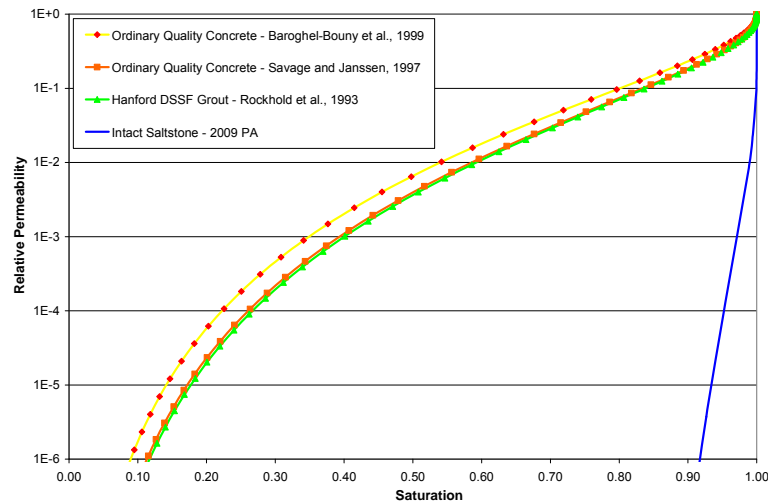


Figure 1: Moisture characteristic curves adapted from the PA and WSRC-STI-2006-00198

RESPONSE SP-3:

The DOE agrees that the moisture curves based on the INL dataset and utilized in the SDF PA are somewhat inconsistent with literature. The INL relative permeability curve, based on a limited moisture retention dataset, suggested that small changes in moisture content near saturation result in a significant decrease in hydraulic conductivity. Characteristic curves have been developed based on our most recent testing which are similar to those derived from the Hanford DSSF grout presented in PA Reference WSRC-STI-2006-00198. The relative permeability curve based on this recent testing resulted in a more gradual decrease in hydraulic conductivity with decreasing moisture content. This most recent testing and the development of the characteristic curves are documented in *Hydraulic and Physical Properties of ARP/MCU Saltstone Grout*, SRNL-STI-2009-00419. Figure SP-3.1 illustrates the comparison of the relative permeability curves based on this recent testing (labeled as Saltstone Relative Permeability using Simulant as Test Fluid), used in the SDF PA (labeled as Saltstone Relative Permeability used in Vadose Zone Model), and derived in WSRC-STI-2006-00198 (labeled as Estimated Saltstone Relative Permeability).

To acknowledge results from this recent testing and to evaluate the impact of using modified moisture characteristic curves, the Base Case was rerun in PORFLOW as a sensitivity case fixing the relative permeability to 1.0 throughout the saltstone saturation range used in the model (1.0 to 0.86). To determine the impact of using this revised relative permeability for saltstone, the radionuclides I-129, Th-230, Pu-238, U-234, and Tc-99 were run in the PORFLOW transport model to determine the flux (in pCi/yr) to the water table from Vault 4 and an FDC. These radionuclides were chosen to address the most dose sensitive radionuclides with Th-230, Pu-238, and U234 included because their decay contributes to Ra-226. Including Th-230, Pu-238, and U234 in the run also allows an assessment of radionuclides that are less mobile in cementitious material.

Figures SP-3.2 through SP-3.4 illustrate the estimated flux at the water table from Vault 4 for I-129, Ra-226, and Tc-99, respectively, during the compliance period of 10,000 years. Figures SP-3.5 through SP-3.7 illustrate the estimated flux at the water table from an FDC for I-129, Ra-226, and Tc-99, respectively, during the compliance period of 10,000 years. These figures

indicate that the value of relative permeability used for saltstone has no appreciable impact on the shape of the release rate curve for these dose sensitive radionuclides during the compliance period.

Review of the flux data shows that the magnitude of the release rate from Vault 4 based on this sensitivity case is less than twice that of the Base Case for Tc-99 and less than a 30% increase of the Base Case for either I-129 or Ra-226 during the compliance period. For the FDC, the magnitude of the release rate from the FDC based on this sensitivity case is approximately twice that of the Base Case during the compliance period. As shown in Table 5.5-4 the FDCs contribute only 0.1 mrem to the Sector B peak dose in the compliance period. Review of PA Table 5.5-1 indicates that these increases in the release rate would not significantly impact the resulting dose to the MOP during the compliance period.

In support of the response for RAI VP-2, the synergistic case discussed in the SDF PA Section 5.6.6.5 was also rerun with the revised saltstone relative permeability (equal to 1.0) as a sensitivity case. The synergistic case assumes earlier degradation of the closure cap, early degradation of the disposal unit concrete, and cracked saltstone with 100% oxygen saturation in the cracks. The results of this sensitivity case also showed no significant impact on the resulting dose to the MOP.

Based on the results indicated here for the Base Case, and the results indicated in the response to RAI VP-2 for a significantly degraded saltstone and disposal unit condition, it is inferred that the saltstone permeability curve used in the PA analysis does not appreciably impact the estimated dose results to the MOP during the compliance period for any of the cases analyzed in the SDF PA.

Figure SP-3.1: Relative Permeability for Saltstone (SRNL-STI-2009-00419)

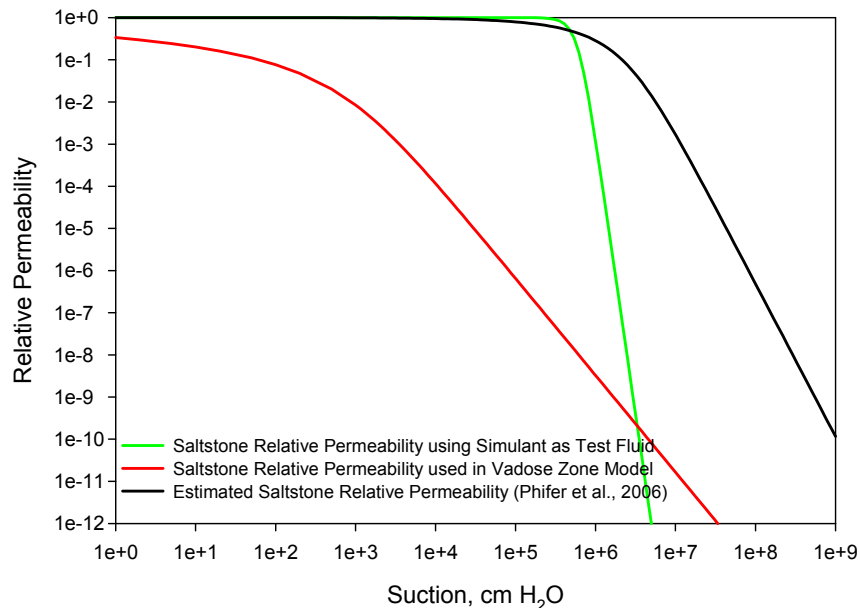


Figure SP-3.2: I-129 Flux at Water Table from Vault 4

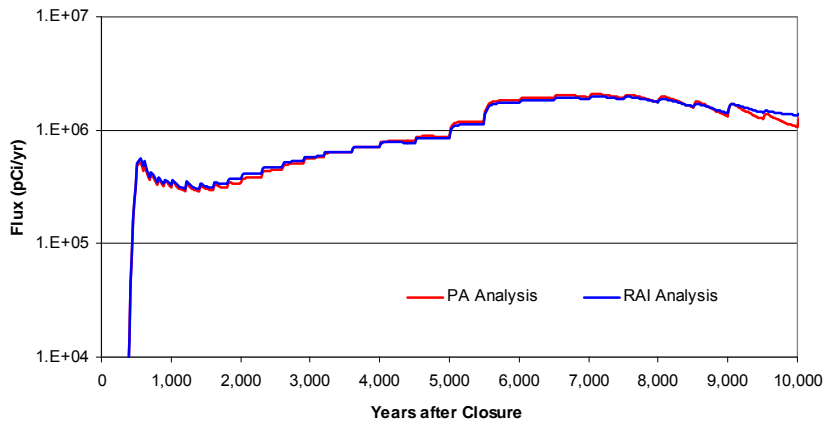


Figure SP-3.3 Ra-226 Flux at Water Table from Vault 4

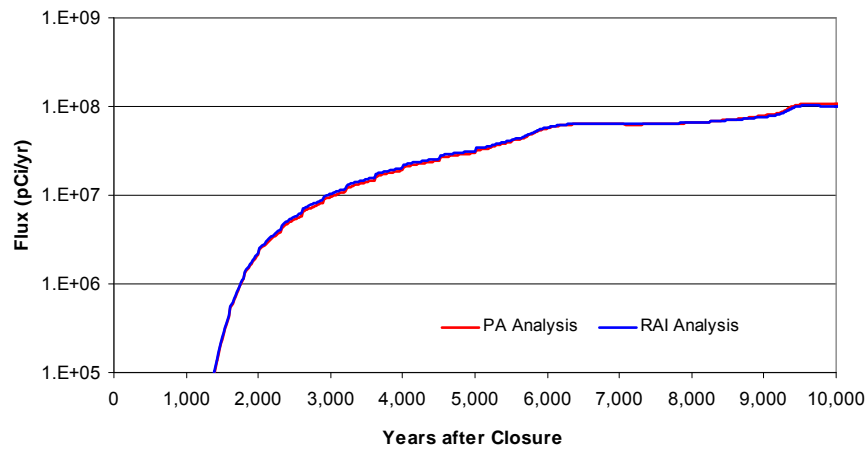


Figure SP-3.4: Tc-99 Flux at Water Table from Vault 4

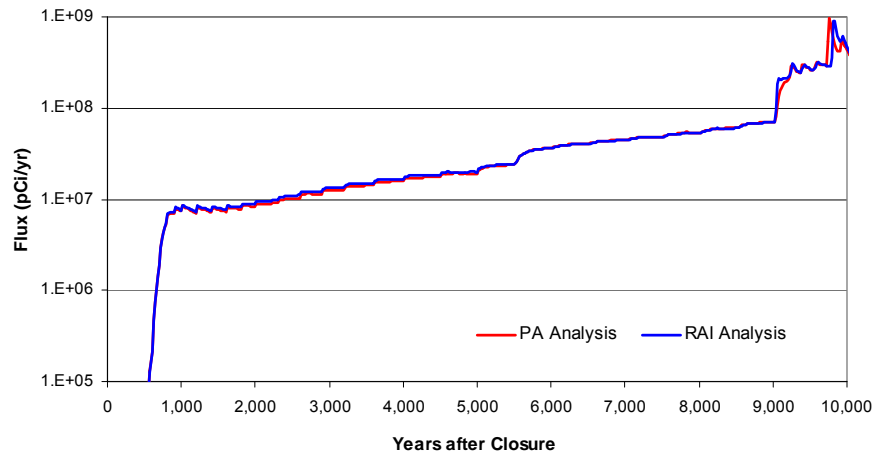


Figure SP-3.5: I-129 Flux at Water Table from an FDC

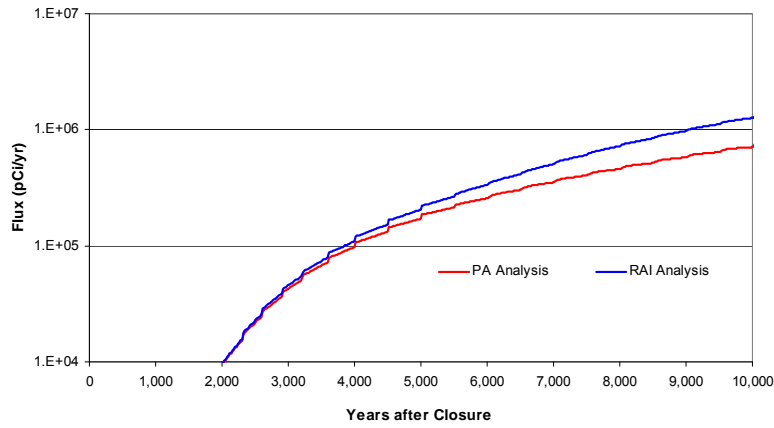


Figure SP-3.6: Ra-226 Flux at Water Table from an FDC

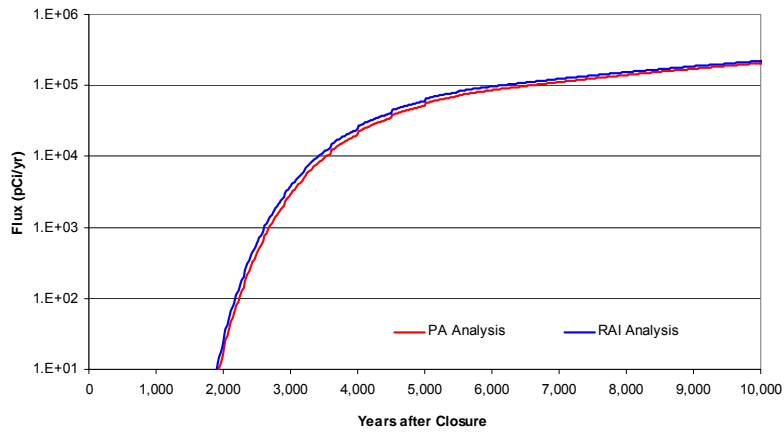
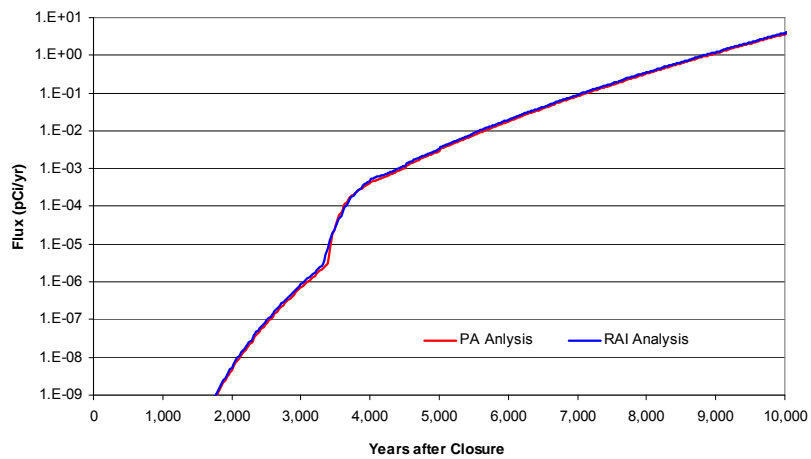


Figure SP-3.7: Tc-99 Flux at Water Table from an FDC



SP-4

Characteristic curves implemented in the PA are based on a continuum approach that does not reflect non-equilibrium flow.

Basis

The characteristic curves developed by INL (referred to in SP-3) were also used as the basis for the fractured saltstone and concrete characteristic curves (see Figure 2 below) that were developed in “Numerical Flow and Transport Simulations Supporting the Saltstone Disposal Facility Performance Assessment” (SRNL-STI-2009-00115). The authors discuss the use of an analytical approach developed by Or and Tuller (2000) to adapt INL moisture characteristic curves for cracked cementitious materials because experimental characteristic data for cracked vault concrete and saltstone grout are not available (SRNL-STI-2009-00115). However, use of moisture characteristic curves combined with coarse spatial and temporal averaging can result in an inadequate representation of non-equilibrium flow.

Path Forward

Provide additional support for the modeled flow through fractures. Model support could include field observations and laboratory experiments that verify consistency between numerical results and physical measurements.

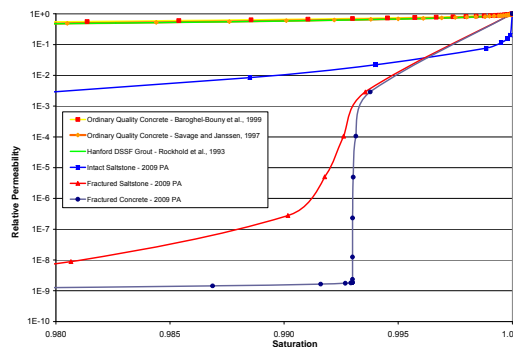


Figure 2: Characteristic curves for the intact and fractured saltstone and concrete as adapted from the 2009 PA and SRNL-STI-2009-00115

RESPONSE SP-4:

The continuum approach used to generate effective characteristic curves for fractured cementitious materials implicitly assumes chemical equilibrium between fractures and matrix. This assumption may over predict contaminant leaching, depending on fracture spacing.

The PORFLOW vadose zone flow simulations do not consider the possibility of episodic or other transient flow behavior. The cover system tends to dampen rainfall events, effectively insulating the vaults and FDCs from transient boundary conditions and lessening the possibility of a transient flow. Transient flow, if it occurs nonetheless, would presumably be in the form of periodic pulses, largely through the fracture network. This behavior would minimize contact time between water in fractures and the matrix, and potentially reduce contaminant leaching. The matrix is effectively saturated, so episodic flow would not lead to saturation fluctuations that could enhance contaminant transport within the matrix.

<p><u>SP-5</u></p>	<p>Additional support is needed for the hydraulic conductivity of intact saltstone that is used in Case A, Case B, Case C, Case D and the synergistic case.</p> <p><u>Basis</u></p> <p>In response to NRC Issue 2007-1, (NRC, 2008) DOE is in the process of completing an analysis of saltstone core samples to determine the hydraulic properties of as-emplaced saltstone grout, as described in “<i>NRC Salt Waste Monitoring Open Item Status</i>” (SRR-CWDA-2010-00009). However, because of the sensitivity of SDF performance to hydraulic properties of saltstone grout, additional information is needed to support the review of the updated PA prior to the completion of DOE’s analysis of saltstone core samples.</p> <p>The hydraulic conductivity value in the PA for intact saltstone is 2.0E-9 cm/s for Case A, Case B, Case C, Case D and the synergistic case. This value represents the recommended value for saltstone samples made from SWPF treated waste (SRNL-STI-2008-00421). Because this value represents a best estimate based on laboratory measurements of simulated samples (rather than as-emplaced saltstone), these results may not accurately reflect the hydraulic conductivity of as-emplaced saltstone. Until the testing program described in SRR-CWDA-2010-00009 is complete, a more conservative assumption may be required to account for these differences.</p> <p>The hydraulic conductivity of as-emplaced saltstone may not be well represented by the hydraulic conductivity of small laboratory-prepared samples because laboratory measurements on samples that are small relative to the field scale are unlikely to capture the heterogeneities that tend to dominate hydraulic properties. In addition, variations in field placement, consolidation, and curing conditions that are discussed in the SRS report on “<i>Hydraulic Property Data Package for the E-Area and Z-Area Soils, Cementitious Materials, and Waste Zones</i>” (WSRC-STI-2006-00198) can result in cementitious materials that vary by several orders of magnitude in hydraulic conductivity. A hydraulic conductivity value that is derived from laboratory samples may result in a value that varies significantly from as-emplaced conditions.</p> <p>In addition to the difficulty in scaling results from a laboratory-prepared sample to a large field-scale wastefrom, experimental and analytical uncertainties involved in the measurement of hydraulic conductivity should be addressed in the basis for a hydraulic conductivity value used in modeling. For example, the hydraulic testing used as a basis for the hydraulic conductivity value used in SRS’s PA model (SRNL-STI-2008-00421) does not discuss the potential reactions of Ca(OH)_2 with CO_2. As stated in the report, “<i>Hydraulic and Physical Properties of MCU Saltstone</i>” (WSRC-STI-2007-00649), the high pH of the saltstone permeant promotes the rapid dissolution of atmospheric CO_2, which readily reacts with Ca(OH)_2 to precipitate CaCO_3. The formation of CaCO_3 would significantly and perhaps artificially decrease the hydraulic conductivity of cementitious materials. Although this concern was discussed in WSRC-STI-2007-00649 for MCU samples, the hydraulic tests that form the basis for the hydraulic conductivity value used in the PA model (SRNL-STI-2008-00421) do not seem to have been conducted in a CO_2-free atmosphere, which could lead to the underestimation of hydraulic conductivity.</p>
---------------------------	---

In addition, a monitoring follow-up item (ML091320439-11) is open on the impact of varying pore solution concentration on the measured hydraulic conductivity of certain simulated samples, including the samples used as the basis for the hydraulic conductivity value used in the PA (SRNL-STI-2008-00421). In response to NRC's comment, report SRR-CWDA-2009-00009 stated that simulants were adjusted based on geochemical modeling to preclude the formation of any precipitates that would artificially lower the hydraulic conductivity SRS. In addition to the potential impacts of precipitates, there are potential impacts of the varying pore solution concentration on hydraulic conductivity. As the salt concentration in the pore water decreases with time, the permeability may increase due to changes in permeant viscosity and density caused by the significant change in salt concentration.

A second monitoring follow-up item (ML091320439-13) is currently open regarding logarithmic averaging of hydraulic conductivities of saltstone samples used as the basis for the value used in the PA (SRNL-STI-2008-00421). In response to NRC's comment, SRS discussed the basis for logarithmic averaging for skewed distributions in general (SRR-CWDA-2009-00009). However, the specific concern remains that insufficient data were collected to determine the distribution for hydraulic conductivity as hydraulic tests were only conducted on three samples. Although potential outliers may bias the data, the use of logarithmic averaging over a limited data set may not be conservative.

Although the potential for increased hydraulic conductivity is addressed non-mechanistically in the PA by sensitivity Case E and the increased hydraulic conductivity case in Section 5.6.6.7, as discussed in other comments in this section (Saltstone Performance), the conservatism of these cases is not clear. In addition, because the base case result is an important factor in compliance determination, it is important for the assumptions regarding the hydraulic conductivity used in the base case to be well supported. Accordingly, additional support is needed for the hydraulic conductivity value that was implemented in the PA for the base case.

Path Forward

Provide additional support for the hydraulic conductivity value that is implemented in the PA for intact saltstone. Additional support should include a description of how data from laboratory samples is scaled to represent full-scale, as-emplaced saltstone. Additional support should also address the specific analytical concerns raised in the basis of this comment, including the potential impact of atmospheric CO₂ on the results. Demonstrate that analyses for intact saltstone saturated hydraulic conductivity are valid over the range of pore water concentrations expected to occur over the 10,000 year compliance period. Provide justification for the logarithmic averaging of hydraulic conductivity for a limited data set or provide additional data to characterize the distribution. Alternatively, provide an updated base case analysis that uses a hydraulic conductivity value that is well supported.

RESPONSE SP-5:

Additional testing of the hydraulic and physical properties of saltstone has continued to be performed and the most recent results are documented in SRNL-STI-2009-00419. Summary hydraulic properties for saltstone samples are provided in Table 11 of SRNL-STI-2009-00419

and are reproduced below.

As noted in the comment, the hydraulic conductivity value utilized in the PA for intact saltstone is 2.0E-9 cm/s based on the saltstone testing data available at the time from SRNL-STI-2008-00421. The baseline test results from the latest testing (e.g., Batches 2-5 in Table 11) are all approximate to the Base Case hydraulic conductivity value, with the test results ranging from 1.3E-09 to 4.0E-09. SRNL-STI-2009-00419 documented the results of various tests that were performed to investigate the impact of 1) admixtures, 2) organics, 3) water to premix ratio (w/pm), 4) aluminate concentration, and 5) temperature of curing on the performance properties of saltstone. The test results suggest that the addition of admixtures, organics, and a combination of admixtures and organics did not significantly affect the performance properties of saltstone compared to the baseline saltstone mix.

Because of the uncertainty regarding parameters affecting hydraulic conductivity, several SDF PA sensitivity analyses were performed to address hydraulic conductivity variability (e.g., Section 5.6.6.7, "Increased Saltstone Hydraulic Conductivity Sensitivity Analysis") and these sensitivity analyses show that the uncertainty around hydraulic conductivity does not have a significant (e.g., less than four times) impact on the peak dose results.

The SDF PA Section 5.6.6.7 sensitivity case utilized a saltstone hydraulic conductivity of 1E-7 cm/sec, which is more pessimistic than the Base Case and represents a value higher than the baseline test results provided in SRNL-STI-2009-00419. The results of the pessimistic hydraulic conductivity sensitivity case are shown in Table 5.6-22 and Figure 5.6-85 of the SDF PA. Even with a saltstone hydraulic conductivity of 1E-7 cm/sec, the estimated dose to the MOP is much less than 25 mrem/yr.

As noted in the SDF PA Section 8.2 "Further Work of the SDF PA", the need to perform additional studies to address saltstone hydraulic properties was identified and remains an area of ongoing work. Additional information on planned work on saltstone hydraulic properties is included in SRR-CWDA-2010-00015, Section 2.3.5.

Table 11 of SRNL-STI-2009-00419: Summary Hydraulic Properties for ARP/MCU Saltstone Grout Samples

Batch	Mix ID	Description	Bulk Density (g/cm ³) ¹			Saturated Hydraulic Conductivity (cm/sec)			Permeability (darcy)			Porosity (fraction) ¹		
			Min	Max	Avg ²	Min	Max	Avg ²	Min	Max	Avg ²	Min	Max	Avg ²
1	TR545, TR546	Control - BFS/OPC	0.981	1.077	1.055	1.1E-09	2.4E-09	1.9E-09	2.3E-06	4.9E-06	4.0E-06	0.540	0.578	0.571
2	TR547, TR548	Baseline	0.924	0.970	0.951	8.8E-10	9.9E-09	4.0E-09	1.8E-06	2.0E-05	8.2E-06	0.595	0.640	0.623
2	TR548	Baseline (2 inch samples)	0.907	0.956	0.945	9.6E-10	2.1E-09	1.4E-09	2.0E-06	4.3E-06	2.8E-06	0.597	0.637	0.626
3	TR549, TR550	Baseline with Admixtures	0.935	0.979	0.960	1.1E-09	2.1E-09	1.6E-09	2.3E-06	4.3E-06	3.2E-06	0.601	0.625	0.618
4	TR557, TR558	Baseline with Organics	0.907	0.962	0.949	1.2E-09	1.8E-09	1.4E-09	2.5E-06	3.7E-06	2.9E-06	0.597	0.642	0.627
5	TR565, TR566	Baseline with Organics and Admixtures	0.952	0.967	0.959	8.4E-10	1.6E-09	1.3E-09	1.7E-06	3.3E-06	2.6E-06	0.608	0.633	0.622
6	TR575, TR576	Impact of Water to Premix Ratio	0.977	1.006	0.991	8.8E-10	2.0E-09	1.4E-09	1.8E-06	4.1E-06	2.8E-06	0.600	0.632	0.615
7	TR577, TR578	Impact of Water to Premix Ratio	0.911	0.957	0.920	8.0E-09	9.1E-09	8.4E-09	1.6E-05	1.9E-05	1.7E-05	0.623	0.672	0.638
8	TR582, TR583	Impact of Increased Aluminate	0.992	1.035	1.018	1.7E-10	4.2E-10	2.8E-10	3.9E-07	9.7E-07	6.5E-07	0.565	0.593	0.583
9	TR588, TR589	Impact of Increased Aluminate	0.923	0.963	0.945	1.9E-10	3.6E-10	2.5E-10	4.4E-07	8.3E-07	5.9E-07	0.598	0.619	0.610
10	TR602, TR603	Baseline with Organics, Admixtures, and Increased Aluminate	0.935	0.986	0.960	7.8E-10	1.4E-09	1.0E-09	1.8E-06	3.2E-06	2.4E-06	0.589	0.613	0.601
11	TR604, TR605	Baseline with Organics and Admixtures at 60° C Cure Temperature	0.910	0.958	0.939	7.5E-07	8.6E-07	8.0E-07	1.7E-03	2.0E-03	1.9E-03	0.628	0.653	0.641

¹ Includes measurements from the MCT permeability samples, the MCT moisture retention samples, and SRNL moisture retention samples.

² Arithmetic average.

<p><u>SP-6</u></p>	<p>Comment: Additional basis is required for the values of the effective diffusivity of intact and degraded saltstone used in the base case and sensitivity cases.</p> <p><u>Basis</u></p> <p>As discussed in comment SP-1, the effects of degradation of bulk saltstone (as compared to fractures in otherwise intact saltstone) are addressed in sensitivity Case E, in the synergistic case discussed in Section 5.6.6.5, and in an increased saltstone hydraulic conductivity case discussed in Section 5.6.6.7. In each of these cases, the hydraulic conductivity of saltstone is adjusted, but the effective diffusivity is kept constant at the base-case value. Because both the effective diffusion coefficient and hydraulic conductivity are intimately related to pore structure in cementitious materials, it is reasonable to expect that both coefficients would increase as saltstone degrades. The basis for adjusting the hydraulic conductivity in the sensitivity cases but maintaining the effective diffusivity at the base-case value does not appear to be addressed in the PA.</p> <p>In addition, clarification is needed of the basis for the effective diffusivity of intact saltstone. The supporting document "Numerical Flow and Transport Simulations Supporting the Saltstone Disposal Facility Performance Assessment" (SRNL-STI-2009-00115) indicates that the effective diffusivity is based on a comparison to other cementitious materials with similar hydraulic conductivities, but the specific materials used for comparison and the process by which an effective diffusivity value was selected are not provided. Table 4.4-16 of the PA indicates that the effective diffusion coefficient is based on the effective diffusion coefficient of high quality concrete in the supporting document "Hydraulic and Physical Properties of Saltstone Grouts and Vault Concretes" (WSRC-STI-2006-00198). However, the actual value of the effective diffusion coefficient for high quality concretes provided in Tables 6-44 and 6-47 of WSRC-STI-2006-00198 is 5 E-8 cm²/s, which does not match the value of 1.0 E-7 cm²/s used in the PA for saltstone. Furthermore, it is not clear why an effective diffusivity value appropriate for high quality concrete, which has a porosity of 0.11 (PA Table 4.2-16) would be appropriate for saltstone, which has a porosity of 0.58 (PA Table 4.2-16). While the choice of an effective diffusion coefficient of 1.0 E-7 cm²/s is more pessimistic than the value provided for high quality concrete in the supporting document, the basis for the effective diffusivity value chosen should be clarified.</p> <p><u>Path Forward</u></p> <p>Provide a basis for using the effective diffusivity of intact saltstone in the two sensitivity cases that address degraded saltstone listed in the basis or update the sensitivity cases that address degraded saltstone with a value of effective diffusivity that reflects the physical degradation of the wasteform. Clarify the basis for the value of the effective diffusivity of intact saltstone.</p>
<p><u>RESPONSE SP-6:</u></p> <p>While the diffusion coefficient would be expected to increase as the saltstone degrades, the transport is advection dominated except during the first few hundred years after closure as indicated by the Peclet number for Case A for Vault 4 as presented in Figure SP-6.1. As indicated in Figure 5.5-1 in the SDF PA, the peak dose in 10,000 years is in Sector B at year</p>	

10,000 and is dominated by releases from Vault 4. At year 10,000 the Peclet number is greater than 10 indicating the dominance of advective versus diffusive transport. Therefore, any change in the diffusion coefficient will not have a noticeable impact on the calculated peak dose results.

Similarly, for Case E (the configuration case with significantly degraded saltstone properties) Figure SP-6.2 presents the Peclet number for Vault 4 within 10,000 years. As indicated in Figure 5.6-72 in the SDF PA, the peak dose in 10,000 years is in Sector B at approximately year 9,400 and the Peclet number is greater than 10,000 indicating the dominance of advective versus diffusive transport. As in Case A, any change in the diffusion coefficient will not have a noticeable impact on the calculated peak dose results.

Table 4.4-16 in the SDF PA should refer to the ordinary quality concrete effective diffusion coefficient from WSRC-STI-2006-00198 rather than high quality concrete. The saturated hydraulic conductivity of the ordinary quality concrete presented in WSRC-STI-2006-00198 is $5.0E-09$ cm/s which is similar to the $2.0E-09$ cm/s modeled value used for saltstone in the SDF PA. For this reason, the ordinary quality concrete effective diffusion coefficient was used for modeling purposes as presented in SRNL-STI-2009-00115.

Figure SP-6.1: Calculated Peclet Number for SDF PA Case A

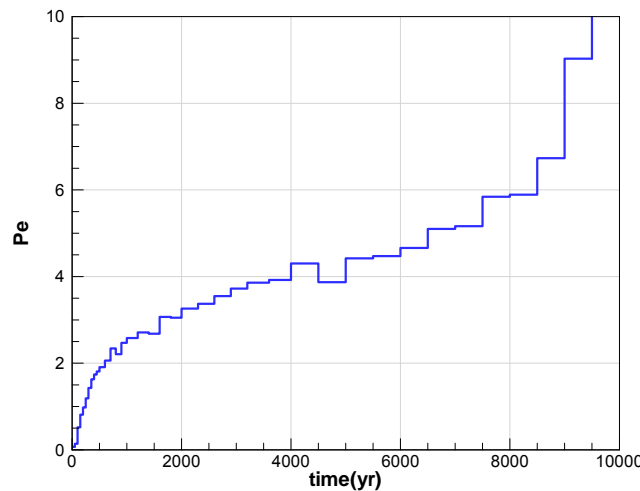
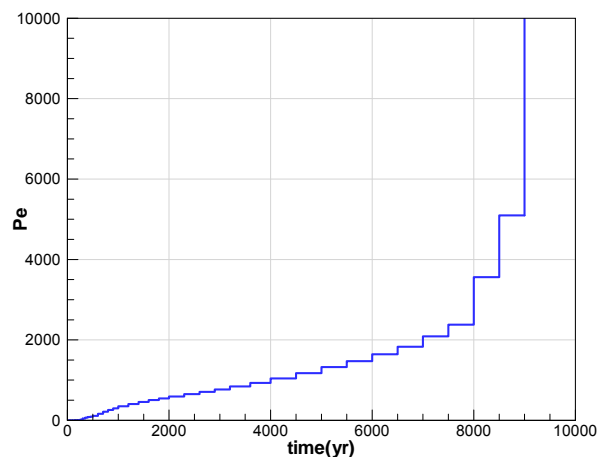


Figure SP-6.2: Calculated Peclet Number for SDF PA Case E



<p><u>SP-7</u></p>	<p>Additional bases are needed for key assumptions used in the simulation of sulfate attack with the STADIUM code.</p> <p><u>Basis</u></p> <p>SRS modeled the degradation of Vault 1 and 4 and FDC concretes due to sulfate attack using the STADIUM code. The STADIUM input parameters included the initial mineralogy, which was derived using the Samson and Marchand (2007) mass balance method that was developed for ordinary Portland cement. In SRNS-STI-2008-0050, the initial grout mineralogy for the Vault 1 and 4 surrogate and FDC surrogate was calculated using a mass balance, assuming the initial paste is made of portlandite, CSH, monosulfates, and ettringite. However, in Samson and Marchand (2007), the calculation method was applied to hydrated paste prepared from ordinary Canadian Type 10 Portland cement. The initial mineralogy for blended cements (Portland cement mixed with fly ash, silica fume, and blast furnace slag) is different from that of Portland cement, and the degree of sulfate attack also could be different. It is not evident that the mass balance method applies to blended cements. If it does not, the results of the sulfate attack calculations could change.</p> <p>The STADIUM model also relies on assumptions about CSH phase solubility. The SIMCO sulfate attack model used a simplified approach to represent the CSH phase solubility, in which the Ca/Si ratio was kept constant at 1. The approach is simpler than that of Berner (1988), who represented the CSH solid solution using different model solids for different Ca/Si ratios of 0, 0 to 1, 1 to 2.5, and >2.5. The approach used by SIMCO was validated for sulfate attack cases by Samson and Marchand (2007) and Maltais et al. (2004). However, the validation cases used Portland cements, not blended cements that are to be used for the future disposal cells. During a review of the sulfate attack model, the NRC staff questioned the use of this approach to CSH solubility (NRC, 2009). In response (SRR-CWDA-2009-00010), SRS indicated that the approach had been validated for high alkaline and high pH conditions by Henocq et al. (2007). Because this reference was not available at the web address SRS provided, it is not clear if the validation performed by Henocq et al. (2007) was based on Portland cements or blended cements similar to those that are to be used for the future disposal cells. Because of the coupled processes involved in sulfate attack, it is not evident how a more detailed model for CSH would change the results of the sulfate attack analysis.</p> <p>During the review of the sulfate attack model, the NRC staff also questioned basis for neglecting minor species such as AlO_2^-, Fe^{3+}, SiO_3^{2-}, CO_3^{2-}, and PO_4^{3-} (NRC, 2009a). In response, SRS indicated that minor species are not expected to significantly influence sulfate attack in particular or the evolution of the concrete matrix in general (SRR-CWDA-2009-00010). SRS explained that speciation of cement components such as calcium or silica are dependent on pH and that, at high pH, the concentrations of various species would be low (SRR-CWDA-2009-00010). However, the explanation did not provide a basis for concluding the concentrations would be low enough to be neglected. Because of coupled processes involved in sulfate attack, it is not evident how inclusion of these species would affect the sulfate attack analysis. Inclusion of CO_3^{2-} (due to ingress of CO_2 dissolved in groundwater or present in air) could result in the formation of CaCO_3, which also could reduce the tendency to form ettringite (and gypsum) by reducing</p>
---------------------------	---

the available Ca^{2+} in solution. On the other hand, CO_2 ingress would reduce the concrete pore water pH, which could depassivate the steel components and cause corrosion-induced cracking of the concrete.

Path Forward

Provide additional bases for the sulfate attack model, addressing the points described in the basis of this comment. Specifically, provide a basis for applying the Samson and Marchand (2007) calculation method to determine the initial methodology blended cements. Additional information could include a comparison of the calculated mineralogy of hydrated blended cements with phase composition derived using x-ray diffraction or other measurements.

Provide a basis for applying the simplified Berner (1988) approach to determining the solubility of CSH, including a basis for assuming that the approach can be applied to blended cements representative of those that are to be used for the future disposal cells (i.e., grout formulations including fly ash, silica fume, and blast furnace slag). Provide a basis for neglecting minor species, including AlO_2^- , Fe^{3+} , SiO_3^{2-} , CO_3^{2-} , and PO_4^{3-} .

RESPONSE SP-7:

The model STADIUM® was specifically developed to handle reactive transport in cementitious materials. The STADIUM® model has been applied to numerous concretes containing a variety of Portland cement and blended cement binders exposed to typical environmental conditions. Simco Technologies has assembled an extensive data basis of concrete properties that affect reactive transport and have used these properties as input to the code. Field observations and laboratory testing have been performed by Simco Technologies Inc. personnel, and the model results have been validated for numerous Portland cement and blended cement concretes. (Note: Some SIMCO tests involving blended cements were performed with private funds and are part of a proprietary material database. These data are unpublished.)

The SIMCO sulfate attack model takes into account electro-diffusion coupling between species in the flux equation in order to maintain electrical balance in the pore solution.

Given the high concentration in alkalis and hydroxide found in the sulfate solutions that are expected to come in contact with the saltstone disposal unit concretes, this approach seems justified. This strongly affects the modeling performed for the saltstone disposal unit concretes. Instead of dealing with mass balance equations that are decoupled, the equations are coupled and strongly nonlinear.

Also, the self-diffusion coefficient of each species must be provided. This sulfate attack model prevents using the common approach where the addition of transport equations allows eliminating some interaction terms and introduces the total concentration variable. Considering minor species becomes complicated by the fact that self-diffusion data are not available. It was thus decided to neglect complexation of secondary species.

Although different types of cement and supplementary cementing materials have different initial mineralogies, the bulk chemistry is basically that of clinker material made of CaO , SiO_2 , Al_2O_3 , Fe_2O_3 and SO_3 .

As reported in *Cement Chemistry* (ISBN: 0-12-683900-X), the hydration products of the different types of Portland cement are for practical purposes the same. Also reported in ISBN:

0-12-683900-X is several studies showing that Portland cement blended with slag or fly ash yielded the same hydration products as an ordinary Portland cement (i.e., CSH, portlandite, ettringite, monosulfates, etc.). However the proportions of the different minerals will be affected by the proportions of the cement and supplemental cementing materials. For instance, the addition of slag, fly ash or silica fume usually translates into more CSH being formed, at the expense of portlandite.

Calculating the initial equilibrium mineral assemblage based on the bulk chemistry (i.e., total amount of SiO₂, Al₂O₃, Fe₂O₃ and SO₃ is reasonable). However, the contribution of the different cementitious materials must be adjusted for the degree of hydration. For instance, it is well known and reported in many papers that fly ash hydrates poorly. Accordingly, the calculations can be made by assuming that 85% of cement reacts while only 40% of fly ash reacts.

A feature of reactive transport codes is that porosity is updated based on the changes in equilibrium mineralogy. The approach in *Modeling the Incongruent Dissolution of Hydrated Cement Minerals* (ISSN: 0033-8230) is an example of CSH dissolution using non-ideal solid solutions where the apparent solubility product depends on the solid composition. The simplified approach in ISSN: 0033-8230 was used to keep the calculation time over 10,000 years as short as possible, since it allows neglecting one species. Before this model was used, it had been compared to the complete model and no significant differences were observed in degradation rates.

The basis for applying the approach in ISSN: 0033-8230 was stated above (i.e., the bulk composition, thermodynamic equilibrium, of blended cements is very similar to that of ordinary Portland cement). The supplementary cementing materials used do not change the fundamental chemical characteristics of a mixture.

The measurements discussed in ISSN: 0016-7037 were performed on lab-synthesized CSH. The equilibrium results obtained for CSH at pH of 7 were in line with the experimental data compiled in ISSN: 0033-8230. (Note: ISSN: 0016-7037 pertained to the influence of alkali adsorption on CSH particles, surface properties, and solubility.)

Considering minor species becomes complicated by the fact that there is no self-diffusion data available. The model was therefore simplified to neglect complexation of secondary species. The simulation results presented in *Modeling the Effect of Temperature on Ionic Transport in Cementitious Materials* (ISSN: 0008-8846) do not discount electro-diffusion, but the model has been shown to successfully reproduce experimental observations even though secondary species are neglected. The argument for electro-diffusion coupling is supported by a recent paper "Cement and Concrete Composites", Volume 32, Issue 5, *On the Relevance of Electrochemical Diffusion for the Modeling of Degradation of Cementitious Materials*. [ISSN: 0958-9465]

SP-8

The initial grout mineralogy used in evaluating expansive phase precipitation is inconsistent with the initial mineralogy used to determine Eh and pH transitions in pore fluids. Depending on which initial mineralogy is more appropriate, the conclusions of either report could change.

Basis

WSRC-STI-2008-00236 and SRNL-TR-2008-00283 address expansive phase precipitation in saltstone and the Eh and pH transitions in pore fluids, respectively. In both reports, normative calculations were done to estimate the initial mineralogy

of saltstone and concrete. However, in WSRC-STI-2008-00236, the saltstone initial mineralogy comprised CSH, hydrotalcite, gibbsite, quartz, hematite, and gypsum; the concrete initial mineralogy comprised CSH, hydrogarnet, ettringite, and portlandite. On the other hand, in SRNL-TR-2008-00283, the saltstone initial mineralogy comprised CSH, hydrotalcite, kaolinite, quartz, hematite, gypsum, and pyrrhotite; the concrete mineralogy comprised CSH, hydrotalcite, gibbsite, quartz, hematite, gypsum, and pyrrhotite. In addition, the initial mineralogies in the two reports are inconsistent with that in SRNS-STI-2008-00050, which used a different normative method. Using a different initial mineralogy could result in a different conclusion regarding the likelihood of expansive phase formation or the calculated pore volumes for Eh and pH transitions.

Path Forward

Provide a basis for using different initial mineralogies in the calculations described in the basis of this comment, or provide information that demonstrates the calculation results are not significantly affected by the differences in initial mineralogy.

RESPONSE SP-8:

The mineralogy used in WSRC-STI-2008-00236 and SRNL-TR-2008-00283 reflect the evolution of the saltstone formula. WSRC-STI-2008-00236 was initially prepared in 2006, though not issued until 2008. It used the saltstone formulation listed in the 1992 radiological performance assessment (WSRC-RP-92-1360) for the SDF. SRNL-TR-2008-00283 used an updated formulation from WSRC-TR-2008-00037. WSRC-STI-2008-00236 was intended as a preliminary look at the potential for expansive phase formation in saltstone. Experimental analysis is ongoing and will be reported when the results become available.

Major differences in the saltstone and disposal unit formulations used in the type of simulations done in SRNL-TR-2008-00283 will result in differences in the calculated pore volumes for E_h and pH transitions. In these simulations the E_h transition is directly related to the amount of slag in the formulation. The pH transition from Region II to Region III is related to the amount of CSH in the cementitious mineralogy. In the normative mineralogical calculations, CSH is formed from calcium, added as Portland cement, and silica added as fly ash, blast furnace slag, or silica fume. If the amount of silica exceeds the amount of calcium, then the formation of CSH is calcium limited. In this case, the case for the formulations used in SRNL-TR-2008-00283, the amount of normative CSH will be proportional to the amount of Portland cement.

The UA/SA were performed for the SDF PA using a probabilistic model (i.e., the GoldSim model). To provide insight into the effects of source term release model uncertainty on the dose results, variability was incorporated into the model for the transition times between chemical states (detailed in the SDF PA Section 5.6.3.4). While the Base Case modeling represents the best estimate of source term release behavior, the impact of uncertainty in calculating pore water transitions which will affect the E_h and pH transitions has been addressed in the UA/SA.

The analysis conducted to calculate these transition times is provided in SRNL-TR-2008-00283 and recommends a $\pm 50\%$ modeling uncertainty on the pore volumes. Thus, the GoldSim model includes a stochastic analysis on transition times as shown in SDF PA Table 5.6-6 using a uniform distribution with the mean value being the calculated values taken from Table 4.2-1. This uncertainty directly addresses the variability in the source term release

behavior noted above.

SP-9

Uncertainty in groundwater composition was not considered in the Geochemist's Workbench simulations to estimate Eh and pH transitions in pore fluids.

Basis

Supporting reference SRNL-TR-2008-00283 indicates that the groundwater composition used in all the simulations of Eh and pH evolution is based on an analysis of a sample from a water table monitoring well in the vicinity of the Saltstone facility reported in WSRC-RP-92-450. The referenced report tabulates numerous groundwater compositions, and the basis for selecting the specific groundwater composition for the Geochemist's Workbench simulations is not evident. Furthermore, it is not clear whether a water sample taken from the water table aquifer would be representative of water chemistry in the unsaturated zone.

Path Forward

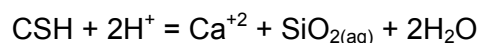
Clarify the basis for the selected groundwater composition used in SRNL-TR-2008-00283, addressing how well it represents the chemistry of water in the unsaturated zone. Alternately, provide information showing the effect of variation in SRS groundwater composition on the Eh and pH transitions, including any expected differences between the chemistry of the water samples addressed in WSRC-RP-92-450 and water in the unsaturated zone, is bounded by the estimated ± 50 percent uncertainty in Eh and pH transition pore volumes. Provide reference WSRC-RP-92-450.

RESPONSE SP-9:

The groundwater composition used to simulate E_h and pH transitions in cementitious materials was an analysis from the background well P27D. [WSRC-RP-92-450] The P-well clusters were installed across SRS to serve as background wells. P27D is a water table well located approximately 1.8 km south of the SDF.

The primary parameters in infiltrate pertinent to the E_h and pH transitions of cementitious materials are pH and dissolved oxygen concentration. A dissolved oxygen concentration in equilibrium with atmospheric oxygen (8.0 mg/L) was used rather than the dissolved oxygen concentration measured in the well (1.2 mg/L). This was done to account for the possibility of higher dissolved oxygen in unsaturated zone pore water. Equilibrium with atmospheric oxygen provides the highest possible dissolved oxygen concentration, and hence the quickest E_h transition possible for the type of analysis done in SRNL-TR-2008-00283. Had 1.2 mg/L been used for the dissolved oxygen concentration, the E_h transition times (number of pore volumes of infiltrate) would have been approximately 6.7 times longer.

The pH transition time (Region II to Region III) is controlled primarily by the reaction:

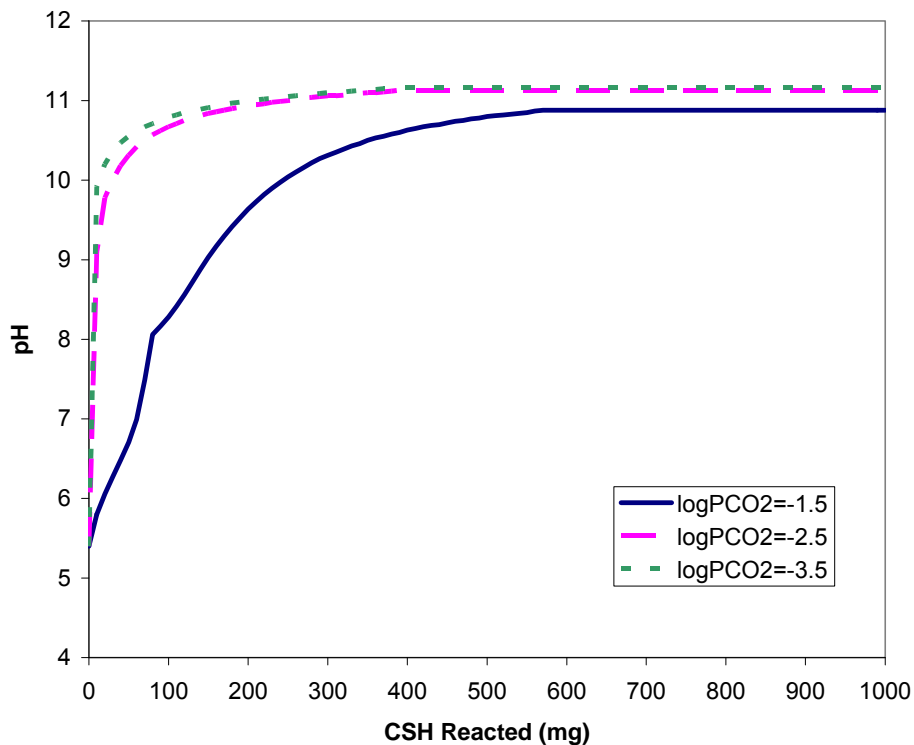


The transition from Region II to Region III in these simulations occurs when all the CSH is dissolved. Therefore, the transition time is related to pH of the infiltrate. Lower infiltrate pH results in faster transition from Region II to Region III. The median and the mean of the pH values of water table wells reported in WSRC-RP-92-450 is 5.6. The pH of the groundwater

composition used in SRNL-TR-2008-00283 was 5.4.

The composition of a water table well that is screened in a lithology that is similar to the unsaturated zone is likely to be a good estimate of the unsaturated zone pore water composition. The primary difference might be the dissolved O₂ and CO₂ concentrations. The dissolved O₂ concentration is addressed above. Partial pressures of CO₂ in soil gas are often higher than atmospheric and this is reflected in the P27D groundwater composition. The calculated log PCO₂ is -2.6 compared to -3.5 for log PCO₂ of the atmosphere. At the pH of the groundwater, variations in PCO₂ do not significantly change the groundwater pH. Nor do variations in PCO₂ significantly alter the equilibrium pH of CSH reacted with the groundwater. Figure SP9-1 shows the pH evolution as CSH is reacted with a groundwater at pH 5.4 at different log PCO₂ values. The equilibrium pH is identical for log PCO₂ values of -3.5 and -2.5. For log PCO₂ = -1.5 the equilibrium pH of CSH is 10.9. What does change is the amount of CSH dissolution required to reach equilibrium. Again, this is nearly identical for log PCO₂ values of -3.5 and -2.5, but is about 50% more for log PCO₂ = -1.5. Thus, if there were a rather extreme partial pressure of CO₂ in the unsaturated zone it could reduce the transition time from Region II to Region III. However, there is no reason to expect such a condition at the SDF.

Figure SP9-1: pH Evolution as CSH is Reached



The UA/SAs were performed for the SDF PA using a probabilistic model (i.e., the GoldSim model). To provide insight into the effects of source term release model uncertainty on the dose results, variability was incorporated into the model for the transition times between chemical states (detailed in the SDF PA Section 5.6.3.4). While the Base Case modeling represents the best estimate of source term release behavior, the impact of uncertainty in calculating pore water transitions has been addressed in the UA/SA.

SP-10

There are indications that some measured plutonium and neptunium sorption

coefficients in cementitious materials could reflect solubility rather than sorption, which could lead to a significant overestimate of plutonium and neptunium sorption.

Basis

The PA radionuclide release model uses K_d values to simulate the release of radionuclides from the saltstone waste form. A recent DOE-sponsored saltstone and concrete sorption study found that dissolved plutonium and neptunium concentrations were actually controlled by solubility during experiments originally thought to measure sorption (SRNL-STI-2009-00636). If a dissolved concentration in a sorption experiment is controlled to the solubility limit, the apparent K_d calculated from the experiment will be an overestimate. It is not clear from the sorption studies forming the basis for the K_d values for plutonium and neptunium used in the PA (WSRC-STI-2007-00640, SRNS-STI-2008-00045, and SRNL-TR-2009-00019) whether solubility effects had been ruled out. The use of K_d values based on sorption experiments in which solubility was actually the controlling process could lead to underestimates of radionuclide release rates.

Path Forward

Provide a basis for concluding that the K_d values for plutonium and neptunium used in the PA were not influenced by solubility limits during the sorption experiments used as a basis for the values, or analyze the effects of using alternate (non-solubility limited) K_d values on the performance assessment results.

RESPONSE SP-10:

As stated in the SDF PA Section 8.2, the PA will be reviewed as additional information and studies are conducted to verify that it continues to adequately bound the SDF model inputs. New information regarding plutonium and neptunium sorption in concrete and saltstone cementitious material has been reported since the issuance of the SDF PA, in SRNL-STI-2009-00636, and the impact of the new data to the expected dose calculated in the PA is small, for the reasons outlined below.

SRNL-STI-2009-00636 states that plutonium and neptunium dissolved concentrations remain relatively constant in recent batch sorption experiments, and are therefore interpreted as being solubility limited rather than sorption controlled. The models supporting the SDF PA (i.e., PORFLOW and GoldSim) do not use solubility constraints to control the dissolved concentration of plutonium and neptunium released from the saltstone wasteform, but instead use apparent K_d values.

As indicated in the Basis section above, it is possible that the K_d s used in the PA are an overestimate, if the process controlling the experimentally derived K_d s were, in fact, controlled by solubility rather than sorption. However, as indicated in the SDF PA Section 5.6.5 and in Tables 5.6-14 and 5.6-15, plutonium and neptunium K_d s for cementitious material did not show up as being important dose drivers (as are certain K_d s in soils) in the parameter sensitivity analysis performed with the GoldSim model. This is supported by results from a new sensitivity run conducted using the SDF GoldSim deterministic model for Case A and Case C with the plutonium and neptunium K_d s for cement and saltstone material set equal to zero. Although setting the plutonium and neptunium K_d s equal to zero is unreasonably bounding, even for a solubility controlled environment, the sensitivity run provides bounding information regarding the impact of potentially overestimating plutonium and neptunium K_d s on dose results.

Sensitivity runs were made with the GoldSim transport model to estimate the impact of the dose to the MOP during the compliance period if neptunium and plutonium were solubility controlled. The GoldSim transport model was utilized with the K_d values for neptunium and plutonium set to effectively zero to simulate no retardation of neptunium and plutonium in cementitious material. The results of these sensitivity runs indicate that the dose to the MOP during the compliance period is increased by a factor of less than 3 for the Base Case and less than a factor of 1.1 for Case C.

Therefore, based on the analysis presented in the SDF PA Section 5.6.5 and the sensitivity runs mentioned above, DOE concludes that any overestimation of plutonium or neptunium K_d s on cementitious material would not impact the overall conclusions of the PA.

SP-11

In recent experiments used to help define K_d values for cementitious materials, the distinction between “middle” and “old” age conditions was based chiefly on water chemistry—not on the mineralogical assemblage. It is not clear whether the differences in solid phases for the different stages can be neglected.

Basis

Recent SRS experiments (SRNS-STI-2008-00045) studied sorption coefficients for middle- and old-aged cementitious materials by using aqueous solutions equilibrated with portlandite and calcite, respectively. The two sets of experiments used essentially the same solid phase assemblages, whether fresh concrete or saltstone, or partially oxidized saltstone. This approach neglects the potential differences in mineralogical assemblage under the two sets of conditions. For old materials (i.e., Region III of Bradbury and Sarott, 1995), no portlandite is present and CSH phases continually decline in favor of other minerals (e.g., quartz and calcite). This transition could lead to less sorptive minerals and lower available surface areas for sorption.

Path Forward

Comment on the potential effect of mineralogical changes on K_d values as the concretes and saltstone transition from middle to old age, and whether neglecting the potential effects of mineralogical differences on K_d values could have led to underestimates of radionuclide release rates.

RESPONSE SP-11:

As described in the SDF PA Section 4.2.2, source term release from the saltstone waste form and the concrete of the vaults and FDCs is a function of the K_d s used for the different states of the cementitious materials. K_d s are estimated for middle-age (pH above 11) and old-age (pH below 11) concretes using aqueous solutions equilibrated with portlandite and calcite, respectively. [SRNS-STI-2008-00045] Aqueous portlandite is used to represent pore water in a young saltstone under oxidizing conditions, and aqueous calcite is used to represent pore water in an aged saltstone under reducing conditions. These sorption tests are meant to represent benchmarks to help in the selection of K_d values in the different cement stages. The different experimental conditions are used to estimate sorption under extreme sets of conditions. In general, the recommended values are reduced from the measured experimental values to account for uncertainty, such as the uncertainty associated with the solid mineral phases.

Decreased sorption as a result of evolving mineral assemblage is not expected to be

significant in the wastefrom because the timing of re-crystallization of reducing old-age concrete is after the performance period, and because a decreasing trend between middle-age and old-age cement K_d s was implemented in the PA to account for this type of uncertainty.

ISSN 1019-0643 suggest that for redox sensitive radionuclides, sorption could decrease with decreasing CSH content, resulting from the lower pH levels (approximately 10) reached in old-age cements. Although the gradual re-crystallization process to calcite and quartz minerals may lead to a reduction in the surface area for sorption, it is not expected to lead to any sorption site saturation effects due to the generally very low concentrations of radionuclides present. In fact, re-crystallization could result in sorbed radionuclides incorporated within the re-crystallized structure, thus limiting radionuclide releases as discussed in ISSN 1019-0643.

It is also likely, that the decreasing pH of the pore waters expected in old-age concrete will lead to increased precipitation of iron as iron oxyhydroxides-ferrihydrite, which increases the surface areas available for sorption. Additionally, as the pore waters approach more neutral values the actinide (e.g., plutonium, americium, thorium, uranium) solubility decreases and these radionuclides are more likely to precipitate out (e.g., see decreasing concentration with increasing pH in WSRC-TR-2006-00004, Figure 2). Therefore it is likely that any decreased sorption effects of the evolving mineral assemblage with pH is counteracted by both the increased sorption onto iron oxyhydroxides and the immobilization of actinides as they precipitate.

The chemical transition (from reducing to oxidizing and from middle-age to old-age) times for cementitious materials in SDF are presented in Table 4.2-17. The table indicates that some of the concrete within the roof, wall, and floors of Vaults 1, 4 and in the FDCs may transition within 20,000 years. However, based on the experiments in SRNL-TR-2008-00283 and assuming Base Case infiltration rates through the closure cap and disposal units, the reducing to oxidizing and middle-age to old-age transition for saltstone is not expected to occur during the performance period (SDF PA Section 4.2.2), therefore any potential K_d variations as a result of evolving mineralogic assemblage would be precluded.

Table 4.2-18 provides K_d values used in the PA for cementitious materials in different age states. For the risk significant radionuclides that are redox sensitive (i.e., I-129, Np-237, and Pa-231), K_d values are modeled as decreasing from middle-age to old-age, while Tc-99 is handled separately using the shrinking-core model. The K_d values in the PA model do follow the general trend of decreasing sorption with increasing quartz precipitation, and therefore do not underestimate radionuclide releases. For additional information and justification for the iodine and radium (not redox sensitive) K_d used in the model, please see the response to RAI SP-14.

As identified above, there is a potential for sorption of key radionuclides onto old-age concrete to decrease with increasing precipitation of quartz as CSH gel dissolves. Any potential impact this may have on underestimating releases from the wastefrom are considered insignificant, because countering factors would tend to immobilize these same radionuclides under the old-age conditions, either by incorporation into the re-crystallized structures, increased sorption to iron oxyhydroxides, or by increased precipitation of the radionuclide itself, effectively canceling out the effects. It is also proposed that the K_d s used in the PA are conservative in that they do reflect a decreasing trend in K_d s from middle-age to old-age cementitious material.

<p><u>SP-12</u></p>	<p>Model support is needed for the process models supporting PA predictions of Eh–pH evolution for cementitious materials.</p> <p><u>Basis</u></p> <p>In the report SRNL-TR-2008-00283, SRS developed a geochemical model for transitions in Eh and pH in pore waters of concrete and saltstone using Geochemist’s Workbench. The calculated pore volumes required for the transitions were used directly in the PA to establish appropriate K_d values for radionuclide release. The calculations were used, for example, as a basis for the conclusion that saltstone will remain reducing and middle-aged throughout the period of performance. This model is subject to uncertainties discussed in the report and others not discussed (e.g., mineralogical assemblage). The model results have not been validated by any objective comparisons to data or other information independent of model development.</p> <p><u>Path Forward</u></p> <p>Provide model support for the Geochemist’s Workbench results regarding pore fluid volumes necessary for transitions in Eh and pH of pore fluids in cementitious materials (SRNL-TR-2008-00283). For example, model support could include a comparison of model results with the results of pH and Eh measurements in accelerated physical testing using higher flow rates than anticipated in full-scale saltstone.</p>
<p><u>RESPONSE SP-12:</u></p> <p>The lack of experimental data is the primary reason the calculations in SRNL-TR-2008-00283 were done, so that there would be an analytical basis for incorporating chemical changes of pore fluid with aging into the PA modeling. As acknowledged in the SDF PA Section 8.2 (“Further Work”), the PA is considered a living document for the closure of the SDF and additional studies may be conducted to verify that it continues to bound the SDF model inputs. It is recognized that one area of future work is further support for the source term release model, potentially including physical testing in those areas currently addressed through Geochemist’s Workbench simulations.</p> <p>The UA/SAs were performed for the SDF PA using a probabilistic model (i.e., the GoldSim model). To provide insight into the effects of source term release model uncertainty on the dose results, variability was incorporated into the model for the transition times between chemical states (detailed in the SDF PA Section 5.6.3.4). While the Base Case modeling represents the best estimate of source term release behavior, the impact of uncertainty in calculating pore water transitions has been addressed in the uncertainty and sensitivity analyses.</p>	
<p><u>SP-13</u></p>	<p>The effect of limiting the shrinking-core model to the effects of the Eh evolution of saltstone on Tc should be analyzed.</p> <p><u>Basis</u></p> <p>A shrinking-core model was used to calculate the K_d value for release and transport of technetium from individual model cells. This approach represents an enhancement in the PA treatment of release and transport. The shrinking-core</p>

model, however, does not track pH, which also affects release and transport by way of pH-dependent K_d values. As shown in Table 4.2-18, many elements experience significantly less sorption in old age grout, which may appear near fractures and edges of the saltstone wasteform, than they do in middle-age grout. The shrinking-core model also is not used to model the release of other contaminants that may show Eh dependence (e.g., neptunium and uranium). Instead, K_d values for elements other than technetium are selected based on calculated step changes in the system Eh and pH.

In general, a shrinking-core model would be expected to predict a more gradual release of radionuclides than a step-change model and, therefore, predict a lower peak dose. However, because saltstone is predicted in the base case to remain reducing middle-age grout for the entire performance period and beyond 30,000 years (Table 4.2-17), the release of some redox and pH sensitive elements may be underestimated in the base-case analysis.

Path Forward

Discuss the basis for and effects of limiting the shrinking core model to technetium and Eh only, to the exclusion of pH and other elements.

RESPONSE SP-13:

Those radionuclides with at least 0.05 mrem contribution to the all-pathways Base Case dose are Tc-99, I-129, Ra-226, Np-237, and Pa-231 (SDF PA Section 5.2.2). The radionuclide parents producing these progeny are U-235 (Pa-231 ingrowth), and Th-230, U-234, and Pu-238 (Ra-226 ingrowth). The Base Case “Key radionuclides” are defined as the set of radionuclides defined by the union of these groups. The K_d values for the key radionuclide decay chains are tabulated in Table SP-13.1 below.

Table SP-13.1: K_d Value for Key Radionuclide Decay Chains

Nuclide chain	ReMiddle K_d (mL/g)	OxMiddle K_d (mL/g)	OxOld K_d (mL/g)	OxMiddle / ReMiddle ratio	OxOld / OxMiddle ratio
Pu-238	10,000	10,000	1,000	1	0.1
U-234	2,500	250	70	0.1	0.28
Th-230	5,000	5,000	500	1	0.1
Ra-226	3	100	70	33	0.7
(Pb-210)	-	-	-	-	-
U-235	2,500	250	70	0.1	0.28
Pa-231	5,000	1,600	250	0.32	0.16
(Ac-227)	-	-	-	-	-
Np-237	4,000	1,600	250	0.4	0.16
(U-233)	-	-	-	-	-
(Th-229)	-	-	-	-	-
I-129	9	15	4	1.7	0.27
Tc-99	5,000	0.8	0.5	0.00016	0.62

Based on geochemical calculations, the E_h transition from reducing to oxidized conditions is predicted to occur before the pH transition from middle-aged to old-aged material. Therefore the K_d transitions are in the order ReMiddle → OxMiddle → OxOld for saltstone and vault/FDC concrete.

As indicated by the OxMid/ReMiddle ratio, for radionuclides other than Tc-99 there is not a significant K_d value impact as a result of the E_h transition from reducing to oxidized conditions.

In fact, the predominant contributors to dose are Ra-226 and I-129 which actually have K_d values that increase due to the E_h transition.

As indicated by the OxOld/OxMiddle ratio, there is not a significant K_d value impact as a result of the pH transition from middle-age to old-age. For radionuclides other than I-129 and Tc-99, the OxOld K_d values are lower than the OxMiddle values but are still high enough to provide retardation to movement.

For I-129 and Tc-99, the OxOld K_d values are also lower, but the OxMiddle values are already low enough to provide minimal retardation to movement so there is no significant impact. The shrinking core model for Tc-99 assumed that the K_d value becomes zero after the E_h transition and thus no pH transition was necessary after making this pessimistic assumption.

SP-14

Additional information is needed about the basis for the K_d values used for iodine and radium in cementitious materials.

Basis

The most recent report on SRS sorption studies of cementitious materials shows that a number of measurements of iodine sorption for "old" materials (i.e., equilibrated with a calcite-saturated solution) yielded negative values, indicating essentially no sorption (SRNS-STI-2008-00045, Tables 2 and 3). That report and the PA, however, retained a previously recommended K_d of 4 mL/g for iodine. If iodine does not effectively adsorb to cementitious materials under old oxidizing conditions, the use of this nonzero value could lead to underestimation of iodine release rates. (This comment applies also to old reducing conditions, but this state is not obtained in the PA.)

It is not clear why the K_d for radium in cementitious materials differs substantially for reducing and oxidizing conditions. The PA assigns a much higher radium K_d for middle oxidizing conditions (100 mL/g) and old oxidizing conditions (70 mL/g) than for middle reducing conditions (3 mL/g). In geochemical systems, radium is not redox sensitive. The large increase in radium K_d , and attendant decrease in radium release rate, as conditions become oxidizing is, therefore, unexpected. In addition, reference information was not provided for the Berry, et al. document cited in the discussion of radium K_d values under oxidizing conditions in the source document WSRC-STI-2007-00640 (Table 10).

Path Forward

Provide the basis for neglecting recent observations of a lack of iodine sorption in recommending a non-zero K_d for iodine for old cementitious materials.

Discuss the geochemical justification for the radium K_d values for cementitious materials, particularly with respect to the large increase as conditions become oxidizing. Provide information on the Berry et al. reference cited in WSRC-STI-2007-00640 Table 10.

RESPONSE SP-14:

The recommended partition coefficients used for iodine and radium in cementitious materials are reproduced here (Table SP-14.1) from Table 4.2-18 of the PA, and are discussed in the SDF PA Section 4.2.3.2.4. The iodine K_d values for all three stages of cement in a reducing environment are updated in SRNS-STI-2008-00045, based on recent batch sorption experiments. Results for iodine partition coefficients onto old-age cements in an oxidizing environment from the same report were not recommended for update because the new results do not correspond to previously reported values (Table 2, WSRC-STI-2007-00640).

Table SP-14.1: Recommended K_d s for cementitious materials from Table 4.2-18 of the SDF PA

	Reducing				Oxidized			
	Young (mL/g)	Middle (mL/g)	Old (mL/g)	reference	Young (mL/g)	Middle (mL/g)	Old (mL/g)	reference
Iodine	5	9	0	(b) Table 2 and 3	8	15	4	(a) Table 4
Radium	0.5	3	20	(a) Table 11	100	100	70	(a) Table 10

(a) WSRC-STI-2007-00640

(b) SRNS-STI-2008-00045

The recent batch experiment reported in SRNS-STI-2008-00045 analyzed I-125 as a proxy for I-129. The negative K_d values reported from the experiments suggest possible analytical error in the measurements. Therefore, the negative results for iodine K_d s for oxidized old-age cementitious material recorded in SRNS-STI-2008-00045 were not utilized and the previous “Best” estimate (4 mL/g) from Table 4 of WSRC-STI-2007-00640 is maintained for use in the PA.

The “Best” estimate K_d value for iodine is considered justified because 1) results from the batch sorption experiments shown in Table 2 of WSRC-STI-2007-00640 record values well above zero for old-age oxidized cement (14.4 mL/g +/-7.3 mL/g) indicating that using a mean value of 4 mL/g is conservative, and 2) any uncertainty in the value is captured in the uncertainty and sensitivity analysis presented in the SDF PA Sections 5.6.4 and 5.6.5.

The uncertainty distribution for old-age oxidized cements is defined by a log normal distribution surrounding the mean value of 4 mL/g +/- 1.5 mL/g with minimum and maximum values equal to 1 mL/g and 7 mL/g, respectively. Taking these factors into consideration, the “Best” estimate of 4 mL/g is considered appropriate for oxidized old-age cement.

In addition, saltstone is not expected to reach the old-age oxidizing transition time before 20,000 years (Table 4.2-17).

Table SP-14.1 provides the recommended radium K_d s for reducing and oxidizing cementitious materials used in the SDF PA. The alkali-earth metal, radium is not expected to be redox sensitive (ISSN 1019-0643). However, because the reducing values for radium are based on measured strontium K_d values, whereas the oxidizing values are based on literature reports of measured radium values, an apparent redox dependency occurs.

Radium K_d values in an oxidizing environment are selected based on the low end of the measured K_d range (50 to 530 mL/g) reported in ISBN: 1-55899-151-4 and DOE-HMIP-RR-92.061-(Pt.1), for radium onto ordinary Portland cement as a function of radium concentration. In contrast, no experimental data is available for radium K_d s in reducing environments. Therefore, the measurements for strontium sorption onto cementitious material under reducing

conditions are used as a proxy for radium. It was assumed that radium would exhibit similar sorption properties to strontium based on their chemically similar properties and their close proximity on the periodic table. However, the measured values for radium in an oxidizing environment are, in some instances, an order of magnitude greater than the measured strontium values in a reducing environment. The use of strontium K_d values in a reducing environment as a proxy for radium K_d values in a reducing environment is considered a conservative estimate (as opposed to using the oxidizing K_d values for radium). In other words, radium is not actually redox sensitive, however, since the basis for the values in the reducing environment uses strontium as a proxy, an apparent redox sensitivity is exhibited.

SP-15

The basis for the adopted technetium pseudo- K_d of 1,000 mL/g for reducing conditions is not clear.

Basis

In the shrinking core model for cementitious materials, DOE used a technetium pseudo- K_d of 1000 mL/g for reducing conditions, applied to both middle-age and old-ages. The technical basis for this value is not clear, particularly in light of uncertainties regarding recent data on technetium sorption (SRNS-STI-2008-00045) and the scarcity of other applicable data. Among the data reported in two recent site-specific studies (SRNS-STI-2008-00045 and WSRC-STI-2007-00640), only one set of technetium values—obtained from fresh reducing grout—yielded values on the order of 1,000 mL/g (WSRC-STI-2007-00640 Table 2). Values for aged reducing grout were much lower.

Additional measurements have recently been performed for the sorption of Tc and other radionuclides to saltstone formulations (SRNL-STI-2009-00636). In this report, the sorption of Tc was measured on saltstone formulations containing 45 dry wt-% (i.e., the formulation for saltstone assumed in the PA) and 90 dry wt-% reducing slag. The K_d values reported in Figure 6.16 for sample TR547 (45 dry wt-% slag) were less than 100 mL/g for both 1 and 4 days; thus, this data also does not seem to support a technetium pseudo- K_d of 1000 mL/g for reducing conditions. Note the text of the executive summary of SRNL-STI-2009-00636 states “Saltstone formulations under reducing conditions had K_d values between 32 (0 dry wt-% slag) and 4,370 mL/g (45 dry wt-% slag)”. However, the data presented in Figure 6.16 and Tables 10.22 and 10.30 of SRNL-STI-2009-00636 implies that these K_d values correspond to 45 and 90 dry wt-% slag instead of 0 and 45 dry wt-%.

Section 4.2.3.2.4 of the PA indicates that the pseudo- K_d for Tc used in the shrinking-core model is pessimistic compared to the value of 5000 mL/g recommended in Table 11 of the PA. The recommendation in Table 11 appears to be based (1) data from experiments described in SRNS-STI-2007-00640 and (2) text in Bradbury and Sarott (1995) (although not the value of 1000 mL/g actually recommended by Bradbury and Sarott [1995]). As previously discussed, the experiments in WSRC-STI-2007-00640 were based on fresh grout, which is expected to have significantly different properties from aged grout. The text of Bradbury and Sarott (1995) indicates that distribution ratios of ~5,000 mL/g have been reported using Tc (IV) at trace levels ($<10^{-11}$ M) and the reducing agent sodium dithionite. However, these results do not appear to be applicable to saltstone because saltstone does not contain a strong reducing agent such as sodium dithionite. Site-specific values based on measurements of Tc sorption to

	<p>simulated saltstone, such as the measurements recently reported in SRNL-STI-2009-00636 are expected to be more relevant.</p> <p><u>Path Forward</u></p> <p>Provide further support for the adopted technetium pseudo-K_d of 1,000 mL/g for reducing conditions in light of the data reported in SRNL-STI-2009-00636 and the uncertainties in K_d values for Tc discussed in the basis. Clarify whether the K_d values reported in the executive summary of SRNL-STI-2009-00636 apply to saltstone formulations containing 0 and 45 dry wt-% slag or formulations containing 45 and 90 dry wt-% slag.</p>
<p><u>RESPONSE SP-15:</u></p> <p>The technetium K_d value selected for the shrinking core model (1,000 mL/g) is a lower bound on the values recommended in SRNL-STI-2009-00636 for cementitious materials of varying age. The selected value also creates margin in comparison to the recommended value (5,000 mL/g) for young and medium age cementitious material. This margin can be used to account for uncertainty in the recommended value. Tc-99 release is controlled primarily by the oxidation of the initially reduced saltstone grout and concrete vault in the shrinking core simulation. The precise K_d value under reducing conditions is unimportant to the model simulation, as long as the K_d value used is relatively high in comparison to the oxidized value. Additional research activities are in progress for reduction capacity and K_d measurements.</p> <p>The SRNL-STI-2009-00636 Executive Summary should read:</p> <p><i>“Saltstone formulations under reducing conditions had K_d values between 32 (45 dry wt-% slag) and 4,370 mL/g (90 dry wt-% slag), but the system had not achieved steady state conditions at the time of measurement, thus greater sorption may likely occur under natural conditions”.</i></p>	
<p><u>SP-16</u></p>	<p>The basis for the range of reduction capacities over which the shrinking-core model transitions to oxidizing K_d values for technetium is not clear.</p> <p><u>Basis</u></p> <p>PA Figure 4.2-41 shows how the shrinking core model varies the technetium K_d for cementitious materials based on the calculated reduction capacity for a cell. Neither the PA nor the cited supporting report (SRNL-STI-2009-00115) explains how the modelers chose the reduction capacity value of 0.005 meq e-/mL at which the K_d begins to change from reducing to oxidizing. This transition is critical to the model’s prediction of when technetium becomes mobile and influences groundwater-based dose.</p> <p><u>Path Forward</u></p> <p>Provide the technical basis for the reduction capacity range over which the shrinking core model varies the technetium K_d for cementitious materials.</p>

RESPONSE SP-16:

The initial reduction capacities of the saltstone and vault concrete are 0.822 and 0.240 meq e-/g respectively. The K_d value transitions from 0 to 1,000 mL/g between 0 and 0.005 meq e-/g. The conceptual model is that Tc-99 becomes mobile when the local reduction capacity is exhausted, defined in practice to be less than 0.005 meq e-/g remaining. A relatively small value (i.e., 0.005 meq e-/g) was chosen in order to produce a smooth curve in the transition between 0 and 1,000 mL/g, which serves to both minimize the potential for numerical instabilities and eliminate the acute effects of a step change.

SP-17

Neglecting gas-phase diffusion of oxygen appears to be inconsistent with the PORFLOW result that saltstone fractures are not completely saturated.

Basis

The PA indicates that gas-phase diffusion of oxygen is neglected because saltstone is assumed to be nearly 100 percent saturated. However, the PORFLOW model indicates in some cases, fractures may experience much lower saturations. For example, the PORFLOW model indicates that, at maximum infiltration, fractures in Case C are 40 to 50 percent saturated. At lower infiltration rates, the cracks are expected to be less saturated. It appears saltstone oxidation may be underestimated in cases representing fractured saltstone (e.g., Sensitivity cases B, C, D, E, and the synergistic case).

Furthermore, as described in “*Numerical Flow and Transport Simulations Supporting the Saltstone Disposal Facility Performance Assessment*” (SRNL-STI-2009-00115) the elevated hydraulic conductivity of Case E is intended to represent “an extensive network of smaller-scale cracks”. Thus, an additional concern is that, because of the relatively larger number of (small-scale) cracks in Case E as compared to the other cases, the effect of neglecting gas-phase diffusion may be more pronounced in this case.

Path Forward

Provide additional basis for neglecting gas-phase oxygen diffusion in cases representing fractured and degraded saltstone or provide updated dose estimates for cases representing fractured and degraded saltstone considering the potential effects of gas-phase oxygen diffusion.

RESPONSE SP-17:

The SDF saltstone is assumed intact in the Base Case (Case A) simulation. The assumption of saturated conditions is considered well justified for the Base Case (Case A). In Case C and other similar fast-flow scenarios, the flow of fresh, oxygenated, water into fast-flow paths keeps the oxygen concentration near saturation, except at early times (<1,000 years) when flow through the cover system (and fractures) is very low. Oxygen delivery via the liquid phase transport alone is generally sufficient to keep fracture faces near the oxygen solubility limit for fast-flow paths that fully penetrate the entire system. The impact of not directly addressing the impact of gas phase diffusion for Case E is considered minimal during the period of performance since Case E assumes, along with extensive cracking in saltstone grout at time zero, the surrounding FDC concrete barrier is intact and effectively would maintain saturated conditions until failure of the concrete, thus supporting the assumption of saturated conditions

being a barrier to gas-phase oxygen transport.

The effect on system performance of gas-phase oxygen diffusion through vertical fractures spaced every 2.5 feet was examined in the "Synergistic Sensitivity Analysis using the PORFLOW Deterministic Model" in SDF PA Section 5.6.6.5. These fractures do not extend through the concrete barrier, but oxygen delivery via the gas-phase is assumed to occur nonetheless. Conceptually, oxygen in the air gap between fracture faces is assumed to keep dissolved oxygen at its saturation level in the matrix immediately adjoining the fracture face. In the PORFLOW implementation, the dissolved oxygen concentration in the fracture is held constant at the saturation value.

SP-18

Additional justification is required for the uncertainty ranges used for K_d values in cementitious materials.

Basis

SRNL-STI-2009-00150 uses site-specific sediment sorption data from WSRC-STI-2008-00285 (specifically, for sandy soils) as the basis for the 95 percent confidence levels applied to K_d s for cementitious materials that are used in the PA GoldSim stochastic analyses. This approach results in a range of uncertainty for K_d values of only a factor of seven (PA Table 5.6-5). No basis was presented for applying these limits, which were based on analysis of natural system media, to the cementitious materials distributions. If the true uncertainties or variabilities in cementitious material K_d values were underestimated, the PA may not have adequately represented the uncertainty of dose evaluations.

Path Forward

Provide the rationale for using the sandy-soil-based uncertainty distribution for cementitious materials K_d values and the basis for concluding that this approach does not underestimate uncertainty in radionuclide sorption to cementitious materials.

RESPONSE SP-18:

The uncertainty ranges used for K_d values in site soils are bounded as indicated in Table 5.6-5 of the SDF PA, and reproduced below as Table SP-18.1. The basis for the selection of the uncertainty distribution is presented in WSRC-STI-2008-00285. The distributions were based on >730 K_d measurements of nine radionuclides taken from 27 samples collected from the E-Area vadose and aquifer zones at SRS. The variability, range, and distribution types (log-normal or normal) were assigned and statistical tests were conducted. The variability in the distributions is attributed to general geochemical/geological differences in site soils. The general rules presented in Table SP-18.1 were applied to >50 radionuclides in the PA based on the 9 radionuclides reported in WSRC-STI-2008-00285.

An evaluation of the uncertainty ranges surrounding the site-specific cementitious K_d s is not available, therefore the general uncertainty rules used for bounding the sandy sediment was applied to cement. A larger uncertainty range was used for sandy sediments, and therefore it was deemed more conservative for the cements than the narrower band of uncertainty applied to clayey sediment. This uncertainty range is considered conservative because it is expected that SRS sediment is more heterogeneous than cementitious materials given that the latter is mixed and is composed of much fewer minerals than natural sediments. Until additional work is done to constrain the uncertainty associated with radionuclide sorption onto cementitious

material, the distributions presented are proposed as a conservative estimate, and therefore are unlikely to underestimate the true variability.

Table SP-18.1: Distribution Coefficient Variability in the GoldSim Model (reproduced from Table 5.6-5 of the PA)

Material Zone	Minimum	Maximum	Log-Normal Geometric Standard Deviation	
			GM < 4.0 mL/g	GM = 4.0 mL/g or greater
Clayey Soils (Backfill Layer)	0.5 x GM ^a	1.5 x GM	1.001 mL/g	0.25 x GM
			GM < 2.7 mL/g	GM = 2.7 mL/g or greater
Sandy Soils (Vadose Zone)	0.25 x GM	1.75 x GM	1.001 mL/g	0.375 x GM
			GM < 2.7 mL/g	GM = 2.7 mL/g or greater
Cementitious Materials	0.25 x GM	1.75 x GM	1.001 mL/g	0.375 x GM
			GM < 2.7 mL/g	GM = 2.7 mL/g or greater

(a) GM = Geometric Mean of the log-normal distribution defined as the baseline value presented in Table 4.2-15 for soils and Table 4.2-18 for cementitious materials.

Vault Performance (VP)

<p><u>VP-1</u></p>	<p>Additional analysis is needed to assess the applicability of the degradation mechanisms responsible for the observed fracturing of Vault 1 and 4 walls and the degradation mechanisms described in SRS-REG-2007-00041 to the FDCs and to other parts of Vaults 1 and 4.</p> <p><u>Basis</u></p> <p>The PA and supporting documents predict the FDC walls, floors, and roofs as well as the floors of Vaults 1 and 4 to remain essentially intact with hydraulic conductivities increasing by less than an order of magnitude by the end of a 10,000 year compliance period. This prediction is based on the conclusions of “<i>Numerical Flow and Transport Simulations Supporting the Saltstone Disposal Facility Performance Assessment</i>” (SRNL-STI-2009-00115). The walls of Vaults 1 and 4 have already shown cracking and were modeled in the PA with an increased saturated hydraulic conductivity and a relative permeability curve for fractured concrete.</p> <p>As discussed in report “<i>Z-Area Industrial Solid Waste Landfill Vault Cracking</i>”, the reinforced concrete construction of Vaults 1 and 4 was designed for gravity loads plus the hydrostatic pressure associated with saltstone grout (ESH-WPG-2006-00132). According to the report “<i>Savannah River Site Saltstone Disposal Facility Vaults 1 and 4 Overview</i>”, cracking developed in Vault 1 that may have stemmed from construction and operational events that date back to 1988 (LWO-CES-2006-00010).</p> <p>The cause of observed fracturing in the walls of Vaults 1 and 4 was determined to be (i) the hydrostatic pressure exerted by 25 ft of hydrostatic head in the gap between the cured saltstone and the vault wall, (ii) thermal shock, and/or (iii) drying shrinkage from non-ideal concrete mixing and inadequate curing practices (SRNL-STI-2009-00115). Sheet drains were installed to remove any free liquid near the inside of the wall as a defense in depth, as the FDCs are designed to handle hydrostatic fluid pressure. However, as discussed in ESH-WPG-2006-00132, Vaults 1 and 4 were also designed to handle hydrostatic pressures (although it is not clear if Vault 1 was damaged during construction and operation).</p> <p>In addition to the vault wall degradation that has been observed, additional long-term failure mechanisms may exist within the 10,000 year compliance period. Report SRS-REG-2007-00041 discussed sensitivity cases that were conducted to account for the following potential degradation mechanisms:</p> <ul style="list-style-type: none">• Cracking from seismic events and settlement• Cracking due to external static loading (weight of overburden and cap)• Chemical reactions involving the waste components in saltstone which could result in expansion and cracking• Chemical reactions involving ions in the soil which could result in expansion and cracking• Chemical reactions involving corrodents in the soil which could cause leaching and an increase in porosity and/or cracking in the vault• Physical process such as freeze-thaw cycles
---------------------------	--

Path Forward

If construction and operational events were responsible for the cracking of Vault 1 walls, discuss the current and future construction and operational activities that will prevent this type of cracking in the FDC roofs, floors, and walls as well as the floors of Vaults 1 and 4.

Provide engineering calculations to demonstrate whether the hydrostatic head of the water in the annulus between the saltstone and the vault walls was responsible for the cracking of vault 4 walls (e.g., by comparing the hydrostatic head to expected wall strength and the pressure from grout lifts). Provide engineering calculations for the hydrostatic pressure resulting from the grouting of FDCs and compare this pressure to the expected FDC wall strength.

If the failure mechanisms for the Vault 1 and 4 walls are thermal gradients or drying shrinkage, which can be expected for all cementitious material, provide a basis for assuming FDCs and the floors of Vaults 1 and 4 have not degraded similarly to the Vault 1 and 4 walls.

Provide the basis for excluding the degradation mechanisms discussed in SRS-REG-2007-00041 from the analysis of the predicted performance of the FDCs over the 10,000 year period of performance.

RESPONSE VP-1:

Design Enhancements of FDC's

The new FDC's adopt a pre-stressed cylindrical design that is similar to leak tight water tanks available in commercial service. The design incorporates Class III sulfate resistant concrete with a 28 day compressive strength rating of 5,000 psi for the cell floor, walls, and roof. Outside the cell wall is a steel shell which is covered with shotcrete. Pretensioning wires are incorporated into the design to counteract the stress of free standing salt solution in the cell. The cell roof is cast in place, Class III sulfate resistant concrete that is tied into the wall rebar. This creates an integrated structure with horizontal rather than vertical concrete interfaces that would invite rainwater infiltration. The interior of the cell is coated with an epoxy based material to protect the concrete walls from liquids (primarily bleed water) during the operational life. The entire cell structure is encased in 100 millimeters HDPE before backfill and closure cap materials are applied.

The source of cracking in Vaults 1 and 4 is due to hydrostatic pressure buildup of liquids in the spaces between the saltstone monolith and the vault wall (ESH-WPG-2006-00132). A calculation (C-CLC-Z-00016) was performed to evaluate the Vault 1 hydrostatic head stresses. This calculation concluded that the hydrostatic water head pressure exerted on the Vault 1 wall would cause deflection and cracking. Because the Vault 1 and Vault 4 wall designs are not appreciably different, a separate hydrostatic head failure calculation was not performed for Vault 4. The saltstone production process introduces liquid in the form of bleed water into the cells during filling operations. The FDC construction incorporates multiple engineered systems, structures and components to address the potential buildup of liquids inside the cell. First, a system of sheet drains is installed to collect liquid that accumulates between the saltstone monolith and the cell wall such that significant head pressure does not accumulate. The sheet drain and associated drain water piping collect liquids from the space between the saltstone monolith and the cell walls so that it can be pumped out during the operational life of the cell. Second, the cylindrical design incorporates pre-stressing wires around the outside of the concrete walls that are used to counteract the stress of free standing salt solution in the cell (T-CLC-Z-00022). Thus, if salt solution did accumulate to the full height of the

wall, this condition would not induce cracking of the wall. In addition, an interior coating is used to preclude liquids from penetrating the concrete walls during filling operations and to protect the walls from sulfate attack during the operational life.

Construction of Vaults 1 and 4 used cast in place concrete for the walls. Construction techniques for the FDC walls allow for wall panels to be cast in beds rather than cast in place. The beds maximize control over the standard curing techniques. Early in the construction process the Disposal Unit 2 walls did experience some cracking from shrinkage during the curing process. However, these cracks were identified by the QAP and repaired using standard concrete repair methods. More rigorous attention to the curing process has been effective in addressing shrinkage cracking due to the curing process.

Vault 1 and 4 Floor Cracking

SRS-REG-2007-00041 attempted to address the presence of a source term (salt solution) in the walls of the existing vaults. The mechanisms leading to the presence of source term in the wall are 1) the presence of free liquid (salt solution) in contact with the wall, and 2) a force driving the salt into the wall (head pressure). These mechanisms are absent from an analysis of the floor.

Although there may be free liquid (salt solution) in the initial saltstone introduced into the cell, it is not in significant quantities or exposure times when compared to the free liquid available to interact with the vault walls. Unlike the vault walls, that could be exposed to free liquids for the duration of salt disposal operations, once the initial layer of saltstone is poured, free liquid from subsequent pours is shed towards the walls, and not down through the hardened saltstone below. This assumption is supported by the fact that, absent any attempt to remove free liquids, there is liquid present at the saltstone/wall interface. Therefore, the source term incorporated into the vault floor is negligible when compared to the source term assumed in the vault walls.

The following addresses specific mechanisms and were qualitatively addressed in SRS-REG-2007-00041.

Seismic events are considered in the design of the FDC's. [T-CLC-Z-00022] Seismic restraints are included outside the concrete walls to address potential movement during a seismic event.

Differential settlement of the FDC's is a potential mechanism to induce cracking. As part of the overall FDC design and construction process, extensive soil investigation is performed (K-ESR-Z-00001 for Disposal Unit 2, K-ESR-Z-00002 for Disposal Units 3 and 5) and incorporated into the design calculations (T-CLC-Z-00022).

Stresses induced from overburden and the closure cap are a potential source of cracking. Stresses induced from cracking have been anticipated. [T-CLC-Z-00022] The interior coating system is flexible enough to span cracks anticipated from stress induced from overburden and the closure cap. [WB00001K_Sh 32]

Reactions from contact with Saltstone

The Class III sulfate resistant concrete credited in the PA is used in the cell itself. Components of the cell that have the potential to come in contact with the saltstone waste are limited to the walls and floor (the roof is excluded since gravity precludes a plausible mechanism which would put the roof in contact with the saltstone).

The interior coating system is installed on the walls and floor of the cell so that they do not come in direct contact with the saltstone during the operational life.

Reactions from contact with soils

The Class III sulfate resistant concrete credited in the PA does not come in direct contact with soils. The mechanisms that preclude chemicals from the soil from attacking the exterior of the cell are addressed by individual component as follows:

Cell floor: As indicated on construction drawings, a minimum 4 inches of lower concrete mud mat is poured directly on the soil. This is followed by a 100 millimeters HDPE liner, a GCL layer, and a minimum 4 inch upper mud mat. The floor of the cell is poured on top of these components. Thus, the Class III sulfate resistant concrete credited in the PA does not contact the soil directly.

Cell walls: As indicated on construction drawings, the cell wall is surrounded by a steel shell. The steel shell is covered by shotcrete. This is followed by a 100 millimeters HDPE liner. Thus, the soil backfill contacts the outer layer of HDPE and not the Class III sulfate resistant concrete. Thus, the Class III sulfate resistant concrete credited in the PA does not contact the soil directly.

Cell roof: As indicated on construction drawings, the cell roof will be covered with a 100 millimeters HDPE liner. Thus, the soil backfill contacts the outer layer of HDPE and not the Class III sulfate resistant concrete. Thus, the Class III sulfate resistant concrete credited in the PA does not contact the soil directly.

Physical process such as freeze-thaw cycles

“Deterioration of concrete exposed to freezing conditions can occur when there is sufficient internal moisture present that can freeze at the given exposure conditions. The source of moisture can be either internal (water already in the pores of concrete that is redistributed by thermodynamic conditions to provide a high enough degree of saturation at the point of freezing to cause damage) or external (water entering the concrete from an external source, such as rainfall).” [ACI 201.2R]

“The likelihood of damage from freezing and thawing is reduced by reducing the amount of water in concrete. For conventional mixtures, this has generally been accomplished by the use of a low w/cm (maximum of 0.50 for mild exposure and 0.45 for severe exposure), combined with adequate curing to ensure a minimum compressive strength of approximately 3,600 psi before exposure to repeated cycles of freezing and thawing.

Limiting the w/cm to a specified maximum value has the effect of reducing the amount of freezable water in the cured concrete initially, and requiring a minimum strength before freezing helps ensure that the fractional volume that could be occupied by freezable water in saturated concrete has been adequately reduced by the formation of hydration products.” [ACI 201.2R]

The water to cement ratio specified for FDC Class III concrete is 0.38. [C-SOW-Z-00001] This value is below the ACI water/cement ratio of 0.45 which is recommended for concrete exposed to severe conditions.

FDC Concrete Exposed to Freezing Conditions

After the operational life, the units will be surrounded with backfill and a closure cap installed so that exposure to freezing conditions is not expected. FDC concrete has the potential to be exposed to freezing conditions during the construction and operational life of the unit. The concrete itself has a low hydraulic conductivity (on the order of 1.0E-12) so rainwater infiltration adds little to the internal water available to freeze during construction. After construction is complete, the 100 millimeters HDPE precludes infiltration of rainwater.

VP-2	Additional basis is required for neglecting disposal unit degradation mechanisms other than sulfate attack.
-------------	---

Basis

Section 4.2.3.2.4 of the PA indicates that degradation of disposal unit concrete is believed to be dominated by external sulfate attack. However, the basis for neglecting other forms of degradation of the Vault 1 and 4 roof and floor, as well as the FDC roof, walls, and floors is not discussed, although other forms of degradation are possible.

For example, one of the key references supporting the calculation of sulfate attack "*Evaluation of Sulfate Attack on Saltstone Vault Concrete and Saltstone*" (SRNS-STI-2008-00050) recommends that, given the high alkalinity of the solutions used in the model, the risk of alkali silica reaction should be considered in a more global performance assessment study.

As another example, the design of Disposal Unit 2 includes significant amounts of carbon steel components (e.g., rebars, prestressing wires, diaphragms). These components could corrode, leading to expansive reactions that could cause cracks to form in the concrete. In addition, the roofs of Vault 4 and the FDCs have a significant number of steel penetrations. It does not appear that corrosion cracking around these penetrations was considered as a degradation mechanism of the Vault 4 or FDC roofs. Furthermore, because carbonate was not included in the sulfate attack model, decreasing pH due to carbonation also was excluded from the model. In particular, groundwater was assumed to be pure water at pH 7. Thus, any pH output resulting from the STADIUM sulfate attack simulations could not be relied upon to indicate whether carbon steel depassivation would occur.

Early hydraulic degradation of disposal unit roofs, floors, and walls is addressed non-mechanistically in the synergistic case discussed in PA Section 5.6.6.5. The results of this modeling case (Table 5.6-20) indicate that, even if the Vault 1 and 4 floors and roof, and the FDC floors, roofs, and walls are assumed to be hydraulically degraded to have soil properties at 500 years, the performance objective for an off-site member of the public would still be met. However, as discussed in SP-3 and SP-4, it is unclear whether the synergistic case is based on unrealistically optimistic hydraulic characteristic curves for saltstone, and, therefore, its degree of overall conservatism is unclear. It also is unclear whether a potential update to the synergistic case would also show that the performance objectives are met. Furthermore, because the base-case result is an important factor in the compliance determination, it is important to be able to understand the potential for increased hydraulic degradation of the disposal unit floors, walls, and roofs in the base case.

Path Forward

Provide justification for neglecting other forms of degradation of disposal unit cementitious materials, including alkali silica reaction, corrosion cracking, and other relevant forms of degradation. The justification should address Vault 1 and 4 floors and roofs as well as FDC walls, roofs, and floors. Alternately, the base-case model could be updated to reflect the potential effects of applicable degradation mechanisms.

If maintenance of an alkaline pH near steel components of the disposal units is relied upon to demonstrate steel passivity, the model generating predicted pH values should account for local effects near steel components (e.g., pH depression by carbonation in fractures near steel components) or address why such phenomena can be neglected.

A summary of observed reinforcement corrosion of concrete at SRS should be provided. Provide information to demonstrate that modeling of engineered systems in

	<p>this application is consistent with observed performance of analogous systems at SRS.</p> <p>If the justification for neglecting other forms of degradation is based on the results of the synergistic case, the response should be consistent with the response to other comments in this document.</p>
--	---

RESPONSE VP-2:

It is recognized that there are other concrete degradation mechanisms that may be important to the SDF PA model. Investigations on potential concrete degradation mechanisms are ongoing.

In this current PA, sulfate attack has been identified as one of the more aggressive potential degradation mechanisms. Thus, state-of-the-art computer modeling has been utilized to estimate the rate and consequences of concrete degradation from sulfate attack as described in the SDF PA Section 4.2.3.2.4.

Recognizing that other mechanisms may potentially degrade the disposal unit concrete, sensitivity analyses have been conducted and presented in the SDF PA Sections 5.6.6.3 (increased sulfate attack), Section 5.6.6.5 (synergistic case), and Section 5.6.6.6 (walls and floor of Vaults 1 and 4 are oxidized at closure). Of these sensitivity cases, the synergistic case provided the most pessimistic dose to the MOP within the compliance period of 10,000 years. Based on the concerns raised by RAI SP-3 and RAI SP-4, the synergistic case was rerun in PORFLOW using a constant saltstone permeability value of 1.0 for Vault 4 and an FDC. Further discussion on the use of a constant relative permeability value of 1.0 in saltstone is provided in the response to SP-3. The response to SP-3 evaluated the impact of this constant permeability value on the Base Case. In this response this similar sensitivity case is used to evaluate the impact of this constant permeability value on the synergistic case.

The results of this sensitivity case on the synergistic case are presented in the following figures. These figures provide the flux (pCi/yr) at the water table from Vault 4 (Figures VP-2.1 through VP-2.3) and from an FDC (Figures VP-2.4 through VP-2.6) for the most dose sensitive radionuclides: I-129, Ra-226, and Tc-99.

Figures VP-2.1 through VP-2.3 indicate that the flux curve from Vault 4 for the sensitivity case has a similar pattern as the PA Synergistic Case for the dose sensitive radionuclides. In addition, after year 1,300, the magnitudes of the individual fluxes for this sensitivity case are less than a factor of 1.1, 1.2 and 1.8 for I-129, Ra-226, and Tc-99, respectively, of the PA synergistic case during the compliance period of 10,000 years.

Figures VP-2.4 through VP-2.6 indicate that the flux curve from an FDC for the sensitivity case has a similar pattern as the PA synergistic case for the dose sensitive radionuclides. In addition, the magnitudes of the individual fluxes for this sensitivity case are less than a factor of 1.5, 1.8 and 1.6 for I-129, Ra-226, and Tc-99, respectively, of the PA synergistic case during the compliance period of 10,000 years.

The SDF PA Figure 5.6-83 shows the dose to the MOP at 100m in Sector B for the Base Case and the synergistic case. Figure VP-2.7 illustrates the contribution of the dose sensitive radionuclides to the dose in Sector B for the synergistic case. As indicated in this figure, Ra-226 is the dominant contributor to the dose in Sector B. Inspection of Figures VP-2.2 and VP-2.5 indicates that the flux from Vault 4 is more than a thousand times greater than from an FDC; thus the contribution of Ra-226 is dominated by Vault 4. Because this dose to the MOP in Sector B is driven by Vault 4 and Ra-226, the potential increase in the dose to the MOP in Sector B is estimated to be equivalent to the increase in the Ra-226 flux of approximately 10%. Thus, the estimated dose to the MOP in Sector B

is approximately 10% greater than the dose reported in PA Table 5.6-20, approximately 19 mrem/yr.

As shown in Figures VP-2.1 and VP-2.4 the I-129 flux from an FDC is greater than that from Vault 4 at later time periods and thus the dose in Sector I is dominated by the FDCs. Because this dose to the MOP in Sector I is driven by the FDCs and I-129, the potential increase in the dose to the MOP in Sector I from a single FDC is estimated to be equivalent to the increase in the I-129 flux of approximately 50%. Since multiple FDCs would contribute to the MOP dose in Sector I, the estimated dose to the MOP in Sector I would be greater than 50% of the dose reported in Table 5.6-20 for Sector I; but it would be less than the estimated dose to the MOP in Sector B reported above.

Based on this revised synergistic case sensitivity analysis, which conservatively considered the degradation of the disposal unit concrete and of the saltstone as well as a more pessimistic relative permeability for the saltstone in addition to the early degradation of the closure cap, saltstone cracked at closure to allow for oxygen diffusion with a non-depleting source of oxygen, and the FDC concrete degraded chemically to oxidizing, old-aged concrete at year 500, it is concluded that the dose to the MOP at 100m is less than 25 mrem/yr.

As stated above, the mechanisms of concrete degradation continue to be investigated as evidenced by the development of the CBP project which is a multi-disciplinary partnership of federal, academic, private sector, and international expertise. The objective of the CBP project is to develop a set of tools to improve understanding and prediction of the long-term structural, hydraulic, and chemical performance of cementitious barriers used in nuclear applications. The partners in the CBP project are the U.S. Department of Energy, the U.S. Nuclear Regulatory Commission, the National Institute of Standards and Technology, the Savannah River National Laboratory, Vanderbilt University/Consortium for Risk Evaluation with Stakeholder Participation, the Energy Research Center of the Netherlands, and SIMCO Technologies, Inc.

Further work described in the SDF PA Section 8.2 recognizes the importance of understanding and modeling of the mechanisms of concrete degradation. The PA maintenance activities (SRR-CWDA-2010-00015) which address the eight factors identified in the NRC Technical Evaluation Report on the DOE waste determination for salt waste disposal at SRS (ML053010225) include the development of a long-range program plan for on-going testing of degradation mechanisms associated with cementitious hydraulic properties.

Figure VP-2.1 I-129 Flux from Vault 4 at the Water Table for the Synergistic Case

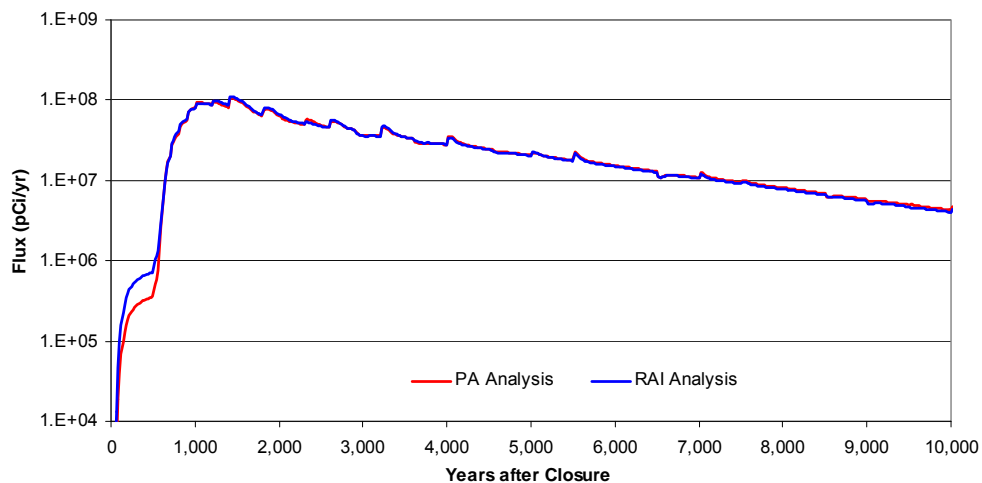


Figure VP-2.2 Ra-226 Flux from Vault 4 at the Water Table for the Synergistic Case

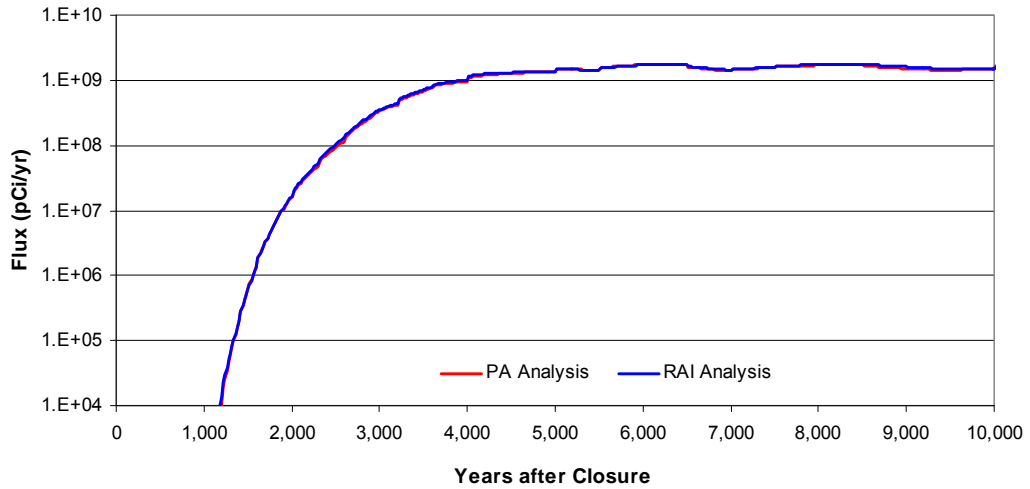


Figure VP-2.3 Tc-99 Flux from Vault 4 at the Water Table for the Synergistic Case

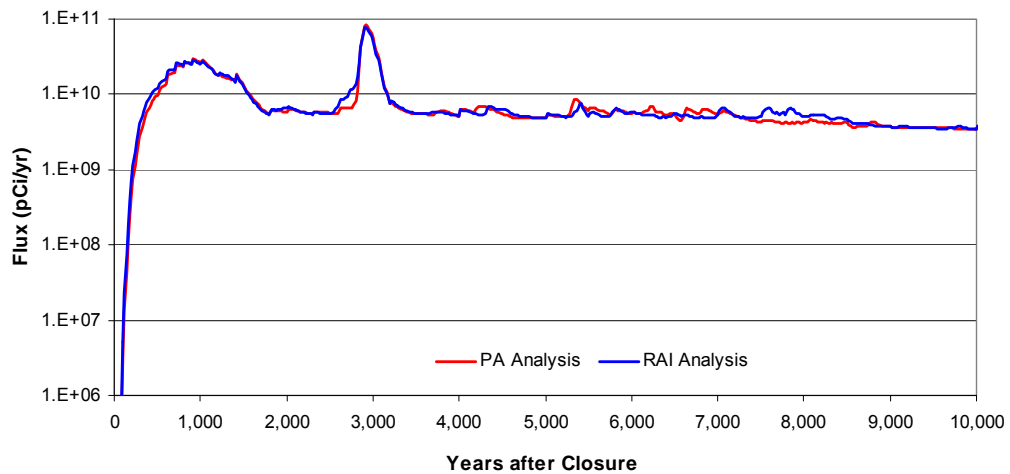


Figure VP-2.4 I-129 Flux from an FDC at the Water Table for the Synergistic Case

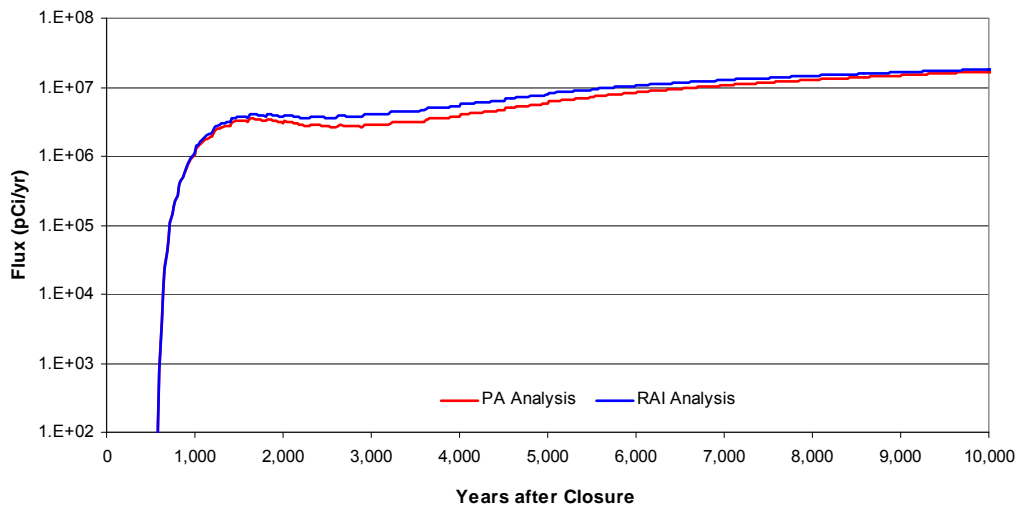


Figure VP-2.5 Ra-226 Flux from an FDC at the Water Table for the Synergistic Case

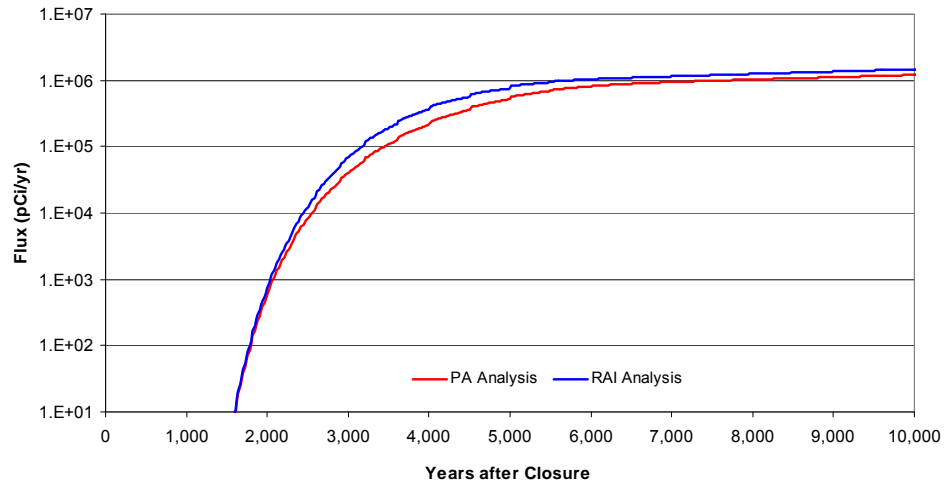


Figure VP-2.6 Tc-99 Flux from an FDC at the Water Table for the Synergistic Case

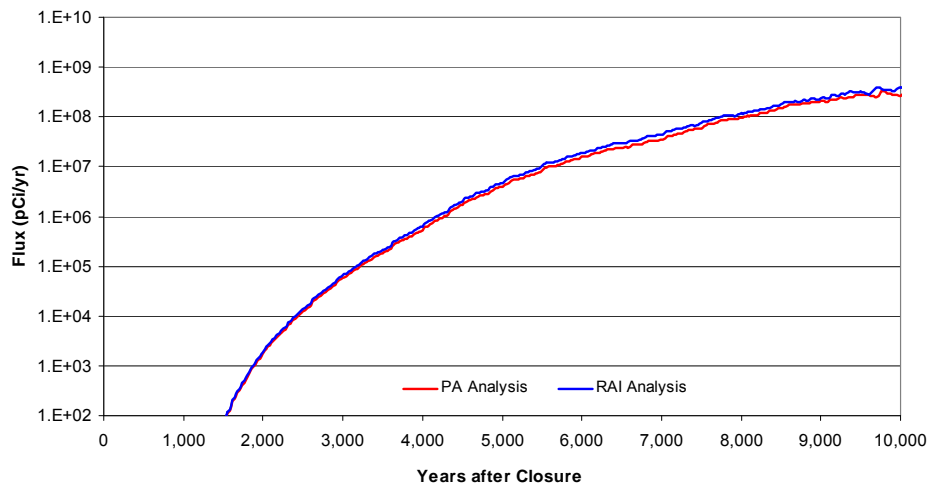
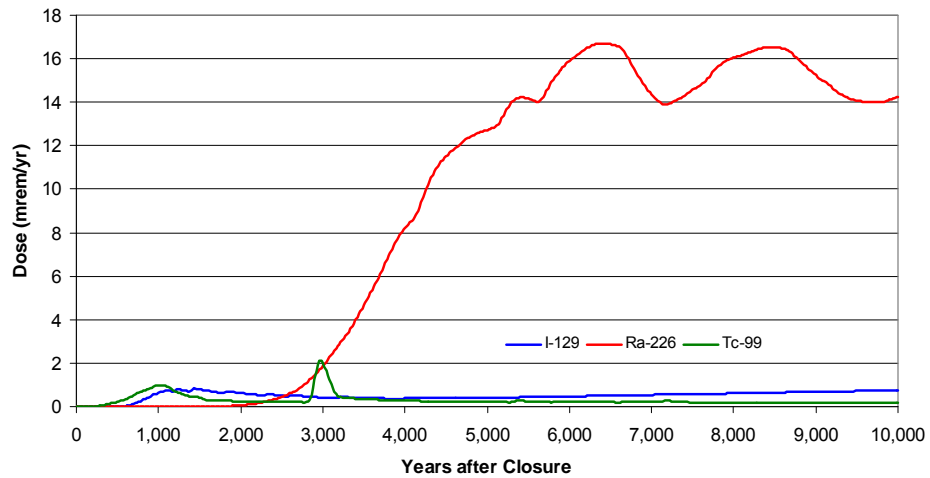


Figure VP-2.7 Contribution to the MOP Dose in Sector B for the Synergistic Case



VP-3

The effect of modeling disposal unit floors as completely reducing for the entire performance period, and beyond 20,000 years, should be analyzed.

Basis

Although a shrinking-core model was used to model the release of Tc-99 from saltstone, the vault walls and floor were presumed to be completely reducing until completely oxidized. This assumption seems unrealistic, as the vault walls and floors would be expected to oxidize near exposed surfaces and fractures just as the saltstone does. This assumption appears to be conservative with respect to the vault walls, because a more gradual release would produce a lower peak than a sudden release when the wall is presumed to fully oxidize. However, this assumption appears non-conservative in the case of the floor, which is modeled as remaining reducing beyond 30,000 years (Table 4.2-17). Thus Tc-99 release may be underestimated, because once released from the saltstone it is modeled as being strongly held in the unoxidized floor during the entire performance period, whereas chemical oxidation is expected to occur around the edges of the floor and near fractures.

Although complete oxidation of Vault 1 and 4 floors was addressed non-mechanistically in the oxidized concrete sensitivity case discussed in Section 5.6.6.6, this case does not address oxidation of the FDC floors or walls.

Path Forward

Address the effect of limiting release of Tc from the disposal unit floors by presuming the floors remain 100% reducing instead of becoming partially oxidized, as would be predicted by a shrinking-core model.

RESPONSE VP-3:

The shrinking core model for Tc-99 release and migration considered oxidation of FDC concrete (e.g. floor) in the same manner as saltstone, with the only difference being the initial reduction capacity of the two materials. The initial reduction capacities of the saltstone and vault concrete are 0.822 and 0.240 meq e-/g respectively. As such, the exposed surfaces of the vault concrete floor begin oxidizing at time zero. The SDF PA Table 4.2-17 presents the transition times for the various cementitious materials as computed within the PORFLOW model, but only applies to non-shrinking core (non-Tc-99) simulations. The shrinking core model explicitly simulates oxidation of both the saltstone and vault/FDC concrete for Tc-99 simulations.

SDF PA Table 4.2-17: Chemical Transition Times for Cementitious Materials

Cementitious Material	Vault 1		Vault 4		FDCs	
	E _h Transition (years)	pH Transition (years)	E _h Transition (years)	pH Transition (years)	E _h Transition (years)	pH Transition (years)
Roof	N/A ¹	25,400	N/A ¹	16,547	25,640	27,387
Clean Grout	NR	NR	NR	NR	NR	NR
Saltstone	NR	NR	NR	NR	NR	NR
Wall	20,781	21,043	15,519	16,018	16,334	16,753
Floor ²	NR	NR	NR	NR	22,498	23,274

(1) Material is oxidized at the start of the model.

(2) Includes the Upper Mud Mat for the FDCs.

NR = Not reported, computed transition time greater than 30,000 years.

[SRNL-STI-2009-00115]

<p><u>VP-4</u></p>	<p>The effects of the potential inventory in Vault 1 and 4 floors on radionuclide release should be analyzed.</p> <p><u>Basis</u></p> <p>The PA indicates that salt waste is assumed to fill the pore spaces in Vault 1 and 4 walls. However, no similar inventory is considered in Vault 1 and 4 floors. It is not clear why inventory could fill the pore spaces of the walls but not the pore spaces in the floors.</p> <p><u>Path Forward</u></p> <p>Justify why the Vault 1 and 4 floors are not assumed to contain inventory in the pore spaces, or estimate the effect on dose to an off-site member of the public of assuming the Vault 1 and 4 floors contain salt waste in the pore spaces.</p>
<p><u>RESPONSE VP-4:</u></p> <p>Based on the history of Vault 1 and Vault 4 crack sites, an initial inventory is assumed to be present in the walls. The Vault 1 and 4 Vault floors are not assumed to be cracked such that they contain inventory. The forces acting to induce contaminants into Vaults 1 and 4 walls are fundamentally different from the forces acting on the floor. To understand the difference it is important to understand the operation of Vaults 1 and 4.</p> <p>The initial introduction of saltstone into the cell introduces potential contamination to the floor slab as saltstone settles on the floor of the cell. However, the saltstone quickly sets up and begins to cure. Although the saltstone appears level, it slopes slightly to the outer edges of the cell. The saltstone is not “finished” as would be expected of conventional concrete structures so there are imperceptible undulations in the saltstone surface. After saltstone is poured into the cell, bleed water from the saltstone is typically observed both on the top of the saltstone as well as shedding to the edges of the cell. Over a few hours the bleed water will either be shed off the sides of the saltstone layer or will be reabsorbed as the saltstone cures.</p> <p>As the saltstone layer cures the layer experiences a small amount of shrinkage from curing. As the saltstone shrinks, a thin gap forms between the saltstone layer and the wall. Successive layers of saltstone contain bleed water which also sheds to the shrinkage gaps near the wall. Operationally, the bleed water is collected and periodically pumped back to the production facility for incorporation into successive saltstone pours. This effectively manages the bleed water level and associated hydrostatic pressure at the saltstone-wall gap.</p> <p>In order for source term to be driven into the Vault 1 and Vault 4 walls, two conditions must be met. First, a source term capable of penetrating the wall must be present. Second, there must be pressure acting on the source term to force it into the wall. The surface of the wall potentially experiences both of these conditions during the operational life of the cell. The bleed water being shed from successive saltstone pours contains the contaminants intended for incorporation into the saltstone waste form. As bleed water accumulates between the saltstone monolith and the wall the hydrostatic pressure increases. Bleed water is then forced through the microstructure of the wall concrete where it can remain in the pore volume of the wall.</p> <p>Contamination of the floor is fundamentally different from contamination of the walls. The floor is exposed to a single layer of saltstone from the initial pour. Although there may be small amounts of bleed water present at the saltstone-floor interface which could penetrate the floor pore spaces, this condition is only present during the initial pour. Subsequent saltstone pours are laid on top of existing saltstone so that the bleed water does not contact the floor concrete. Thus the quantity of</p>	

material available for contamination of the floor concrete is limited. The hydrostatic pressure experienced by the wall during operations is absent from the floor. To reach the floor, bleed water must be acted on by gravity or by the pressure from accumulated bleed water.

Since the floor is covered by the initial and subsequent layers of saltstone from multiple saltstone pours, bleed water is either shed to the edges of the pour or reabsorbed in the saltstone itself during curing. Bleed water that is shed from the top of the saltstone layer is not available to induce hydrostatic pressure over the saltstone layer. Bleed water that does remain on the saltstone surface is reabsorbed during the curing process and becomes incorporated into the saltstone. Thus gravity does not induce movement of bleed water through the saltstone monolith to the floor of the cell.

The presence of source term in the walls and floor of Vaults 1 and 4 requires two fundamental conditions:

1. The presence of source term in a form that can penetrate the concrete surface.
2. A force acting on the source term sufficient to force the source term into the surface.

As discussed in the preceding information, the walls experience both conditions required to induce source term in the surface during the operational life of the cells. Thus, source term was assumed present in the walls of Vaults 1 and 4 in the PA modeling. The Vault 1 and Vault 4 floors however, are exposed to a very limited quantity of source term and the forces acting to force the source term into the floor are absent. Thus, no inventory was assumed present in the floors of Vaults 1 and 4 in the PA modeling.

Far-field Transport (FFT)

<p><u>FFT-1</u></p>	<p>Additional justification is required for the uncertainty ranges used for K_d values in site soils.</p> <p><u>Basis</u></p> <p>The basis for the distribution coefficient variability used in the GoldSim model (Table 5.6-5) is not clear. In general, distribution coefficient uncertainty distributions are expected to be element-specific because of the varying quality of information available for each element. For example, distribution coefficients based on several site-specific samples are expected to be less uncertain than literature values. Table 5.6-5 indicates that the ranges are based on the report “<i>Distribution Coefficients (K_ds), K_d Distributions, and Cellulose Degradation Product Correction Factors for the Composite Analysis</i>” (SRNL-STI-2009-00150). However, this report (SRNL-STI-2009-00150) does not provide a discussion of the basis for uncertainty ranges, and instead references “<i>Distribution of Sorption Coefficients (K_d Values) in the SRS Subsurface Environment</i>” (WSRC-STI-2008-00285).</p> <p><u>Path Forward</u></p> <p>Provide a basis for the uncertainty distributions provided in Table 5.6-5 of the PA. If WSRC-STI-2008-00285 provides a discussion of the bases for the distributions used in Table 5.6-5 of the PA, provide this reference.</p>
----------------------------	---

RESPONSE FFT-1:

The uncertainty ranges used for K_d values in site soils are bounded as indicated in Table 5.6-5 of the SDF PA, and reproduced here as Table FFT-1.1. The basis for the selection of the uncertainty distribution is presented in WSRC-STI-2008-00285. The distributions were based on >730 K_d measurements of nine radionuclides taken from 27 samples collected from the E-Area vadose and aquifer zones at SRS. The variability, range, and distribution types (log-normal or normal) were assigned and statistical tests were conducted. The variability in the distributions is attributed to general geochemical/geological differences in site soils. The general rules presented in Table FFT-1.1 were applied to >50 radionuclides in the PA based on the 9 radionuclides reported in WSRC-STI-2008-00285.

Table FFT-1.1: Distribution Coefficient Variability in the GoldSim Model (Reproduced from SDF PA Table 5.6-4)

Material Zone	Minimum	Maximum	Log-Normal Geometric Standard Deviation	
Clayey Soils (Backfill Layer)	0.5 x GM ^a	1.5 x GM	GM < 4.0 mL/g	GM = 4.0 mL/g or greater
			1.001 mL/g	0.25 x GM
Sandy Soils (Vadose Zone)	0.25 x GM	1.75 x GM	GM < 2.7 mL/g	GM = 2.7 mL/g or greater
			1.001 mL/g	0.375 x GM
Cementitious Materials	0.25 x GM	1.75 x GM	GM < 2.7 mL/g	GM = 2.7 mL/g or greater
			1.001 mL/g	0.375 x GM

(a): GM = Geometric Mean of the log-normal distribution defined as the baseline value presented in SDF PA Table 4.2-15 for soils and Table 4.2-18 for cementitious materials.

<p><u>FFT-2</u></p>	<p>It is unclear whether any site-specific K_d value measurements have been performed for the sorption of radium to soil.</p>
----------------------------	--

	<p><u>Basis</u></p> <p>The results of the performance assessment indicate that radium is a key radionuclide. In addition, Table 5.6-14 indicates that the peak dose to a member of the public within 10,000 years in the base case is sensitive to the K_d for radium in sandy soil. According to Table 4.2-15 in the PA (“Recommended K_d Values for Backfill and the Vadose Zone”), a K_d value of 17 mL/g was selected for the backfill and a K_d value of 5 mL/g was used for the vadose zone. These K_d values were based on information provided in Kaplan (WSRC-TR-2006-00004). Table 10 of Kaplan 2006 implies that the K_d values for radium were based on measured K_d values for strontium.</p> <p><u>Path Forward</u></p> <p>Clarify if radium K_d values have been measured for soil at SRS. If these measurements have been performed, provide information on the results of these measurements.</p>
<p><u>RESPONSE FFT-2:</u></p> <p>No site-specific K_d measurements for the sorption of radium to soil have been reported; however tests are presently being conducted. Preliminary testing during FY10 has shown that subsurface, sandy sediment had a batch radium K_d of 35 and strontium K_d of 5 mL/g; a subsurface clayey sediment had a radium K_d of 150 and a strontium K_d of 35 mL/g. [SRR-CWDA-2010-00057] These results will be documented in a report scheduled to be issued in September 2010.</p> <p>For purposes of the current PA, strontium is used as a chemical analogue for radium because both are in the IIA Group in the periodic table. Radium is assumed to have partition coefficients onto SRS soils similar to those for strontium. [WSRC-RP-2004-00593, Table 1] The affinity between radium and strontium during chemical reactions is a logical consequence of the similarity in ionic radii (215 pm for radium vs. 200 pm for strontium), electronegativities (0.9 for radium vs. 0.95 for strontium) and electronic configurations. The general trend is as one goes down the IA Group (sodium, potassium, rubidium, cesium, to francium) and IIA Group (calcium, strontium, barium, to radium) in the periodic table, the K_d values systematically increase due to the concomitant increase in size of the cation. Furthermore, based on strontium’s slightly higher electronegativity, (and based on the preliminary results mentioned above) strontium is expected to yield lower sorption values than radium to the same soils; therefore using strontium K_d’s for radium is a conservative assumption.</p>	
<p><u>FFT-3</u></p>	<p>Additional justification is needed for the K_d of selenium in vadose and backfill soils.</p> <p><u>Basis</u></p> <p>The PA references the report “Geochemical Data Package for Performance Assessment Calculations Related to the Savannah River Site” (WSRC-TR-2006-00004) as the basis for a K_d of 1000 mL/g for Se in backfill and vadose zone soil (Table 4.2-15 in the PA). In general, literature values are two to three orders of magnitude lower than the values cited in WSRC-TR-2006-00004 (e.g., Fuhrmann and Schwartzman, 2008; PNNL-13895). Site-specific values are, in general, far preferable to literature values. However, it is important to understand the basis for large deviations from expected values (e.g., particular properties of the site-specific soil or water chemistry).</p> <p>Furthermore, in the reference used in the PA (WSRC-TR-2006-00004), the authors note the K_d for sandy soils exhibits a “characteristic decrease in K_d values as the pH</p>

	<p>increased” in the range from pH 3.9 to pH 6.7, with no additional data available above pH 6.7. In the reference the K_d in sandy soil was 1311 ± 384 mL/g at pH 5.3 and 601 ± 65 mL/g at pH 6.7 (WSRC-TR-2006-00004). The basis for choosing a K_d representative of low-pH soil as compared to a more neutral soil is unclear, especially in light of the potential for alkaline buffering of the vadose zone soils by the significant quantity of cementitious materials in the SDF.</p> <p><u>Path Forward</u></p> <p>Provide a basis for choosing a K_d value representative of low pH soils as compared to more neutral soils. In determining an appropriate pH for modeled soils, consideration should be given to the potential impact of the cementitious materials in the SDF on the pH of water in the vadose and backfill soils.</p>
--	--

RESPONSE FFT-3:

A K_d value of 1,000 mL/g is used in the SDF PA (Table 4.2-15) for selenium in backfill and vadose zone soil, which is representative of low pH soil. A low pH soil value is considered appropriate over more neutral soil, because measurements range from 5.3 to 5.7 in Z-Area background sediments (monitoring well ZBG-1; SRNS-TR-2009-00452). Site-specific selenium K_d measurements suggest that sandy soil selenium K_d s are pH sensitive, with measured values for sandy soil equal to $1,311 \pm 384$ mL/g at pH 5.3, and 601 ± 65 mL/g at pH 6.7. [WSRC-TR-2006-00004]

This pH dependency explains the discrepancy between the PA recommended K_d value and literature K_d values. For instance, the selenium K_d values reported in PNNL-13895 are lower than PA values because they were measured under very different site conditions, e.g., pH >8, sandy sediments with essentially no anion exchange capacity dominated with permanent charge minerals, and an aqueous phase dominated with carbonate (and in at least one case, a carbonate dominated solid phase; PNNL-11966).

The impact of alkaline buffering on selenium K_d s in soil is accounted for in the uncertainty analysis described in the SDF PA Section 5.6. Lacking site-specific measurements from soils with pH > 6.7, selenium K_d values in young-age (pH > 11) cementitious materials provide a proxy K_d value for soils impacted by groundwater traveling through cements. As indicated in Table 4.2-15 of the PA, the selenium K_d in reducing and oxidizing, young-age cements (300 mL/g) is expected to be lower than in backfill and vadose zone soils (1,000 mL/g). Therefore, one would expect vadose zone soils impacted by leaching of the young-age cements to have mean selenium K_d values less than or equal to 1,000 mL/g but greater than or equal to 300 mL/g. The selenium sandy soil K_d in the probabilistic GoldSim model is described by a truncated log-normal distribution centered around 1,000 mL/g, with a minimum value of 250 mL/g, which is 50 mL/g less than the minimum proxy cementitious value. Therefore, the PA does account for the range of uncertainty that leaching through young-age cement may have on selenium K_d in soil.

To further quantify the maximum potential impact of lower selenium K_d s resulting from cement leaching, a bounding sensitivity case was run using the deterministic Case A GoldSim model with both soil K_d s for selenium set equal to zero to represent the most conservative condition. Comparison of the Base Case with the “no selenium sorption onto soils” sensitivity case revealed a maximum increase in peak dose in Sector B and J of < 1%. The 20,000 year peak dose in Sector B increased by <3%, and Sector J by <1.5%. The bounding sensitivity analysis provides confidence that lowering the selenium sorption onto soils has a negligible impact on dose results.

Air Pathway (AP)

<u>AP-1</u>	<p>The dose from the radon pathway was not included in the dose assessment of the air pathway (Section 4.5 of the PA).</p> <p><u>Basis</u></p> <p>The flux rates expected from the radon generated by the decay of radium in saltstone were calculated and presented in Section 4.5 of the PA. However, the dose associated with these flux rates of radon for an off-site member of the public or an inadvertent intruder inhabiting the site was not included. As discussed in comment II-1, an inadvertent intruder is assumed to inhabit the site after the end of institutional controls, and may live directly above a disposal unit.</p> <p><u>Path Forward</u></p> <p>Provide a calculation of the expected dose from the radon pathway to an off-site member of the public and to an intruder residing on site.</p>
--------------------	--

RESPONSE AP-1:

The dose to an inadvertent intruder inhabiting the site from the inhalation of Rn-222 has been estimated to be approximately 8.0E-11 mrem/yr. The dose to an off-site MOP from the inhalation of Rn-222 would be significantly less than the estimated dose to the intruder of 8.0E-11 mrem/yr because the residence of the MOP is at least 100m away from any disposal unit and the intruder analysis presented below assumes the Rn-222 concentration to be in equilibrium within the controlled volume of the basement of the residence built directly above the disposal unit with the highest peak radon flux.

The approach used to estimate the dose to the intruder from the inhalation of Rn-222 is summarized below.

The estimated annual dose to an intruder from the inhalation of Rn-222 is dependent on the following:

- a. Concentration of Rn-222 in a controlled volume occupied by the intruder
- b. Intruder occupancy (fraction of year) in the controlled volume
- c. Breathing rate
- d. Rn-222 dose conversion factor

Rn-222 Concentration in a Controlled Volume

The controlled volume assumed in this analysis is a basement in a residential home that has a floor area of 200m² (2,150 ft²) and 2.43m (8 feet) ceilings for a total volume of approximately 500m³. The size of this controlled volume is based on the assumed values presented in NUREG/CR-4370, *Update of Part 61 Impacts Analysis Methodology, Volume 1*, Section 4.2.5.2. This controlled volume is assumed to be situated above the disposal unit with the highest peak radon flux.

The buildup of Rn-222 in the basement is dependent on the production rate (P) and removal rate (R) of Rn-222. Based on the SDF PA Section 5.3.2, the highest peak Rn-222 flux is above Vault 1 and is 2.0E-13 pCi/m²/sec as shown in PA Table 5.3-6. Taking no credit for intervening materials of construction (concrete, cinder block, etc.) the production rate of Rn-222 entering the controlled volume is assumed to be at a constant rate equal to the peak flux times the basement floor area of 200m². Thus, P = 1.3E-3 pCi/yr. Assuming an air exchange rate of 1 vol/hr taken from NUREG/CR-

4370, SDF PA Section 4.2.5.2, the removal rate is $8,760 \text{ year}^{-1}$. The greatest Rn-222 concentration is when the buildup is at equilibrium which equals P/R or $1.5\text{E-}07 \text{ pCi}$.

The peak Rn-222 concentration in the controlled volume is then estimated to be $3.0\text{E-}13 \text{ pCi/m}^3$ ($= 1.5\text{E-}7 \text{ pCi} / 500 \text{ m}^3$).

Intruder Occupancy

For this analysis, the intruder is assumed to occupy the controlled volume 100% of the time.

Breathing Rate

For this analysis, the nominal breathing rate of $5,548 \text{ m}^3/\text{yr}$ is assumed, as shown in PA Table 4.6-7.

Radon-222 Dose Conversion Factor

The dose conversion factor for Rn-222 inhalation is not included in PA Table 4.7-1, but is included here and is estimated based on 10 CFR 20. Assuming the occupational dose limit of 5 rem (5,000 mrem) specified in § 20.1201(a)(1)(i) and dividing by the annual limits on intake for Rn-222 of 100 μCi ($1\text{E+}8 \text{ pCi}$) in air from Table 1, Column 2 of Appendix B; the Rn-222 dose conversion factor is therefore estimated to be $5\text{E-}5 \text{ mrem/pCi}$.

The estimated dose to the intruder from the inhalation of Rn-222 = $3.0\text{E-}13 \text{ pCi/m}^3 \times 5,548 \text{ m}^3/\text{yr} \times 5\text{E-}5 \text{ mrem/pCi} = 8.2\text{E-}11 \text{ mrem/yr}$.

AP-2

The calculations used for the air pathway dose may not have adequately evaluated the dose from this pathway. The materials were assumed to remain constant over the simulation period and degradation of the wasteform and vault does not seem to have been considered. Also, the sensitivity of the calculated land surface flux rates of radionuclides to the assumed moisture content in the cover was also not evaluated.

Basis

As described in Section 4.5 of the PA, the gaseous flux of radionuclides diffusing from the wasteform and through the cover was calculated using PORFLOW. The materials were assumed to remain constant over the simulation period and degradation and cracking of the wasteform and vault does not seem to have been considered. The flux of gaseous radionuclides out of the saltstone and through the vault may be higher if degradation and fracturing of the saltstone and vault ceiling occurs.

The materials in the cover were assumed to be partially saturated at saturation fractions presented in Tables 4.5-4, 4.5-5, and 4.5-6. The assumed saturation fractions for some portions of the cover were high, and it is not clear if these levels of saturation will be maintained at all times throughout the entire performance period.

The rate of diffusion through partially saturated porous media is very dependent on the amount of saturation. The gaseous flux of radionuclides through the cover, and the resulting dose, could therefore vary greatly depending on the moisture content of the cover. The radon flux is particularly dependent on the moisture content of the cover because of its short half-life. Even though the gaseous fluxes calculated were small, it is not clear if the fluxes would remain this small if the cover has a lower amount of saturation than was assumed in the calculations.

In addition, the basis for the emanation coefficient selected for radon is not clear. As noted in the text of the PA, the emanation factor is dependent on the moisture content and is usually higher with higher moisture contents. Section 4.5.2.5 of the PA

indicates that the chosen value is appropriate for a soil with a low moisture content. Thus, the emanation factor selected seems to be inconsistent with the high level of saturation assumed for the saltstone wastefrom.

Section 4.5.2.1 of the PA indicates that the primary uncertainty in the estimation of the apparent Henry's Law constants is the use of lower ionic strengths in the calculations (0.015 molal) than those estimated for saltstone pore fluids (~6 molal). Higher ionic strengths can cause more partitioning into the gaseous phase (i.e., salting out). The PA states that it is unlikely that the activity coefficients would increase by more than a factor of 10 due to this effect, but the basis for this statement is not clear. The reference for this statement is a textbook, and the specific basis for this statement in the textbook is not clear. Thus it is not clear it whether the assumptions on which this conclusion is based are applicable to saltstone.

Path Forward

Evaluate if the calculated air pathway doses are sensitive to the assumption that the material properties remain constant and that degradation of the saltstone and vaults does not occur. Provide an evaluation of the sensitivity of the calculated gaseous flux rates, including the radon flux, to the assumed amount of saturation of the layers of the cap. Provide an evaluation of the sensitivity of the radon flux to the radon emanation factor. Provide more support for the statement that it is unlikely that the activity coefficients would be unlikely to increase by more than a factor of 10 due to salting out.

RESPONSE AP-2:

Sensitivity analyses have been conducted to consider a higher emanation rate for radon and the assumed saturation conditions for the soil layers of the proposed closure cap.

Analysis indicates that the impact on the radon flux is directly proportional to the radon emanation rate. The SDF PA Section 4.5.2.5 provides the modeling assumptions used in the radon analysis and reports that the radon emanation rate can vary from 0.2 to 0.7 based on soil types. The analysis conducted for the PA assumed the default value of 0.25 utilized by the Residual Radioactivity Computer Software model. Thus, assuming an emanation rate of 0.7 (versus 0.25) would increase the radon flux by a factor of 2.8 which is inconsequential to the radon flux reported in the SDF PA Section 5.3.2.

An additional sensitivity analysis was conducted on the assumed saturation conditions associated with the soil layers that comprise the proposed closure cap. The SDF PA Section 4.5.2 summarizes the assumptions utilized in the air pathway and radon models that are reported in PA reference SRNL-STI-2008-00447. The model described in SRNL-STI-2008-00447 uses average values for air-filled porosity and volumetric moisture content calculated in the closure cap performance analysis documented in PA reference WSRC-STI-2008-00244. In this sensitivity analysis minimum volumetric moisture content values and corresponding maximum air-filled porosity values, computed in the closure cap performance analysis were used; rather than average values. The resulting fluxes based on this sensitivity analysis are presented in Tables AP-2.1 and AP-2.2. The fluxes provided in these tables are based on unit flux values taken from SRNL-L6200-2010-00019, disposal unit inventories provided in the SDF PA Section 3.3, and the following disposal unit surface areas: 5,574m² (Vault 1), 11,148m² (Vault 4), and 1,642m² (FDC) (PA Tables 5.3-6, 5.3-7, and 5.3-8 respectively).

There was a transcription error in the inventory values shown in Table 5.3.7 (Vault 4) and Table

5.3.8 (FDCs) which result in the peak Rn-222 fluxes shown for Vault 4 as slightly underestimated and for the FDCs as overly conservative.

The calculated peak flux stated in Table 5.3-6 for Vault 1 remains $2.0E-13$ pCi/m²/sec which is the peak radon flux for the SDF.

The response to AP-1 provides the estimated dose to the intruder from radon exposure of $8.0E-11$ mrem/yr based on the maximum peak radon flux of $2.0E-13$ pCi/m²/sec presented in the SDF PA Section 5.3.2. Using the peak radon flux from Table AP-2.1, the estimated radon exposure to an intruder for this sensitivity analysis is $5E-9$ mrem/yr based on the flux ratio of 60 (= $1.2E-11 / 2E-13$).

Table AP-2.1: Peak Radon Flux from the Disposal Units Using Minimum Moisture Content

Disposal Unit	Vault 1	Vault 4	FDC
Saltstone Source	DDA	DDA	SWPF
Pu-238 (pCi/m ² /sec)	5.9E-18	6.9E-15	1.0E-19
Ra-226 (pCi/m ² /sec)	2.0E-17	1.3E-13	2.0E-23
Th-230 (pCi/m ² /sec)	1.2E-11	2.2E-13	4.4E-18
U-234 (pCi/m ² /sec)	5.8E-13	5.6E-14	2.2E-19
U-238 (pCi/m ² /sec)	1.9E-16	1.5E-17	2.0E-21
Total (pCi/m ² /sec)	1.2E-11	4.1E-13	4.7E-18

Table AP-2.2: Peak Radionuclide Emission Rate from the Disposal Units Using Minimum Moisture Content

Disposal Unit	Vault 1	Vault 4	FDC
Saltstone Source	DDA	DDA	SWPF
C-14 (Ci/yr)	1.5E-13	2.1E-12	9.0E-14
Cl-36 (Ci/yr)	4.2E-30	1.1E-29	9.2E-31
H-3 (Ci/yr)	7.3E-12	2.1E-10	1.4E-11
I-129 (Ci/yr)	2.7E-31	4.6E-31	3.6E-31
Sb-125 (Ci/yr)	3.5E-46	7.2E-45	1.2E-46
Se-79 (Ci/yr)	3.3E-16	3.5E-14	6.2E-16
Sn-126 (Ci/yr)	4.4E-70	1.9E-69	1.4E-69
Tc-99 (Ci/yr)	8.1E-75	2.9E-74	1.6E-74

The impact on the air pathway dose presented in the SDF PA Section 5.3.1 and the potential dose to an intruder residing above the disposal units have been evaluated for this additional sensitivity case. To conservatively assess the potential dose to the intruder, the annual intake of radionuclides for an intruder is assumed to be the peak emission rate provided in Table AP-2.2. Tables AP-2.3, AP-2.4, and AP-2.5 provide the estimated air pathway dose to the intruder and the MOP at 100m for Vault 1, Vault 4, and for an FDC, respectively.

The total peak dose to the MOP at 100m is then the sum of the dose from Vault 1 ($1.1E-15$ mrem/yr), the dose from Vault 4 ($2.5E-14$ mrem/yr) and the dose from the 64 FDCs ($64 \times 1.4E-15$ mrem/yr). The potential peak dose to the MOP by the air pathway, based on this sensitivity case, is $1E-13$ mrem/yr, which is not significantly greater than the Base Case air pathway dose of $8E-14$ mrem/yr (due to a transcription error the reported dose in the PA was overstated).

Table AP-2.3: Estimated Dose from the Air Pathway from Vault 1

Radionuclide	DCF for Intruder (mrem/Ci) ^a	Dose to Intruder (mrem/yr) ^b	DCF for MOP at 100M (mrem/Ci) ^c	Dose to MOP at 100M (mrem/yr) ^d
C-14	7.40E+06	1.1E-06	3.7E-03	5.5E-16
Cl-36	2.70E+07	1.1E-22	7.9E-03	3.3E-32
H-3	1.67E+05	1.2E-06	7.7E-05	5.7E-16
I-129	1.33E+08	3.6E-23	5.5E+00	1.5E-30
Sb-125	1.78E+07	6.2E-39	1.1E-01	3.8E-47
Se-79	4.07E+06	1.4E-09	1.1E-02	3.7E-18
Sn-126	1.04E+08	4.6E-62	4.9E+00	2.2E-69
Tc-99	1.48E+07	1.2E-67	2.9E-02	2.3E-76
Total	--	2.3E-06	--	1.1E-15

^a Based on PA Table 4.7-1

^b Product of DCF for Intruder and Emission Rate from Table AP-2.2

^c Obtained from Table 5 of PA Reference SRNL-STI-2008-00415

^d Product of DCF for MOP and Emission Rate from Table AP-2.2

Table AP-2.4: Estimated Dose from the Air Pathway from Vault 4

Radionuclide	DCF for Intruder (mrem/Ci) ^a	Dose to Intruder (mrem/yr) ^b	DCF for MOP at 100M (mrem/Ci) ^c	Dose to MOP at 100M (mrem/yr) ^d
C-14	7.40E+06	1.6E-05	3.7E-03	7.8E-15
Cl-36	2.70E+07	3.1E-22	7.9E-03	9.1E-32
H-3	1.67E+05	3.6E-05	7.7E-05	1.7E-14
I-129	1.33E+08	6.2E-23	5.5E+00	2.6E-30
Sb-125	1.78E+07	1.3E-37	1.1E-01	7.9E-46
Se-79	4.07E+06	1.4E-07	1.1E-02	3.9E-16
Sn-126	1.04E+08	2.0E-61	4.9E+00	9.5E-69
Tc-99	1.48E+07	4.3E-67	2.9E-02	8.4E-76
Total	--	5.2E-05	--	2.5E-14

^a Based on PA Table 4.7-1

^b Product of DCF for Intruder and Emission Rate from Table AP-2.2

^c Obtained from Table 5 of PA Reference SRNL-STI-2008-00415

^d Product of DCF for MOP and Emission Rate from Table AP-2.2

Table AP-2.5: Estimated Dose from the Air Pathway from an FDC

Radio-nuclide	DCF for Intruder (mrem/Ci) ^a	Dose to Intruder (mrem/yr) ^b	DCF for MOP at 100m (mrem/Ci) ^c	Dose to MOP at 100m (mrem/yr) ^d
C-14	7.40E+06	6.6E-07	3.7E-03	3.3E-16
Cl-36	2.70E+07	2.5E-23	7.9E-03	7.3E-33
H-3	1.67E+05	2.3E-06	7.7E-05	1.1E-15
I-129	1.33E+08	4.8E-23	5.5E+00	2.0E-30
Sb-125	1.78E+07	2.2E-39	1.1E-01	1.4E-47
Se-79	4.07E+06	2.5E-09	1.1E-02	6.8E-18
Sn-126	1.04E+08	1.5E-61	4.9E+00	7.0E-69
Tc-99	1.48E+07	2.3E-67	2.9E-02	4.5E-76
Total	--	3.0E-06	--	1.4E-15

^a Based on PA Table 4.7-1

^b Product of DCF for Intruder and Emission Rate from Table AP-2.2

^c Obtained from Table 5 of PA Reference SRNL-STI-2008-00415

^d Product of DCF for MOP and Emission Rate from Table AP-2.2

As indicated in the SDF PA Section 4.5.1.2.1, the model used to estimate radon and air pathway emission conservatively directs, though boundary conditions, all gaseous emission in the vertical direction; takes no credit for the pore water that moves vertically downward through the model domain; and excludes the HDPE and GCL layers and any material above the erosion barrier that would be present in the proposed closure cap.

The model also assumes that the roof concrete of the disposal units does not degrade during the compliance period of 10,000 years. As indicated in the SDF PA Figures 4.2-36, 4.2-37, and 4.2-39, the concrete degradation of the roof for Vault 1 and an FDC, evidenced by increasing hydraulic conductivity and diffusion coefficient, is insignificant during the 10,000 year compliance period. The concrete roof of Vault 4, however, does experience significant degradation during the compliance period as shown in SDF PA Figure 4.2-38. However, while the increase in hydraulic conductivity and diffusion coefficient would allow greater pore liquid flow through the concrete, it would not increase the gaseous emission rate. The model assumes that the roof is dry thus maximizing the air-filled porosity and diffusion coefficients for this layer, so any degradation of this layer would likely increase saturation and lower the air-filled porosity of the concrete.

The conclusion that higher ionic strengths in the saltstone pore fluid would not be expected to increase the activity coefficients by more than a factor of 10 is based on *Geochemical Thermodynamics*. The effect of higher ionic strengths is shown in Figure 7-8 of *Geochemical Thermodynamics* which is reproduced below as Figure AP-2.1. It shows $\log \gamma$ (log of activity coefficient) for ions associated with CaCl_2 versus the molality of CaCl_2 – experimental data compared to estimation methods. The range of activity coefficients in solutions that range from molalities of 0 to 6 is approximately 1 order of magnitude. [ISBN: 0-86542-319-9]

Data obtained from *Electrolyte Solutions*, (ISBN-10: 0486422259), further supports the statement that activity coefficients would be unlikely to increase by more than a factor of 10 due to higher ionic strengths. Figure AP-2.2, generated from data obtained from *Electrolyte Solutions*, shows the increase in activity coefficients for ions associated with various nitrate salts. Sodium nitrate is the dominant salt accounting for the high ionic strength of saltstone. Hence, the activity coefficients of other cations in saltstone pore fluids will be similar to the values of their nitrate salts. Their range is less than a factor of 10 over the molality range of 0 to 6.

Figure AP-2.1: Figure 7-8 of *Geochemical Thermodynamics*

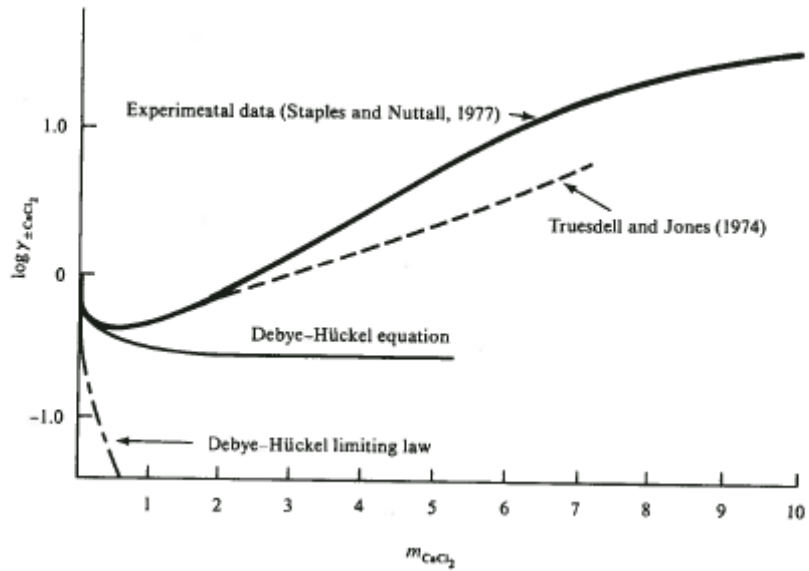
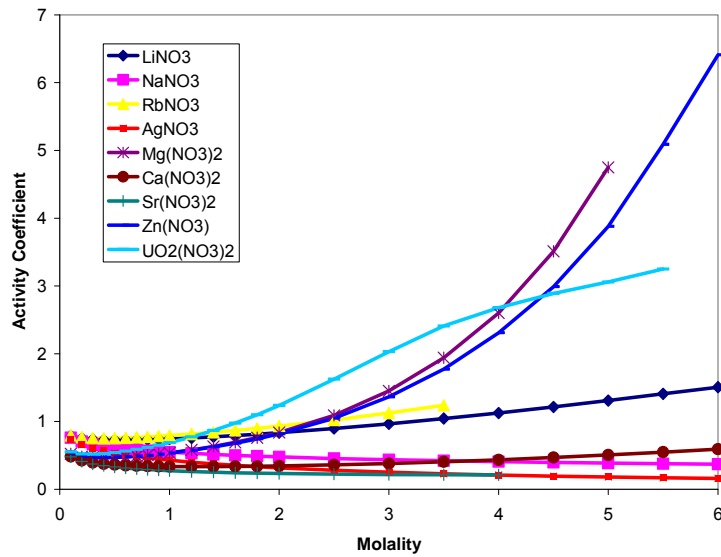


Figure AP-2.2: Increase in Activity Coefficients for Ions Obtained from *Electrolyte Solutions*



Inadvertent Intrusion (II)

<p><u>II-1</u></p>	<p>Key assumptions about the potential pathways of exposure of an inadvertent intruder appear to underestimate dose.</p> <p><u>Basis</u></p> <p>The assumed location of the inadvertent intruder was 1 m from the perimeter boundary of the Saltstone Disposal Facility. The dose to the intruder at this location includes the dose at 1 m from the FDCs nearest to the perimeter boundary as well as the dose from the radionuclides from the upgradient vaults that transport to this location within 10,000 years. This assumed location appears to be optimistic because the dose at a location 1 m from vault 4 would likely be higher than the dose at 1 m from a FDC because the size of vault 4 is larger and because the FDCs have many more engineered features than vault 4. The inventory in the individual FDCs is also expected to vary from vault to vault. The dose to an intruder at 1 m from a vault that had a higher inventory would be higher than the dose to an intruder located 1 m from a FDC with the average inventory. As defined in 10 CFR 61.2, an inadvertent intruder may occupy the disposal site and is not assumed to be confined to the buffer zone of the site.</p> <p>In addition, it is not clear if the 1 m dose corresponds to the dose at the 1 m perimeter or if it corresponds to the dose from soil and water with the average concentration in the grid cell located at approximately 1 m. Because a 50 ft by 50 ft mesh was used to define the grid cells in the saturated zone, the average concentration of radionuclides in the water and soil in these grid cells could be much less than the concentration at 1 m, particularly for those radionuclides that sorb strongly to soil and are not expected to travel quickly in the saturated zone. Although it may be appropriate to average water concentrations over the grid cell, depending on well capture area, it is less clear if it is appropriate to average soil concentrations over a 50 ft by 50 ft grid.</p> <p>The dose from the air pathway was not included in the assessment of the dose to an inadvertent intruder. The calculated inhalation dose from radionuclides that diffused from the saltstone wastefrom to the atmosphere air was small, but this calculated dose is expected to be greater for an intruder residing directly above a disposal unit. In addition, this calculated dose may be very sensitive to the assumed moisture content in the cap. If the response to AP-2 indicates that the air pathway dose, including the dose from radon, could be non-negligible for an intruder residing directly above a disposal unit, the air pathway dose should be included in the assessment of dose to an inadvertent intruder. In addition, as described in B-2, the poultry and egg pathways were not included in the dose assessment. If the response to B-2 indicates that these pathways should be included for the member of the public, then these pathways should be included for the chronic intruder as well.</p> <p><u>Path Forward</u></p> <p>Provide justification for the selected location for the intruder or provide an intruder analysis that considers the dose to an intruder at a location 1 m from Vault 4 and from a FDC that has the maximum expected inventory. Clarify if the 1 m dose is at a distance of exactly 1 m or if this dose corresponds to the average dose over a 50 ft</p>
---------------------------	--

by 50 ft grid cell located at the 1 m perimeter. If appropriate, the intruder dose assessment should be revised to include the dose from the air pathway, including radon, and from animal pathways other than the beef and milk pathway (e.g., poultry and egg pathways).

RESPONSE II-1:

An analysis has been performed to estimate the dose to an inadvertent intruder that draws well water within 1m from Vault 4. This analysis utilizes the flux entering the water table below Vault 4 generated from PORFLOW for Case A. Using the flux data entering the water table is conservative since a travel distance of one meter from the vault is not considered. The flux data obtained from PORFLOW is converted to concentration by dividing the flux (Ci/yr) by the Vault 4 footprint area of 11,148 square meters and by the Darcy Velocity (m/yr) extracted from PORFLOW output for various time steps. The concentrations computed at the water table below Vault 4 are entered into the GoldSim dose calculator model to estimate the dose to the intruder. The finfish ingestion dose is computed by assuming that the intruder ingests finfish from the local stream that is contaminated from all disposal units. The resulting peak dose for the intruder within the 10,000 year compliance period occurs 9,760 years after closure and is 35.3 mrem/yr. The contributions to the total dose from the various pathways are presented in Table II-1.1.

Table II-1.1: Dose to Intruder from Groundwater Pathways 1 Meter from Vault 4

Pathway	Dose (mr/yr)	Percent Total
Water Ingestion	18.1	51.2 %
Vegetable Ingestion	15.3	43.4 %
Inhalation (during irrigating and showering)	1.0	3.0 %
Milk Ingestion	0.4	1.2 %
Finfish Ingestion (stream from all sources)	0.3	0.8 %
Beef Ingestion	0.2	0.4 %
Others	< 0.1	< 0.1 %
Total from all groundwater pathways	35.3	- -

A similar analysis was not conducted for an intruder at one meter from an FDC, rather a PORFLOW run was made considering the release from a single FDC located in the north-eastern corner of the SDF facility. The 1m concentration computed by the PORFLOW run would be essentially 1m from that FDC. These concentrations are entered into the GoldSim dose calculator and increased by a factor of 10 to account for the maximum expected inventory shown in PA Table 5.6-4. The finfish ingestion dose is the same as computed for the intruder located above Vault 4. The resulting peak dose for the intruder within the 10,000 year compliance period occurs 10,000 years after closure and is 1.5 mrem/yr. The contributions to the total dose from the various pathways are presented in Table II-1.2.

Table II-1.2: Dose to Intruder from Groundwater Pathways 1 Meter from an FDC with Maximum Expected Inventory

Pathway	Dose (mr/yr)	Percent Total
Water Ingestion	0.57	37.1 %
Vegetable Ingestion	0.48	31.4 %
Finfish Ingestion (stream from all sources)	0.31	20.2 %
Beef Ingestion	0.10	6.4 %
Milk Ingestion	0.06	4.1 %
Inhalation (during irrigating and showering)	0.01	0.8 %
Others	< 0.01	< 0.1 %
Total from all groundwater pathways	1.54	--

The 1m dose is computed based on the highest average groundwater concentration within the 50 feet x 50 feet grid cells that encroach on the one meter perimeter of the SDF.

Radionuclide concentration in the soil is used in the vegetable ingestion pathway (via vegetable root uptake), milk and beef ingestion (via cow fodder ingestion), soil ingestion, and external exposure to the soil. The SDF PA Section 5.4.1 provides the equations used in the model to estimate dose from the various pathways to exposure. As shown in the SDF PA Section 5.4.1, the concentration in the soil is based on the groundwater concentration and not on a specified "grid volume" of soil. The response to RAI B-3 addresses the build-up of radionuclides in the soil which is solely dependent on the groundwater concentration.

As indicated in the response to RAI B-2, the poultry and egg consumption pathways are not applicable to the SDF compliance model.

Also, as indicated in the responses to RAIs AP-1 and AP-2, the estimated radiological exposure from the inhalation of radon and other gaseous radionuclides do not appreciably contribute to the dose to the intruder.

II-2

The basis for the use of Case A to calculate the intruder dose is not provided. Additionally, the methodology used for determining the key radionuclides for the intruder uncertainty/sensitivity analysis may have resulted in radionuclides that are risk significant to the intruder being excluded from this analysis. As a consequence, the results of the uncertainty/sensitivity analysis may not capture the true uncertainty in the intruder dose.

Basis

In the deterministic calculation of the dose to the chronic intruder, the 1 m groundwater concentrations were calculated using the Case A modeling case in PORFLOW. Because this case does not include degradation or cracking of the saltstone, the dose calculated from this case may not adequately capture the expected intruder dose. A probabilistic uncertainty/sensitivity analysis was performed for the chronic intruder using GoldSim, and as part of this assessment, the effect of the case selection on the dose was evaluated. However, this uncertainty/sensitivity assessment was based on the key radionuclides identified as causing the greatest dose at 100 m. This approach may have excluded radionuclides that have high soil K_d values because they do not travel quickly enough to reach a distance of 100 m within the evaluation period. However, some of these radionuclides could reach a distance of 1 m within 10000 yrs and could cause

	<p>a significant dose to the intruder. Also, as discussed in PA-3, the use of Case A to determine the list of key radionuclides may have led to the omission of some potentially dose-significant radionuclides.</p> <p>In addition, some of the comments in this document related to the calculation of the dose to the member of the public also could apply to the intruder calculation. The chronic intruder calculation should be updated to address these comments if appropriate.</p> <p><u>Path Forward</u></p> <p>Provide justification for the use of Case A in the calculation of the deterministic chronic intruder dose or provide the results of an assessment of the dose to an inadvertent intruder in cases representing degraded saltstone, cap, and vault conditions. Evaluate if any radionuclides that could potentially cause a significant dose to the intruder were excluded from the uncertainty/sensitivity analysis, and if so, provide a revised uncertainty/sensitivity analysis. Evaluate whether the responses to comments on the dose assessment to the member of the public affect the intruder analysis and provide a revised analysis if applicable.</p>
--	--

RESPONSE II-2:

The deterministic intruder analysis results are based on Case A because Case A represents the reasonably expected degradation configuration for the SDF disposal units. The peak total doses for the Chronic Intruder (Post-Drilling) Scenarios were calculated using the maximum 1m concentrations identified in the SDF PA Section 6.1.

The SDF PA Section 6.5 presents results that address the effects of uncertainty on the estimation of intruder dose. The intruder dose results presented in the SDF PA Section 6.5 are based on the complete set of radionuclide inventory present in the SDF disposal units, no radionuclides are excluded based on the determination of "key radionuclides" as discussed in more detail in the response to RAI C-8. As indicated by the uncertainty analysis shown in PA Figure 6.5-1, the mean dose to the intruder for all cases (Cases A through E) is less than 10 mrem/yr during the 10,000 year performance period. For Case C only, SDF PA Table 6.5-2 indicates that the mean dose to the intruder during the 10,000 year compliance period is less than 27 mrem/yr.

Specific intruder analyses have not been conducted for sensitivity cases discussed in the SDF PA Section 5.6.6. However, the potential dose to the intruder associated with these other cases can be inferred based on the dose results at 100m presented in the SDF PA Section 5.6.6. Table II-2.1 provides a summary of the dose to the MOP at 100m for the various cases analyzed in the SDF PA Section 5.6.6. As indicated in Table II-2.1, except for the synergistic case, the other cases are comparable or less than the results indicated for Case A or Case C. Therefore, for these other cases the dose results to the intruder are also expected to be comparable. For the synergistic case, the dose to the MOP is approximately 3.5 times greater than Case C and thus, the mean dose to the intruder for the synergistic case is expected to be approximately 3.5 times the intruder dose for Case C.

Table II-2.1: Dose Summary in Sector B for Various Cases within the 10,000 Year Compliance Period

Case Analyzed	Peak MOP Dose (mrem/yr)	PA Reference
Case A – Base Case	1.4	Table 5.6-16
Case C – Fast Flow Case	5.1	Table 5.6-16
“Soils Only” Closure Cap Case	2.1	Table 5.6-17
10 Times Sulfate Case	1.7	Table 5.6-19
Synergistic Case	17.6	Table 5.6-20
Oxidized Concrete Case	0.4	Table 5.6-21
Increased Conductivity Case	5.4	Table 5.6-22

Based on the responses to the RAIs on the Biosphere (B-1, B-2) no further intruder analysis is required. The responses to RAIs AP-1 and AP-2 indicate that the potential exposure to the intruder from the radon and air pathways do not significantly contribute to the dose to the intruder.

Biosphere (B)

<p><u>B-1</u></p>	<p>The basis for excluding biotic transfer factors from the uncertainty analysis is unclear.</p> <p><u>Basis</u></p> <p>Section 5.6.3.7 indicates that only the most likely values of the transfer factors provided in Tables 4.6-1 through 4.6-4 (i.e., soil-to-vegetable, feed-to-milk, feed-to-meat, and water-to-fish transfer factors) were used in the analysis, although a range of values is presented for each transfer factor for each element in Tables 4.6-1 through 4.6-4. The basis for excluding these transfer factors from the probabilistic analysis is unclear, given that fish and vegetable consumption were two of the three significant pathways identified as contributing to the dose to a member of the public at 10,000 years in the base case in Section 5.5.1.4 of the PA. An understanding of the factors to which dose is most sensitive is important to establishing factors to monitor.</p> <p><u>Path Forward</u></p> <p>Provide a basis for excluding the biotic transfer factors listed in the basis from the uncertainty analysis, or provide an updated uncertainty analysis that includes the uncertainty in the transfer factors.</p>
<p><u>RESPONSE B-1:</u></p> <p>The transfer factors were not included in the probabilistic analysis because a preliminary evaluation concluded that the effect of the variability of biotic transfer factors on the total dose was insignificant and thus the biotic transfer factors were not included in the implementation of the probabilistic analysis. As noted, this decision eliminated the probabilistic analysis of the variability of this parameter on the estimation of total dose.</p> <p>Table B-1.1 supports the above decision and presents the effect of using the maximum transfer factors for all elements for all pathways. The maximum values for the transfer factors presented in SDF PA Tables 4.6-1 through 4.6-4 were used to calculate the dose to the MOP for Case A. This approach clearly maximizes the impact of the transfer factors on the estimation of dose. As expected, individual pathways showed increases in the dose to the MOP, especially in the Beef and Milk pathways which utilize two transfer factors, the soil-to-vegetable transfer factor for fodder coupled with the feed-to-beef transfer factor or the feed-to-milk transfer factor. The increase in the Beef and Milk pathway doses were dominated by levels of Tc-99. The increase in the finfish ingestion pathway dose was dominated by levels of I-129. However, the total dose for Case A is increased by only 0.31 mrem within the 10,000 year compliance period, with the majority of the increase caused by the finfish ingestion pathway.</p> <p>Therefore, the transfer factors' variability were not included in the probabilistic analysis since using the maximum values for the transfer factors resulted in such a small change in the peak dose.</p>	

Table B-1.1: Maximum Transfer Factors For All Elements For All Pathways

Pathway	Peak MOP Dose (mrem/yr) at 10,000 years		
	Current ¹	Revised ²	Difference
Vegetable in Sector B	0.308	0.312	0.004
Vegetable in Sector I	0.0259	0.0261	0.0002
Milk in Sector B	0.0154	0.0225	0.0071
Milk in Sector I	0.00553	0.00729	0.00176
Beef in Sector B	0.00989	0.0570	0.04711
Beef in Sector I	0.0103	0.0104	0.0001
Fish Ingestion	0.310	0.587	0.277
Total Dose in Sector B	1.39	1.70	0.31
Total Dose in Sector I	0.416	0.695	0.279

(Note: Peak doses may appear at different times)

1: Using current PA biotic transfer factors.

2: Using maximum values for biotic transfer factors.

It should also be noted that a previous independent assessment, provided in *Description of Methodology for Biosphere Dose Model BDOSE*, ADAMS Accession Number ML083190829, also concluded that applying a distribution to these transfer factors proved to be of no significant importance.

B-2

Comment: The animal product pathways included in the dose assessment are the beef, milk, and finfish pathways. A basis for excluding the other animal product pathways (e.g., consumption of poultry and eggs) from the dose assessment is not provided.

Basis: According to Table 4.6-7 in the PA, the animal products assumed to be consumed include meat, milk, and finfish. The meat pathway seems to only include the ingestion of beef. For example, based on the reference cited in Table 4.6-7 as the basis for the amount of meat consumed (WSRC-STI-2007-00004), the amount of meat consumed seems to correspond to the amount of beef eaten, not the total amount of meat. The basis for the exclusion of the consumption of other animal products, such as poultry and eggs, is not clear. Animals other than cows might be raised on site, and these animals would likely consume groundwater from the site and may consume feed grown on site.

According to Tables 2.6 and 2.7 in PNNL-13421 the transfer factors for poultry are greater than those for beef, so the dose from the consumption of poultry could be higher than the dose from the consumption of beef. In addition, radionuclides can also concentrate in eggs. This can be particularly true for lead. Because the results of the performance assessment indicate that one of the key radionuclides is Ra-226, a parent radionuclide of Pb-210, the Pb-210 dose from the consumption of eggs produced on-site may not be negligible.

Path Forward: Provide the basis for the exclusion of animal pathways other than the beef, milk, and finfish pathways or provide an analysis of the dose from other

	animal pathways (e.g., poultry, egg).
	<p>RESPONSE B-2:</p> <p>The exposure pathway for poultry and eggs is not included in the SDF PA compliance model based on a survey of local practices within 50 miles of SRS.</p> <p>A survey of land and water usage characteristics within a 50 mile region of SRS was conducted and documented in WSRC-RP-91-17, <i>Land and Water Use Characteristics in the Vicinity of the Savannah River Site</i>, March 1991. The results of this study found that chickens are raised on farms within 50 miles of the SRS; however, chickens are housed in covered shelters and eat feed provided by the parent companies responsible for marketing the final product. Thus, the local consumption of chicken (and eggs) is not considered in the determination of “meat” production or consumption with respect to potential dose exposure pathways.</p> <p>As indicated in NUREG-1854, <i>NRC Staff Guidance for Activities Related to U.S. Department of Energy Waste Determinations, Draft Final Report for Interim Use</i>, August, 2007, Section 4.1.1.2:</p> <p><i>Scenarios used in the performance assessment should generally account for site-specific data and information about the characteristics of the site and surrounding region (including local practices), potential disruptive processes, and temporal behavior of the engineered and natural barriers. As necessary, the scenarios that are evaluated in the performance assessment should be constrained in a manner consistent with the relevant guidance provided in this document (e.g., scenarios should be based on past, current, and projected future activities at the site).</i></p> <p>Therefore, based on the survey of local practices within 50 miles of the SRS, the dose pathway from the consumption of contaminated poultry and eggs is not included in the SDF PA compliance model.</p>
B-3	<p>Comment: The effects of radionuclide build-up in irrigated soils may be underestimated.</p> <p>Basis: Descriptions of the biotic pathways in 5.4.1 appear to present conflicting information about the consideration of radionuclide build-up in irrigated soil. For example, Section 5.4.1.2 describes the calculation of the dose from direct exposure to irrigated soil, but does not specify how soil concentrations are calculated. The equation for the dose from the ingestion of vegetables in Section 5.4.1.1 appears to use groundwater concentrations, and does not appear to account for build-up of radionuclides in irrigated soils after multiple years of irrigation. Because vegetable uptake is a significant pathway (see PA Table 5.5-9), neglecting radionuclide build-up in soil could affect the final dose results.</p> <p>Furthermore, Section 5.6.3.7.4 indicates that for both the intruder and off-site member of the public, irrigation and harvesting of vegetables is assumed to occur during the first year of residence, and only uses a 183 day radionuclide build-up time. No explanation is provided of why irrigation and harvesting of vegetables is not assumed to occur in subsequent years, when radionuclide concentrations in soil could have increased due to build-up.</p> <p>Path Forward: Explain how radionuclide build-up in soils was considered in the</p>

biotic pathways described in Section 5.4 of the PA. If radionuclide build-up is neglected, justify why it is neglected or provide an estimate of the effects on the dose results. Provide an explanation for why a 183 day build-up time is used, as described in Section 5.6.3.7.4, and why irrigation and harvesting of vegetables is assumed to occur for only one year. Alternately, provide an estimate of the effect on dose of considering radionuclide build-up during multiple years of irrigation.

RESPONSE B-3:

As shown in the SDF PA Section 5.4.1.1, the build-up of radioactivity in the soil is calculated in the "ROOT" component of the vegetable pathway. The computation of radionuclide concentration in fodder for the beef cow and milk cow utilizes the vegetable concentration equation (with no washing fraction) and thus includes the "ROOT" component. However, for the ingestion of soil the radionuclide concentration of well water is used rather than the radionuclide concentration in the soil. The expression for external exposure from irrigated soil does not include a soil buildup.

The use of 183 days as buildup in the soil is used to account for the fact that the radionuclide concentration of well water, the source of irrigation, is ever changing and the buildup is conservatively assessed without consideration of rainfall dilution, soil porosity, and K_d values for the soil. However, to examine the impact of a longer buildup time, the current expression for the "ROOT" component of the vegetable and fodder concentrations is used with a buildup time of 10,958 days (30 years) which is one-half of an expected exposure period for an adult. In addition, the soil ingestion pathway and the external exposure pathway from irrigated soil are revised to use a 30 year buildup of radionuclides in the soil.

The equation for dose from soil ingestion is revised for this response (with the density of soil assumed to be 1 kg/L) to read:

$$D = \frac{C_{GW} \times DCF \times U_D \times (1 - e^{-\lambda_i t_b}) \times I}{\lambda_i \times T_D}$$

Where:

- D = dose from soil ingestion (mrem/yr)
- C_{GW} = groundwater concentration (pCi/L)
- DCF = Ingestion dose conversion factor (rem/ μ Ci)
- U_D = human consumption rate of dirt (kg/yr)
- λ_i = radiological decay constant (1/d)
- t_b = buildup time of radionuclides in soil (30 years)
- I = irrigation rate (L/m^2 -d)
- T_D = garden till depth (15 cm)

The equation for external dose from irrigated soil is revised for this response to read:

$$D = \frac{C_{GW} \times DCF \times (1 - e^{-\lambda_i t_b}) \times I \times F_G}{\lambda_i \times T_D}$$

Where:

- D = external dose from irrigated soil (mrem/yr)
- DCF = external dose conversion factor, 15cm (rem/yr per $\mu\text{Ci}/\text{m}^3$)
- F_G = fraction of time spent in garden (unitless)

All other terms are as defined above.

The table below compares the peak MOP dose results between the current dose equations as described in the SDF PA with the 183 day buildup time for the vegetable, beef, and milk pathways and the revised dose equations which includes a 30 year buildup for vegetable, beef, milk, soil ingestion and external soil exposure pathways.

Table B-3.1: Peak MOP Dose vs PA Model with 183 Day Buildup Time

Pathway	Peak MOP Dose (mrem/yr) at 10,000 years		
	Current ¹	Revised ²	Difference
Vegetable in Sector B	0.308	0.321	0.0130
Vegetable in Sector I	0.0259	0.0271	0.0012
Milk in Sector B	0.0154	0.0163	0.0009
Milk in Sector I	0.00553	0.00576	0.0002
Beef in Sector B	0.00989	0.0115	0.0016
Beef in Sector I	0.0103	0.0107	0.0004
Soil Ingestion in Sector B	7.5E-05	1.9E-02	0.0189
Soil Ingestion in Sector I	6.3E-06	1.6E-03	0.0016
Soil Exposure in Sector B	1.9E-06	1.1E-04	0.0001
Soil Exposure in Sector I	1.6E-07	9.8E-06	~0.0000
Total Dose in Sector B	1.39	1.42	0.0300
Total Dose in Sector I	0.416	0.419	0.0030

1: Using current PA dose equations.

2: Using revised dose equations.

As expected, Table B-3.1 shows that the revised dose equations do increase dose from pathways that are functionally dependent on soil buildup of radionuclides. Soil ingestion and soil exposure pathways show the greatest relative change from their SDF PA estimated values however, the change to the total MOP dose remains small. The MOP dose from all groundwater pathways is not appreciably impacted compared to the current PA model.

Recognizing that the revised model presented above conservatively assesses the buildup of radionuclides without the depletion that should be considered from rainfall, soil porosity, and K_d values; the current PA model does not warrant revision to directly incorporate the buildup of radionuclides in the soil.

ALARA Analysis (A)

<p><u>A-1</u></p>	<p>Comment: Social, economic, and public policy considerations do not appear to have been considered in an analysis of maintaining doses “As Low as is Reasonably Achievable” (ALARA).</p> <p>Basis: The performance objectives of 10 CFR Part 61, Subpart C, require that doses to the off-site member of the public and to workers be maintained ALARA. As discussed in Section 5.7 of the PA, the goal of the ALARA process is to attain the lowest practical dose given social, technical, economic, and public policy considerations. The discussion in Section 5.7 provides several examples of technical issues that were considered in the ALARA analysis, but does not include a discussion of social, economic, or public policy considerations. Typically, an ALARA analysis presents dose savings and the economic costs of those dose savings, as well as any other costs, such as potential increases in the dose to site workers.</p> <p>Path Forward: Provide a discussion of any social, economic, and public policy issues that were considered in concluding that doses have been maintained ALARA.</p>
<p><u>RESPONSE A-1:</u></p> <p>The goal of the ALARA process is the attainment of the lowest practical dose level after taking into account social, technical, economic, and public policy considerations. Depending on the situation, the ALARA analysis can range from simple qualitative statements evaluating different operation and disposal options for LLW to rigorous quantitative analyses that consider individual and collective doses to the MOP. The rigor of the ALARA analysis should be commensurate with the magnitude of the calculated dose and the decisions to be made regarding the disposal facility. Based on Table 8.1-1 of the SDF PA Section 8.1, the estimated dose pathways evaluated in the PA are well below the performance objectives; therefore, a qualitative assessment of disposal alternatives is justified.</p> <p>Another alternative to in-situ disposal of the LLW salt fraction in saltstone is to ship the solidified saltstone waste offsite. Public perceptions and resulting concerns about shipping LLW to an off-site facility have the potential to affect the social, political, and economic costs of such actions. Proposed actions that are considered unacceptable by an element of the society often face significant opposition that increases the time and cost required to complete each step of the decision-making and implementation processes. This can lead to large cost-uncertainty associated with shipping waste off-site. Therefore, any potential collective dose savings of shipping the waste off-site is unlikely to outweigh the cost-benefits of processing and disposing of the salt solution waste stream on-site at the Saltstone Facility.</p>	

Clarifying Questions

<u>C-1</u>	Section 3.2.1.1.2 discusses a 3-inch gap between disposal units in Vault 1. Clarify whether the area referred to as a gap is an open area that could fill with rainwater or if it represents a wall or barrier between disposal units.
<p><u>RESPONSE C-1:</u></p> <p>Vault 1 is divided into two units, each 100 by 300 feet, with a 3 inch separation gap between the units. The separation gap is an open area for expansion and contraction purposes. The gap contains a 3 inch Styrofoam gasket. Since the gap contained Styrofoam, it was modeled as a void that would not restrict flow or retard contaminant transport.</p>	
<u>C-2</u>	Section 4.2.1.1 indicates that daughters other than daughters of Cf-249, Pu-244, Pu-242, and Cm-243 were “removed from modeling consideration and were not assigned an initial SDF inventory”. Clarify if the radionuclides removed from consideration were limited to daughters whose initial inventory was determined not to be significant, or if any daughters were removed whose initial inventory was unknown.
<p><u>RESPONSE C-2:</u></p> <p>The intent of the SDF PA statement: “Therefore, the other daughter product radionuclides were removed from modeling consideration and were not assigned an initial inventory” was to acknowledge that these other daughter product radionuclides are not assigned an initial inventory however, the production of these radionuclides via decay are included in the model. The SDF PA Section 4.2.1.1 addresses the rationale used to eliminate from the initial inventory those radionuclides identified in PA Table 4.2.2 that appear as daughters in the principal decay chains presented in PA Table 4.2.3. Of the 60 radioactive isotopes identified in PA Table 4.2.3, only 22 have an initial inventory presented in the SDF PA analysis. The remaining 38 radioactive isotopes from Table 4.2.3 are not included in the initial SDF PA inventory because within 100 years after closure, their initial inventories are assumed to be insignificant due to their short half-lives. Because of their short half-lives, these radionuclides will reach equilibrium with their parents in a short time frame and the modeling software accounts for this in-growth. No radionuclides were eliminated because their inventory was unknown.</p>	
<u>C-3</u>	Clarify points 3 and 4 in Section 4.2.3.2.4 of the PA. Vault 4 walls seem to be assigned two different conflicting sets of material properties (high quality concrete and fractured concrete). Similarly, in the “hydraulic conductivity” column of Table 4.2-16, Vault 4 walls appear in two rows with two different hydraulic conductivities assigned. Clarify under what circumstances, if any, each hydraulic conductivity was used.
<p><u>RESPONSE C-3:</u></p> <p>Points 3 and 4 in the SDF PA Section 4.2.3.2.4 are indicating that the concrete used in the walls of Vault 4 are considered “high quality” concrete as shown in the SDF PA Table 4.4-2 and that the walls of Vault 4 are modeled with the properties of “high quality” concrete with the exception of, 1) a much larger initial value for hydraulic conductivity than what is assumed for “high quality” concrete and 2) a characteristic curve associated with “fractured concrete”. The</p>	

hydraulic conductivity value of $3.1E-10$ cm/sec in Table 4.2-16 is only used for the high quality concrete associated with the Vault 4 floor and is not used at any time for the Vault 4 walls.

C-4

Clarify the basis for the selenium K_d of 150 mL/g for old oxidizing conditions. It is not clear from the PA, or the supporting report WSRC-STI-2007-00640, how the value was selected. Clarify whether the evaluation considered the presence in solution of the selenium as selenate, which is potentially less sorptive than selenite.

RESPONSE C-4:

As indicated in the SDF PA source document, SRNS-STI-2008-00045, site-specific batch experiments intended to replicate all three stages of an oxidizing cementitious environment measured selenium K_d values ranging from 29.7 to 78.5 mL/g. The measured selenium K_d s reported in SRNS-STI-2008-00045 are, in general, lower than values reported in literature (e.g., ISSN: 0956-0536; DOI: 10.1021/es020148d). SRNS-STI-2008-00045 attributed the unexpectedly low experimental values to having aqueous selenium concentrations near the detection limits, therefore the experimental values were not utilized and literature sorption values were used in the selection of an appropriate K_d .

The basis for the selenium K_d of 150 mL/g for old oxidizing conditions relies on the sorption values reported in DOI: 10.1021/es020148d because experimental conditions in *Cementitious Near-Field Sorption Data Base for Performance Assessment of an ILW Repository in Opalinus Clay* (OSTI ID: 20406660) were not consistent with conditions expected in Stage 3 cements. Selenite is expected to be the predominant form of selenium at pH levels of 13.5 and redox potentials equivalent to 80 mV, typically found in the pore spaces of young-aged and middle-age cements such as Stage 1 and 2 as shown in *Handbook of Geochemistry, Vol II* (Dewey Dec No. 551.9), whereas selenate species is typical of oxygen saturated cements.

Sorption of Selenite and Selenate to Cement Materials (DOI: 10.1021/es020148d) reported selenate K_d values between 180 and 380 mL/g and showed strong selenate sorption. The OSTI ID: 20406660 used selenite in cementitious material sorption experiments and reported K_d values of 30 to 100 mL/g. The OSTI ID: 20406660 values were discounted because more oxidized conditions are expected in the Stage 3 cements, which would convert selenite to selenate. The value of 150 mL/g was therefore selected because it was lower than the range reported by DOI: 10.1021/es020148d which represents expected conditions and because it was considered conservative.

Additionally, in Stage 3, as the cementitious materials degrade, the selenium sorption constants approach that of the sediment. Selenate K_d values of 1041 ± 0.7 were measured in background SRS sediments. [WSRC-STI-2006-00037] Selenium sorption in sediments is very high due to the ubiquitous presence of iron oxides and low pH of our sediments. Therefore, comparison of the site-specific sorption studies of selenium with SRS sediment with the selection of 150 mL/g, provides additional confirmation that the Stage 3 K_d value used in the SDF PA is conservative.

C-5	The near field velocity profiles should be included in Section 4.4.4.1.2 as the flow in the saltstone is difficult to ascertain from the velocity vectors provided with the saturation profiles.
------------	--

RESPONSE C-5:

The near field velocity profile figures from the SDF PA Section 4.4.4.1.2 have been recreated showing only the Darcy Velocity and are provided as Figures C-5.1 through C-5.6.

Figure C-5.1: Darcy Velocities (cm/yr) for SDF Vault 1 (Case A) – Log Scale

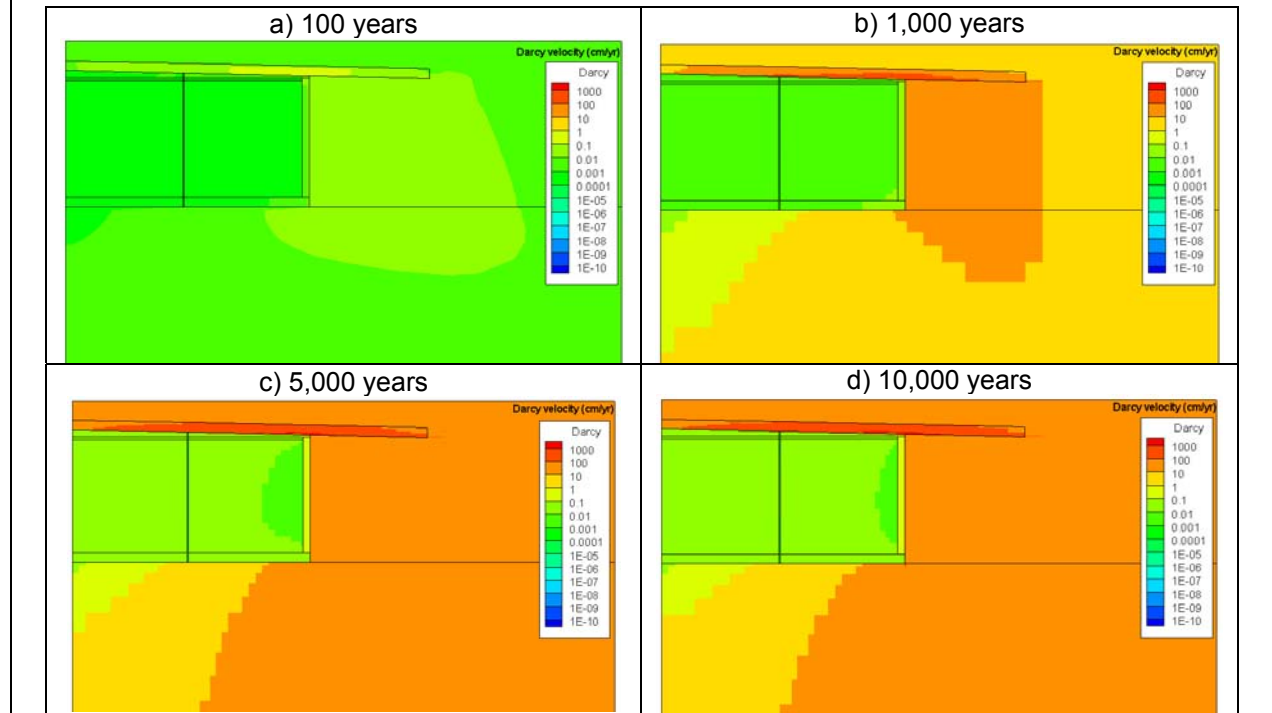


Figure C-5.2: Darcy Velocities (cm/yr) for SDF Vault 1 (Case A) – Log Scale (Bottom Corner)

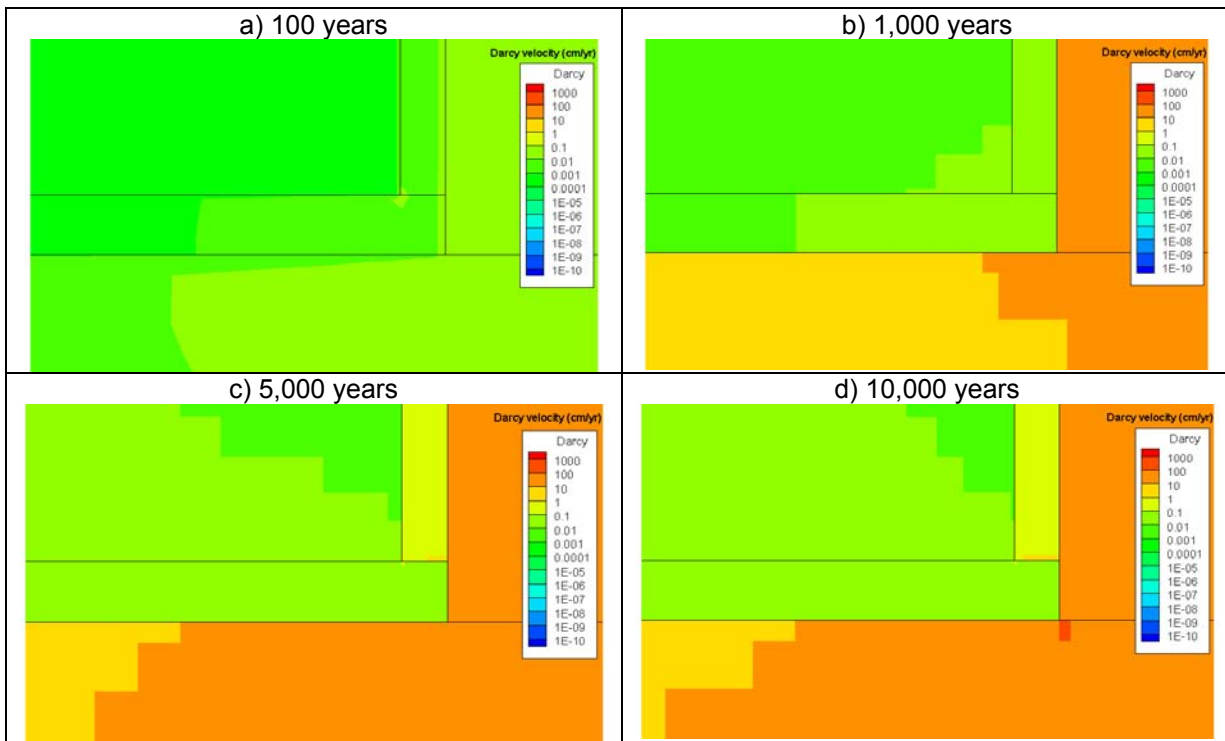


Figure C-5.3: Darcy Velocities (cm/yr) for SDF FDCs (Case A) – Log Scale

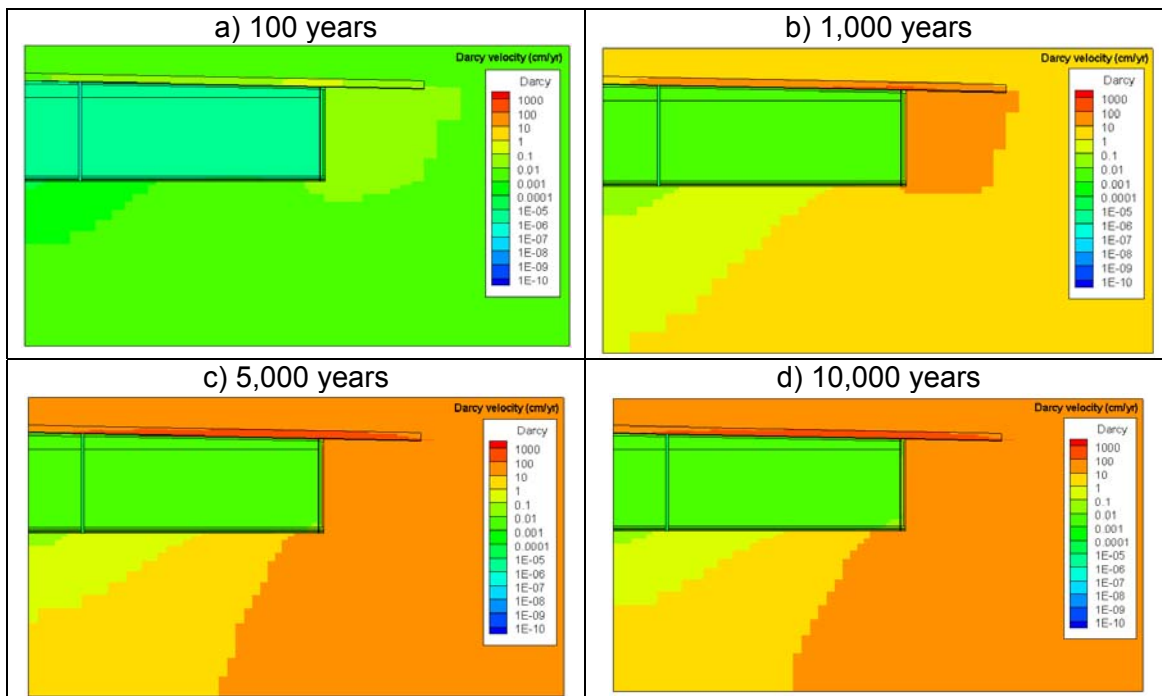


Figure C-5.4: Darcy Velocities (cm/yr) for SDF FDCs (Case A) – Log Scale (Bottom Corner)

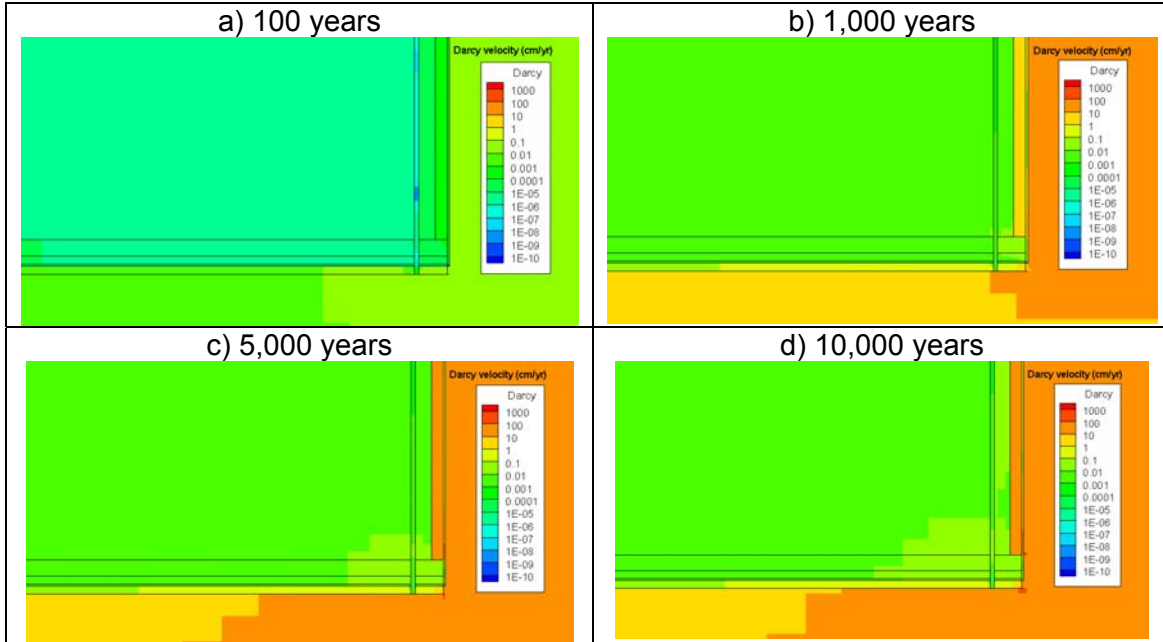


Figure C-5.5: Darcy Velocities (cm/yr) for SDF Vault 4 (Case A) – Log Scale

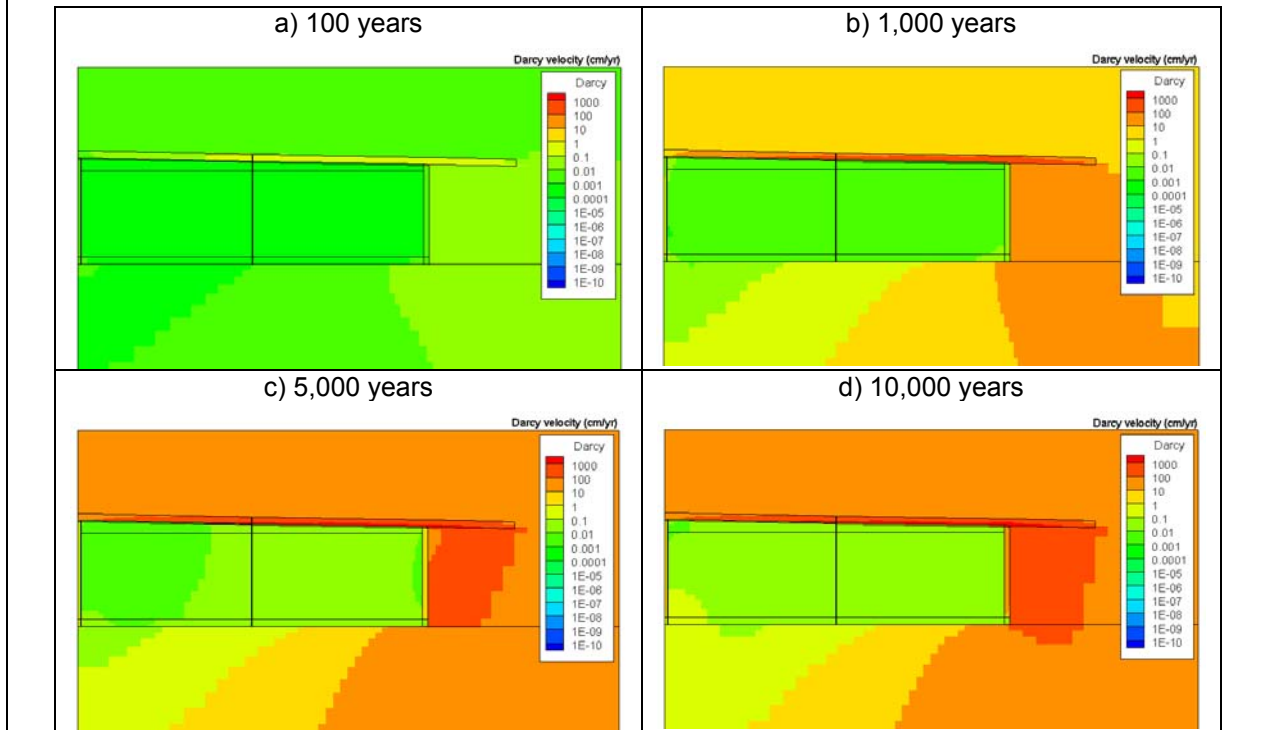
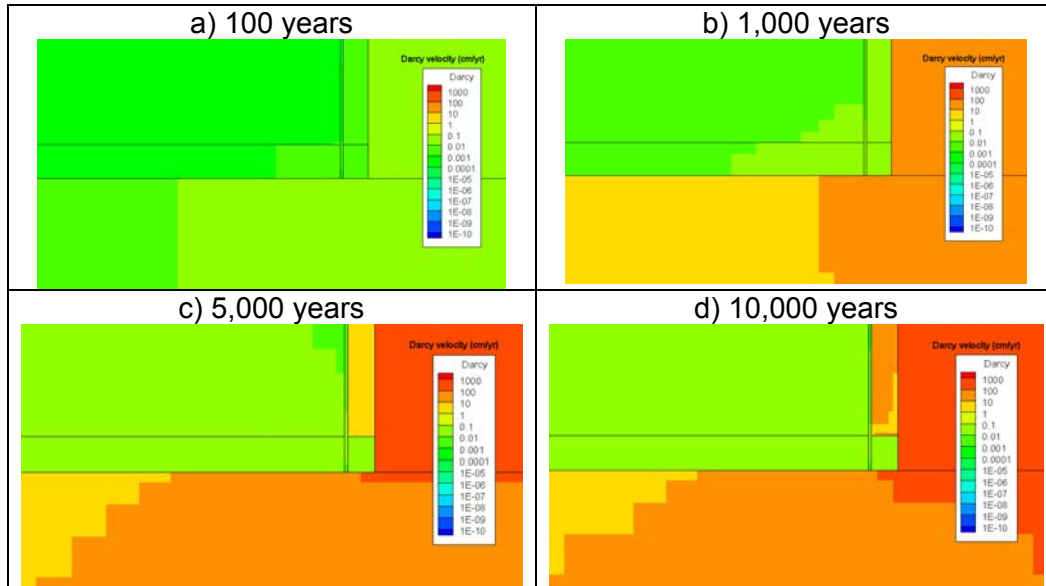


Figure C-5.6: Darcy Velocities (cm/yr) for SDF Vault 4 (Case A) – Log Scale (Bottom Corner)



C-6

The “Diffusion Model Implementation” subsection of Section 4.4.4.2.2 indicates the solution to the diffusion model was valid only for radionuclides existing at time equal to zero, and notes “the model does not explicitly recognize in-growth”. The subsection also indicates “However in-growth was implicit to the model via the species concentrations used as arguments in the model.” The meaning of these statements is not clear, because GoldSim cell networks do account for in-growth.

RESPONSE C-6:

The GoldSim cell networks do account for in-growth. The intention of the statements that the diffusion model “solution was valid only for those radionuclides which exist at time equal to zero”, and “the model does not explicitly recognize in-growth” was to clarify that the analytical diffusion solution is based on the inventory that exists at the beginning of a modeling time step. If a daughter radionuclide were to be produced via in-growth during a time step, it would not be transported by the diffusion equation; therefore, in-growth is not an explicit term in the diffusion equation. The concentrations within a cell will change as a result of the GoldSim transport and decay calculations, so the initial condition (at the beginning of a time step) of the diffusion solution is based on the GoldSim advective transport. The diffusion equation picks up the species vector as its starting point, so that is the manner in which in-growth is “implicit” to diffusion.

C-7

Section 5.5.1.2 indicates the significant spike of I-129 in Sector I at 15,080 years is due to the FDC wall hydraulic conductivity increasing by four orders of magnitude at year 15,080. This result seems to imply that the I-129 peak is seen in the 100 m well the same year the I-129 is released from the FDC walls, and does not appear to allow for transit time. If this result is an artifact of time-stepping, it seems the I-129 should arrive at the 100 m well in the next time step, not in the same time step in which the FDC walls are degraded. Please clarify the statement in Section 5.5.1.2.

RESPONSE C-7:

In clarification of the statement in the SDF PA Section 5.5.1.2, the I-129 spike at year 15,080 is due to the increase of hydraulic conductivity by four orders of magnitude that occurs within 15,000 years, not at 15,080 years after closure. This information is presented in footnote (f) shown below PA Table 4.4-9 on page 263.

C-8

For benchmarking cases B-E (Sections 5.6.2.3.5 through 5.6.2.3.8), the PA compares the doses predicted based on the PORFLOW model and post-benchmarking GoldSim model resulting from “all modeled radionuclides”. Clarify whether the term “all modeled radionuclides” in this context refers to the original list of radionuclides included in the PORFLOW model or a smaller list of radionuclides modeled during the benchmarking effort.

RESPONSE C-8:

As discussed in the SDF PA Section 4.2.1.1, “The inventory of each isotope that was used in the modeling is provided in the SDF PA Section 3.3, which presents the expected inventory in the disposal units at the time of closure. An inventory was developed for the 70 isotopes presented in Table 4.2-5.” For the Base Case PORFLOW modeling, the complete inventory list was addressed, with a shorter list (determined in the SDF PA Section 5.2.2, Key Rad Determination) utilized for sensitivity runs and alternate configurations.

However, the key rad determination was not used to screen radionuclides from the GoldSim model inventory list, and it includes nearly all of the radionuclides included in the Base Case PORFLOW modeling. Some of the radionuclides included in the SDF PA Section 3.3 inventory were not modeled in GoldSim because transport modeling was not required (e.g., their half-lives are so short that they only are significant as a result of in growth at the evaluation location). As noted in the SDF PA Section 4.2.1.1, Appendix Table I6-1 lists those radionuclides not included in the GoldSim modeling (Ba-137m, Bk-249, Ce-144, Cf-252, Cm-242, Cs-134, Eu-155, Na-22, Pm-147, Pr-144, Rh-106, Ru-106, Sb-125, Sb-126, Sb-126m, Te-125m, and Y-90).

The term “all modeled radionuclides” in the referenced context refers to a) the radionuclides included in the SDF PA Section 3.3 inventory for Base Case PORFLOW modeling results, b) the radionuclides listed in the SDF PA Section 5.2.2 Key rad determination for sensitivity and alternate configuration PORFLOW modeling, and c) the radionuclides included in the abridged GoldSim transport inventory (listed in Appendix Table I6-1) for all GoldSim modeling results (e.g., the uncertainty analyses, benchmarking).

C-9

Section 5.6.6.3 indicates the peak dose in Sector B within 10,000 years is 2.1% greater in the sensitivity case representing 10 X faster sulfate diffusion behind the ettringite front than it is in the base case. However, the data in Table 5.6-19 indicate the dose increases from 1.4 mrem/yr to 1.7 mrem/yr (or approximately 21%). Clarify which is the correct information.

RESPONSE C-9:

Table 5.6-19 provides the correct information. Thus, the peak MOP dose in Sector B for the 10 times sulfate case is approximately 21% greater than the Base Case (Case A).

<p><u>C-10</u></p>	<p>As described in Section 5.6.6.3, to test the effects of the assumption that the progress of the ettringite front is unaffected by physical degradation of concrete behind the front, a sensitivity case was run for a case in which the diffusion coefficient is increased by a factor of 10. However, it is not clear whether this diffusion coefficient is applied in the entire block of cementitious material, or if it is applied only behind the ettringite front. The diffusion coefficient value used in this sensitivity case is based on an empirical relationship between the diffusion coefficient and hydraulic conductivity (Equation (1) in Section 5.6.6.3) (Figure 5.6-76), but no reference is supplied for the data. In addition, Section 5.6.6.3 indicates that soil suction levels under nominal saltstone closure cap degradation conditions vary through space and time across a typical range of approximately 0.10 to 0.01 cm, and that the conductivity of cracked concrete ranges up to three orders of magnitude higher than the conductivity for uncracked concrete in this range. However, Figure 5.6-77 does not show this range of suction heads. Clarify whether the modified diffusion coefficient is applied only behind the ettringite front or in the entire block of cementitious material. Supply a reference for the data used in Figure 5.6-76. Clarify whether the reported range of relevant suction heads in Section 5.6.6.3 is correct and, if necessary, modify Figure 5.6-77 to show the applicable range of suction heads.</p>
<p><u>RESPONSE C-10:</u></p> <p>The calculation for ettringite front movement involves estimating the delivery of reactants from the exposure surface to the ettringite front via diffusion. The diffusion coefficient entering the calculation applies to the region behind the ettringite front.</p> <p>The data plotted in Figure 5.6-76 comes from the materials palette used in PORFLOW modeling (Table 4.4-10), as indicated in SRNL-L6200-2009-00011.</p> <p>The range of relevant suction heads in the SDF PA Section 5.6.6.3 should be a "few 10s to a few 100s of centimeters" per SRNL-L6200-2009-00011 (i.e., 10 cm < suction < 1,000 cm).</p>	
<p><u>C-11</u></p>	<p>Section 5.6.6.5 of the PA states that the saltstone is assumed to be cracked at the time of closure in the synergistic case. However, the extent and location of the fractures is not specified. Please provide the number of fractures, the assumed location of the fractures, and the assumed fracture area.</p>
<p><u>RESPONSE C-11:</u></p> <p>In the synergistic case, the fractures are modeled as being vertical and as fully penetrating the saltstone. The fracture spacing is 2.5 feet and their aperture is 0.1 feet. The fracture aperture is assumed to be filled with material having the properties of sand (denoted as "column_crack" material in the materials palette). The "fracture area" (either the cross-sectional area or fracture face surface area) can be calculated using the saltstone dimensions, spacing, and aperture data.</p> <p>In the FDCs calculation, the fractures exist in the form of concentric (thin) cylinders of varying radius. Each perimeter value is the distance around the inside or outside face of the fracture. The crack perimeter and cross-sectional area must be computed individually for each fracture and summed to get the total area.</p>	

The cross-sectional area and fracture face surface area for each disposal unit type is calculated and shown in Table C-11.1.

Table C-11.1: Cross-sectional Area and Fracture Surface Area

Attribute	Units	Vault 1	Vault 4	FDCs
		Value		
Cracks (c)	per width	36	76	29
Aperture (a)	feet	0.1	0.1	0.1
Saltstone Height (H)	feet	24	24.75	20
Nominal Length (L)	feet	600	600	14,188
Cross-sectional Area (c*a*L)	feet ²	2,160	4,560	709
Surface area (c*H*L*2)	feet ²	1,036,800	2,257,200	283,761

C-12 Section 7.1.1.4 indicates that peaks at 15,000 and 16,000 years are due to hydraulic and chemical failures of the FDC walls, respectively. The dose results from the synergistic case (Figure 5.6-83) show the characteristic peak between 15,000 and 16,000 years even though the FDC walls are assumed to fail chemically and hydraulically at 500 years. Clarify the origin of the dose peak between 15,000 and 16,000 years in the synergistic case.

RESPONSE C-12:

The dose peak between 15,000 and 16,000 years in the synergistic case is due to the change in the hydraulic conductivity of the Lateral Drainage Layer placed above the individual disposal units. The Lateral Drainage Layer is designed to divert water away from the disposal units. As the Lateral Drainage Layer degrades over time, as presented in the SDF PA Section 4.2.3.2.2, the hydraulic conductivity decreases which reduces the diversion of water away from the cells and thus, increases the flow of infiltrating water into the disposal units. The SDF PA Figure 4.2-15 illustrates the rate of degradation with respect to the vertical hydraulic conductivity associated with the Lateral Drainage Layer based on the analysis presented in SRNL-STI-2009-00115.

C-13 Section 7.2.2 lists the assumption that there is not HDPE-GCL layer over Vault 1 and 4 as a conservative assumption. Section 4.2.3.2.2 indicates the HDPE-GCL layer that will be placed above each FDC will not be placed above Vaults 1 and 4. Clarify whether this is a conservative assumption or if the HDPE-GCL layers will not be placed above Vaults 1 and 4.

RESPONSE C-13:

The SDF PA Section 4.2.3.2.2 correctly indicates the HDPE-GCL layer will be placed above each FDC, and not above Vaults 1 and 4. This item should be removed from the list in the SDF PA Section 7.2.2 indicating that the exclusion of the HDPE-GCL layer over the roof of Vault 1 and 4 is a conservative assumption.

As noted in the SDF PA Section 3.2.2, the design information provided is for planning purposes sufficient to support evaluation of the closure cap. Final design and a re-evaluation of infiltration will be performed near the end of the operational period. Addition of a HDPE-GCL layer over the roof of Vaults 1 and 4 will be considered in the revision to the SDF Closure Plan.

C-14	Section 8.2 indicates that the probabilistic sensitivity analyses demonstrated that the groundwater doses are most sensitive to the specific radionuclide inventories. Tables 5.6-14 and 5.6-15, however, appear to indicate that the dose in Case A and Case C are most sensitive to parameters related to radionuclide release and transport, and parameters related to vegetable production and consumption. Clarify the conclusion presented in Section 8.2 or the results presented in Tables 5.6-14 and 5.6-15 as appropriate.
<p>RESPONSE C-14:</p> <p>The SDF PA Tables 5.6-14 and 5.6-15 correctly indicate that the most sensitive parameters for the dose endpoints are dominated by elemental-specific K_d values of concrete or soil. The importance of these parameters can be influenced by the estimated radionuclide inventory assumed in the model. Recognizing this influence on the importance of these K_d values in the model, the emphasis on understanding and improving model uncertainty, with respect to radionuclide inventory identified in SDF PA Section 8.2, is warranted.</p>	
C-15	Clarify the technical basis for the plutonium K_d of 1000 mL/g for old oxidizing cementitious materials. The source cited in PA Table 4.2-18 (SRNL-TR-2009-00019) refers to one document (SRNS-STI-2008-00045, Tables 4 and 5) that does not appear to give this value and to another (WSRC-STI-2007-00640, Table 4) that does not appear to include the cited table.
<p>RESPONSE C-15:</p> <p>The technical basis for the recommended plutonium K_d value for old oxidizing cementitious materials is based on measured values reported in Table 2 of WSRC-STI-2007-00640, and confirmed in Table 2 of SRNS-STI-2008-00045 for Pu (IV/V) onto aged cement in CaCO_3 solution, which was taken as an analogue for old-age cement under oxidizing conditions. These measured values are 2 to 3 orders of magnitude greater than the literature values that formed the basis for using the previous recommended value of 500 mL/g for old-age cementitious material (see Table 3 of WSRC-STI-2007-00640).</p> <p>Although not explicitly stated in SRNL-TR-2009-00019, an updated plutonium K_d value for old-age oxidizing cement is recommended to be 1,000 mL/g because doubling the previously used value of 500 mL/g would increase the value to better reflect the information from the new-site specific experimental values reported for plutonium under oxidizing old-age conditions, but would still be conservative.</p>	
C-16	Clarify the difference between the entries “Ancestors not present” and “no decay source” in the column “reason for elimination from initial inventory” of Table 4.2-6.
<p>RESPONSE C-16:</p> <p>“Ancestors not present” refers to those radionuclides that are part of a decay chain in which the parent of that decay chain is not present in SRS waste. “No decay source” refers to a radionuclide that is not produced from decay.</p>	

C-17	Provide the saturation of the vault and FDC walls in Tables 4.5-4 through 4.5-6 to allow independent verification of unsaturated hydraulic conductivities.
<p>RESPONSE C-17:</p> <p>For the Base Case (Case A), the wall saturation is approximately 0.99 for Vaults 1 and 4 and approximately 1.0 for FDCs. The wall saturation average values were generated through a review of the time varying values captured in the PORFLOW output data. The vadose zone flow figures in the SDF PA Section 4.4.4.1.2 provide examples of saturation fields for the different disposal cells at discrete times. Since the saturation value varies through space and time, the approximate values in the tables are averages suitable for use in the air pathway analysis. For unsaturated hydraulic conductivity, the PORFLOW input data electronic files provide more precise values.</p>	
C-18	Tables 5.6-12 and 5.6-13 report doses from the GoldSim model for Cases A and C. Clarify which sectors correspond to the reported maximum dose to a member of the public at any sector within 20,000 years.
<p>RESPONSE C-18:</p> <p>As stated in the SDF PA Section 5.6.4, "Statistics for maximum values for TEDE and groundwater concentrations are summarized in Tables 5.6-12 and 5.6-13 for failure scenarios Cases A and C respectively. The values in the tables show the statistics (mean, median, and 95th percentile) on the maximum." As shown in Tables 5.6-12 and 5.6-13, the results presented correspond to either Sector B, Sector J, or to "any Sector". The data presented for "Maximum MOP dose at any Sector within 20,000 years" includes peak dose data from each realization regardless of the sector associated with the dose. The "any Sector" data tends to resemble the Sector B data within 10,000 years and the Sector J data within 20,000 years because these are the two sectors which tend to contain the peak doses, but there may be individual realizations where the peak dose is not from either Sector B or Sector J.</p>	
C-19	Table 5.6-18 indicates that in the base case, the Vault 4 wall is assumed to be hydraulically failed after 100,000 years. In other locations, the PA indicates that the Vault 4 wall is assumed to be hydraulically failed at time equal to zero. Table 5.6-18 also indicates that in the 10X sulfate attack case, the Vault 4 wall is assumed to be hydraulically degraded at 16,000 years. Clarify whether the Vault 4 wall is assumed to fail hydraulically at 16,000 years in the 10X sulfate case, or whether it is assumed to be failed at time equal to zero. Clarify whether this timing is before or after the wall is assumed to degrade hydraulically in the base case.
<p>RESPONSE C-19:</p> <p>The walls of Vault 4 (and Vault 1) are assumed to be initially degraded (time equal to zero) with a very high hydraulic conductivity of 1.7E-01 cm/sec, as shown in PA Table 4.2-16. The terminology "complete failure" used in Table 5.6-18 is the condition where the Vault 4 wall has degraded to the extent that the hydraulic properties of the concrete are set equal to those of the surrounding soil. In the "10 times sulfate" case the ettringite front from sulfate attack passes through the Vault 4 wall within 16,000 years making the wall "degrade" to a hydraulic conductivity of soil which is 7.6E-05 cm/sec for horizontal hydraulic conductivity and 4.1E-05 cm/sec for vertical hydraulic conductivity.</p>	

<u>C-20</u>	In Table 6.5-2, it is not clear what the difference is between rows 1 and 2 or between rows 3 and 4 of this table. Please clarify the row labels.
<u>RESPONSE C-20</u> Row 2 of Table 6.5-2 indicates the Mean, Median, and 95th percentile values of the dose to the intruder in Sector B for Case A within 20,000 years (not 10,000 years). This information can be seen in PA Figure 6.5-4. Row 4 of Table 6.5-2 indicates the Mean, Median, and 95th percentile values of the dose to the intruder in Sector J for Case A within 20,000 years (not 10,000 years). This information can be seen in SDF PA Figure 6.5-5.	
<u>C-21</u>	Comment response 36 in CBU-PIT-2005-00131 states that any fracturing of saltstone lifts will be filled in by the succeeding pour. However, the “Z-Area Industrial Solid Waste Landfill Vault Cracking” (ESH-WPG-2006-00132) states that saltstone will not flow through any cracks in the vault walls because it is too viscous and sets up very quickly. Clarify the conditions under which saltstone is expected to flow into cracks in cementitious materials and whether these conditions explain the different conclusions made with respect to saltstone flowing into saltstone lifts and vault walls.
<u>RESPONSE C-21:</u> The two scenarios discussed in this clarifying comment are different and do not present a conflict with respect to cementitious materials performance. When comment response 36 in CBU-PIT-2005-00131 states that any fracturing of saltstone lifts will be filled in by the succeeding pour, the scenario being discussed is gaps or cracks that could form in the individual layers of the grout surface from the different pours. The subsequent pour would flow vertically into small-scale shrinkage cracks that could be present at the end of the previous pour. The sentence in <i>Z-Area Industrial Solid Waste Landfill Vault Cracking</i> (ESH-WPG-2006-00132) states that “the saltstone grout cannot flow through the cracks as it is too viscous and sets up very quickly”. This sentence is referencing the side wall cracks in Vaults 1 and 4 caused by hydrostatic pressure buildup of liquids in the spaces between the grout monolith and the vault wall. Since these cracks are in the side wall and formed post-construction as a result of hydrostatic pressures, the grout pours are not expected to flow into them. The horizontal flow into the side wall cracks (which is discussed in some detail in the response to RAI VP-1) is fundamentally different than vertical flow into the small-scale shrinkage cracks in individual pour layers.	

REFERENCES FOR COMMENT RESPONSES

Note: References identified as (Copyright) were used in the development of the Comment Responses, but are protected by copyright laws. No part of the publication may be reproduced in any form or by any means, including photocopying or electronic transmittal in any form by any means, without permission in writing from the copyright owner.

10 CFR 20, *Standards for Protection Against Radiation*, Nuclear Regulatory Commission, Washington DC, January 1, 2010.

ACI 201.2R, (Copyright), ACI Committee 201, *Guide to Durable Concrete*, American Concrete Institute, Rev. 8, June, 2008.

CBU-PIT-2005-00131, *Response To Request for Additional Information on the Draft Section 3116 Determination for Salt Waste Disposal at the Savannah River Site*, Savannah River Site, Aiken, SC, Rev. 1, July 14, 2005.

C-CLC-Z-00016, Reinhardt, P., *Structure Analysis of Saltstone Vault*, Savannah River Site, Aiken, SC, Rev. 0, June 29, 1994.

C-SOW-Z-00001, Chiappetto, C.A., *Storage Tanks for Primary Containment for Saltstone Facility, Statement of Work*, Savannah River Site, Aiken, SC, Rev. 1, January 17, 2006.

C-SPP-Z-00006, *Saltstone Vault #2 Including Excavation, Liner and Backfill*, Savannah River Site, Aiken, SC, Rev. 1, June 2008.

Dewey Dec No. 551.9, (Copyright), Wedepohl, K. H., *Handbook of Geochemistry, Vol II*, Springer-Verlag, New York, NY, 1978.

DOE-HMIP-RR-92.061-(Pt.1), (Copyright), Berry, J. A., *A Review of Sorption of Radionuclides Under the Near and Far-Field Conditions of an Underground Radioactive Waste Repository*, Harwell Laboratory, Oxfordshire, United Kingdom, 1992.

DOI: 10.1021/es020148d, (Copyright), Baur, I., and Johnson, C. A., *Sorption of Selenite and Selenate to Cement Materials*, Swiss Federal Institute for Environmental Science and Technology, Dubendorf, Switzerland, 2003.

ESH-WPG-2006-00132, *Z-Area Industrial Solid Waste Landfill Vault Cracking*, Savannah River Site, Aiken, SC, October 19, 2006.

ISBN: 0-12-683900-X, (Copyright), Taylor, H.F.W., *Cement Chemistry*, Institution of Civil Engineers Publishing, January 1, 1997.

ISBN: 0733-9429/91/0008-0959, (Copyright), Abt, S.R., et al., *Riprap Design for Overtopping Flow*, Journal of Hydraulic Engineering, Vol. 117, No. 8, Reston, VA, August, 1991.

ISBN: 0-86542-319-9, (Copyright), Nordstrom, D.K., *Geochemical Thermodynamics*, The Benjamin/Cummings Publishing Co., Menlo Park, CA, 1985.

ISBN: 1-55899-151-4, (Copyright), Bayliss, S. A., et al., *Radioelement Behavior in A Cementitious Environment*, Materials Research Society Symposium Proceedings, Vol. 257, Warrendale, PA 2007.

ISBN-10: 0486422259, (Copyright), Robinson, R.A., et al., *Electrolyte Engineering*, Dover Publications, 2 Revised Ed., July 24, 2002.

ISSN 1019-0643, (Copyright), Bradbury, M. H., *Sorption Databases for the Cementitious Near-Field of a L/ILW Repository for Performance Assessment*, Paul Scherrer Institute, Villigen, Switzerland, March 1995.

ISSN: 0008-8846_37, (Copyright), Samson, E., et al., *Modeling the Effect of Temperature on Ionic Transport in Cementitious Materials*, Cement and Concrete Research, Vol. 37, March, 1997.

ISSN: 0016-7037, (Copyright), Henocq, P., et al., *The Influence of the Alkaline Earth Cations, Magnesium, Calcium, and Barium on the Dissolution Kinetics of Quartz*, Cement Association of Canada, Montreal, Canada, August, 2007.

ISSN: 0033-8230, (Copyright), Berner, U.R., *Modeling the Incongruent Dissolution of Hydrated Cement Minerals*, Radiochimica Acta, Vol. 44/45, 1988.

ISSN: 0956-053X, (Copyright), Johnson, E. A., et al., *The Sorption of Selenite on Various Cement Formations*, Elsevier Science Ltd., Waste Management, 20 (7): 509-516 2000.

ISSN: 0958-9465, (Copyright), Galindez, J.M., *On the Relevance of Electrochemical Diffusion for the Modeling of Degradation of Cementitious Materials*, Cement & Concrete Composites, Vol. 32, May, 2010.

K-CLC-F-00073, *Static Settlement of F-Area Waste Storage Tanks 18 and 19*, Savannah River Site, Aiken, SC, Rev. 2, June 20, 2006.

K-ESR-Z-00001, Li, W.T., *Saltstone Vault No. 2 Geotechnical Investigation Report*, Savannah River Site, Aiken, SC, Rev. 0, April, 2006.

K-ESR-Z-00002, Williams, R.J., *Saltstone Disposal Cells No. 3 and 5 Geotechnical Investigation Report*, Savannah River Site, Aiken, SC, Rev. 0, July, 2009.

LA-UR-01-4658, Nyhan, J. W., et al., *Estimation of Soil Erosion in Burnt Forest Areas of the Cerro Grande Fire in Los Alamos, New Mexico*, Los Alamos National Laboratory, Los Alamos, NM, April 2001.

ML053010225, Camper, L.W., *U.S. Nuclear Regulatory Commission Technical Evaluation Report for the U.S. Department of Energy Savannah River Site Draft Section 3116 Waste Determination for Salt Waste Disposal*, Office of Nuclear Material Safety and Safeguards, U.S. Nuclear Regulatory Commission, Washington DC, December 28, 2005.

ML083190829, (Copyright), *Description of Methodology for Biosphere Dose Model BDOSE*, Center for Nuclear Waste Regulatory Analysis, San Antonio, TX, Rev. 1, November 30, 2008.

NUREG/CR-4370, *Update of Part 61 Impacts Analysis Methodology*, Vol. 1, U.S. Nuclear Regulatory Commission, Washington DC, January 31, 1986.

NUREG-1623, *Design of Erosion Protection for Long-Term Stabilization*, U.S. Nuclear Regulatory Commission, Washington DC, September 2002.

NUREG-1854, *NRC Staff Guidance for Activities Related to U.S. Department of Energy Waste Determinations, Draft Final Report for Interim Use*, U.S. Nuclear Regulatory Commission, Washington DC, November 2007.

OSTI ID: 20406660, (Copyright), Wieland, E., and Van Loon, L. R., *Cementitious Near-Field Sorption Data Base for Performance Assessment of an ILW Repository in Opalinus Clay*, Laboratory for Waste Management, Paul Scherrer Institute, Switzerland, August 2003.

PNNL-11966, Kaplan, D. I., et al., *Radionuclide Distribution Coefficients for Sediments Collected from Borehole 299-E17-21: Final Report for Subtask 1a*, Pacific Northwest National Laboratory, Richland, WA, October 1998.

PNNL-13895, Cantrell, K. J., et al., *Hanford Contaminant Distribution Coefficient Database and Users Guide*, Pacific Northwest National Laboratory, Richland, WA, Rev. 1, June 10, 2003.

PORTAGE-08-022, *H-Area Tank Farm Model Development for Tanks in the Water Table PORFLOW Version 6.20.0*, Savannah River Site, Aiken, SC, Rev. 0, November 2008.

SRNL-L3100-2009-00189, Reboul, S. H., *Nickel-59, Cerium-144/Praseodmium-144, and Radium-226 in Salt Feed*, Savannah River Site, Aiken, SC, September 8, 2009.

SRNL-L6200-2009-00011, Flach, G., *PORFLOW Sensitivity Cases for Saltstone PA*, Savannah River Site, Aiken, SC, March 18, 2009.

SRNL-L6200-2010-00019, Dixon, K. L., *Sensitivity Simulations for the Saltstone Disposal Facility Radon and Air Pathway Model*, Savannah River Site, Aiken, SC, June 22, 2010.

SRNL-STI-2008-00415, Lee, P.L., et al., *Air Pathway Dose Modeling for the Saltstone Disposal Facility*, Savannah River Site, Aiken, SC, Rev. 0, December 15, 2008.

SRNL-STI-2008-00421, Dixon, K., et al., *Hydraulic and Physical Properties of Saltstone Grouts and Vault Concretes*, Savannah River Site, Aiken, SC, Rev. 0, November 2008.

SRNL-STI-2008-00447, Dixon, K., et al., *Air and Radon Pathway Modeling for the Saltstone Disposal Facility*, Savannah River Site, Aiken, SC, Rev. 0, December 2008.

SRNL-STI-2009-00115, Flach, G., et al., *Numerical Flow and Transport Simulations Supporting the Saltstone Facility Performance Assessment*, Savannah River Site, Aiken, SC, Rev. 1, June 2009.

SRNL-STI-2009-00419, Dixon, K., et al., *Hydraulic and Physical Properties of ARP/MCU Saltstone Grout*, Savannah River Site, Aiken, SC, Rev. 0, May 2010.

SRNL-STI-2009-00636, Kaplan, D. I., *Iodine, Neptunium, Plutonium, and Technetium Sorption to Saltstone and Cement Formulations Under Oxidizing and Reducing Conditions*, Savannah River Site, Aiken, SC, Rev. 0, December 16, 2009.

SRNL-TR-2008-00283, Denham, M., *Estimation of Eh and pH Transitions in Pore Fluids During Aging of Saltstone and Disposal Unit Concrete*, Savannah River Site, Aiken, SC, December 2008.

SRNL-TR-2009-00019, Kaplan, D. I., *Tc and Pu Distribution Coefficients, Kd Values, for the Saltstone Facility Performance Assessment*, Savannah River Site, Aiken, SC, January 2009.

SRNL-TR-2009-00051, Taylor, G., *Saltstone Disposition Facility Stochastic Transport and Fate Model Description*, Savannah River Site, Aiken, SC, Rev. 0, March 20, 2009.

SRNS-STI-2008-00045, Kaplan, D. I., et al., *Saltstone and Concrete Interactions with Radionuclides: Sorption (K_d), Desorption, and Reduction Capacity Measurements*, Savannah River Site, Aiken, SC, October 30, 2008.

SRNS-STI-2009-00477, Langton, C. A., *Saltstone Matrix Characterization and Stadium Simulation Results, Simco Technologies, Inc. Task 6 Report*, Savannah River Site, Aiken, SC, Rev. 0, July 30, 2009.

SRNS-TR-2009-00452, *Z-Area Groundwater Monitoring Report for 2009*, Savannah River Site, Aiken, SC, December 29, 2009.

SRR-CWDA-2010-00015, *Savannah River Site Liquid Waste Facilities Performance Assessment Maintenance Program, FY2010 Implementation Plan*, Savannah River Site, Aiken, SC, Rev. 0, March 31, 2010.

SRR-CWDA-2010-00057, Kaplan, D. I., *Preliminary Ra and SR Kd Values of Subsurface SRS Sediments*, Savannah River Site, Aiken, SC, May 2010.

SRS-REG-2007-00041, Rosenberger, K.H., *Unreviewed Disposal Question Evaluation: Evaluation of Liquid Weeping from Saltstone Vault 4 Exterior Walls*, Savannah River Site, Aiken, SC, April 3, 2008.

T-CLC-Z-00006, Peregory, W., *Saltstone Vault Structural Degradation Prediction*, Savannah River Site, Aiken, SC, Rev. 0, July 10, 2003.

T-CLC-Z-00022, Patel, R.P., *Evaluation of Selected Values from Crom's Calculation for the Z-Area Saltstone Storage Tanks (Vault 2)*, Savannah River Site, Aiken, SC, September 28, 2008.

WB00001K-032, Phillips, J.A., *Tank Surface Preparation, Coating & Testing Instructions*, Savannah River Site, Aiken, SC, Rev. C, June 26, 2010.

WSRC-RP-2004-00593, Kaplan, D. I., and Serkiz, S. M., *Influence of Dissolved Organic Carbon and pH on Contaminant Sorption to Sediment*, Savannah River Site, Aiken, SC, September 2004.

WSRC-RP-91-17, *Land and Water Use Characteristics in the Vicinity of the Savannah River Site*, Savannah River Site, Aiken, SC, March 1991.

WSRC-RP-92-1360, *Radiological Performance Assessment for the Z-Area Saltstone Disposal Facility*, Savannah River Site, Aiken, SC, Rev. 0, December 18, 1992.

WSRC-RP-92-450, Kaback, D. S., and Strom, R. N., *SRP Baseline Hydrogeologic Investigation: Aquifer Characterization, Groundwater Geochemistry of the Savannah River Site and Vicinity*, Savannah River Site, Aiken, SC, March 31, 1992.

WSRC-STI-2006-00037, Kaplan, D. I., et al., *Influence of Dissolved Organic Carbon and pH on Iodide, Perrhenate, and Selenate Sorption to Sediment*, Savannah River Site, Aiken, SC, September 5, 2006.

WSRC-STI-2006-00198, *Hydraulic Property Data Package for the E-Area and Z-Area Soils, Cementitious Materials, and Waste Zones*, Savannah River Site, Aiken, SC, Rev. 0, September 2006.

WSRC-STI-2007-00640, Kaplan, D. I., and Coates, J. M., *Partitioning of Dissolved Radionuclides to Concrete Under Scenarios Appropriate for Tank Closure Performance Assessments*, Savannah River Site, Aiken, SC, December 21, 2007.

WSRC-STI-2008-00236, Denham, M., *Thermodynamic and Mass Balance Analysis of Expansive Phase Precipitation in Saltstone*, Savannah River Site, Aiken, SC, May 2008.

WSRC-STI-2008-00244, Jones, W. E., Phifer, M. A., *Saltstone Disposal Facility Closure Cap Concept and Infiltration Estimates*, Savannah River Site, Aiken, SC, Rev. 0, May 2008.

WSRC-STI-2008-00285, Kaplan, D. I., et al., *Distribution of Sorption Coefficients (Kd Values) in the SRS Subsurface Environment*, Savannah River Site, Aiken, SC, June 30, 2008.

WSRC-TR-2006-00004, Kaplan, D. I., *Geochemical Data Package for Performance assessment Calculations Related to the Savannah River Site*, Savannah River Site, Aiken, SC, Rev. 0, February 26, 2006.

WSRC-TR-2008-00037, Dixon, K. L., et al., *Task Technical and QA Plan: Saltstone Grout and Vault Concrete Sample Preparation and Testing*, Savannah River Site, Aiken, SC, Rev. 0, February 29, 2008.

X-CLC-Z-00027, *Inventory Determination of PODO Radionuclides in Saltstone Vaults 1 and 4*, Savannah River Site, Aiken, SC, Rev. 1, June 2009.